Ring Expansion of Coordinated *N,P*-Heterocyclic Carbenes: Methylene and Imidogen Insertion

Ryan M. Kirk[a] and Anthony F. Hill*[a]

[a] Dr R. M. Kirk and Prof. Dr A. F. Hill
Research School of Chemistry
Australian National University
Canberra, ACT 2601, Australia
E-mail: a.hill@anu.edu.au

1 General Considerations

Unless otherwise stated, all operations were carried out under an atmosphere of commercially purified argon using standard Schlenk techniques. The air stability/sensitivity of each compound is stated in the accompanying text.

The NPHC complexes [M{CNP^{t}Bu$_2$C(CO$_2$Me)=C(CO$_2$Me)}-(CO)$_5$] (**2$_{Cr}$**, **2$_{Mo}$**, **2$_W$**) were prepared by us previously.[3]

[Ph$_3$E-CH$_3$]I (E = P or As) were prepared by addition of methyl iodide (*caution*: **carcinogenic**) to molten Ph$_3$P (80 °C) or Ph$_3$As (60 °C, *caution*: **toxic**), heating continued until solidification (~90 min), and re-crystallised from hot CHCl$_3$/toluene. [Ph$_3$P-NH$_2$]Cl and [Ph$_3$As-NH$_2$]Br were prepared from Ph$_3$P or Ph$_3$As (*caution*: **toxic**), hexachloroethane (*caution*: **toxic**) or Br$_2$ (*caution*: **corrosive**), and anhydrous gaseous NH$_3$ (*caution*: **corrosive**, **asphyxiant**) in THF and isolated according to a published literature method[19a]. Ph$_3$P=CH$_2$ was prepared from [Ph$_3$P-CH$_3$]I and Na[N(SiMe$_3$)$_2$] in Et$_2$O and re-crystallised from hot *n*-hexane according to a published literature method [9] though for convenience it was typically generated *in-situ* as described below.

Other reagents and materials were purchased from commercial suppliers and used without further purification: Ph$_3$P, Ph$_3$As, C$_2$Cl$_6$, Br$_2$, CH$_3$I, ^{t}BuOK, Na[N(SiMe$_3$)$_2$], Li[N^{i}Pr$_2$] solution (1 M in THF), ^{t}BuLi solution (1.7 M in pentane), [Ph$_3$P-CH$_2$Br]Br, silica gel 230—400 mesh (Sigma Aldrich). HPLC-grade solvents were purchased from Merck and re-distilled from an appropriate desiccant under nitrogen: THF, Et$_2$O, toluene, *n*-hexane (sodium or sodium/benzophenone, stored over sodium mirror), CH$_2$Cl$_2$ (P$_2$O$_5$, stored over 4 Å molecular sieves). Solvents for chromatography need not be anhydrous but were sparged with nitrogen for ~10 minutes before use. Benzene-d_6 (*caution*: **carcinogenic**) was purchased from Cambridge Isotopes Laboratories and re-distilled from sodium wire under nitrogen and stored over a sodium mirror.

2 Instrumentation

Solution NMR spectroscopy was conducted on Bruker Avance 400 (400 MHz for ^{1}H, 101 MHz for ^{13}C, 162 MHz for ^{31}P) or 800 (201 MHz for ^{13}C) instruments. Spectra were processed using the MestReNova suite and are referenced to the residual *protio*-solvent impurity (for ^{1}H), the solvent itself (for ^{13}C), or an external standard (for ^{31}P: 85% aqueous H$_3$PO$_4$). Chemical shifts are reported to 2 d.p. for ^{1}H, and 1 d.p. for ^{13}C, ^{31}P, and also coupling constants. We thank Dr Doug Lawes of the ANU for helpful discussion and assistance.

Solution and solid-state IR spectroscopies were conducted on Perkin Elmer Spectrum One and Spectrum Two instruments, respectively, and bond stretching frequencies are reported to the nearest whole number. The following abbreviations are used to denote relative absorption intensities: w (weak), m (medium), s (strong), vs (very strong).

High-resolution mass spectrometry was conducted by the Joint Mass Spectrometry Facility at the Research School of Chemistry (ANU) using a Waters Synapt G2-Si HDMS LC-Q/TOF MS-MS spectrometer. Ion signals are reported to 4 d.p. and specific isotopomers are given for non-C,H,N,O elements. We thank Mrs Anitha Jeyasingham of the ANU for acquisition and processing of spectra.

Elemental microanalysis was conducted in duplicate by the Chemical Analysis Facility at the Department of Molecular Sciences, Macquarie University (NSW, Australia). Analyses are averaged and given to 2 decimal places.

3 Crystallography

Single crystal X-ray diffraction was conducted at 150 K on an Agilent Technologies Supernova equipped with a Rigaku HyPix 6000HE detector using graphite-monochromated Cu-Kα radiation (λ = 1.5406 Å), or New Xcalibur equipped with an Atlas CCD detector using graphite-monochromated Mo-Kα radiation (λ = 0.7107 Å). Selected crystals were mounted in oil on nylon loops and fixed under a cold stream of nitrogen. Data were processed within the *CrysAlisPRO-CCD* and *-RED* software packages.[18] Structures were solved within *Olex2*[19] with *SHELXT* using intrinsic phasing and refined with *SHELXL*[20] using full-matrix least-squares against F^2 in an anisotropic (for non-hydrogen atoms) approximation. Hydrogen atom positions were refined in isotropic approximation in a "riding" model with the U_{iso}(H) parameters fixed to 1.2 (for aromatic hydrogens) or 1.5 (for aliphatic hydrogens) U_{eq}(C$_i$), where U_{eq}(C$_i$) is the equivalent thermal parameter of the carbon atom to which the corresponding

H atom is bonded. Specific absorption correction methods are stated for each crystalline sample in the accompanying text. POV-RAY images of crystal structures were rendered in *Mercury*.[21] We thank Dr Michael Gardiner of the ANU for helpful discussion and assistance.

4 Computational Studies

Computational studies were performed by using the *SPARTAN24* suite of programs.[23] In the first instance, geometry optimisations (gas phase) were performed at the DFT level of theory using the exchange functional (ωB97X-D) of Head-Gordon.[24a] The Los Alamos effective core potential type basis set (LANL2Dζ) of Hay and Wadt[24b] was used for transition metals; the Pople 6-31G* basis sets[24c] were used for all other atoms. Geometry optimisations and single-point energy calculations were performed at the ωB97X-D/6-31G*/LANL2Dζl level; frequency calculations were performed to confirm that the optimized structures were local minima and to identify vibrational modes of interest. For the method's typical reflection of phenomenological Lewis bonds, Löwden bond orders,[25] which emphasise covalency were also calculated. The calculations follow a very similar form to the Wiberg indices, except using the Löwden symmetrically orthogonalized basis set instead of the natural basis. Atom-condensed Fukui functions were calculated as described by Parr and Yang.[26]

5 Synthetic Procedures

5.1 [M(CNHP^{t}Bu$_2$CRCRCH)(CO)$_5$] (R = CO_2Me, $\mathbf{3_M}$)

A typical preparation is as follows: a 250 mL Schlenk tube was charged with ^{t}BuOK and [Ph$_3$P-CH$_3$]I and cooled to -78 °C. To this was admitted ~60 mL THF with rapid stirring resulting in a yellow suspension. Stirring was continued for 1 hour at low temperature before solid $\mathbf{2_M}$ was added and the mixture allowed to warm to ambient temperature. The reaction was monitored by TLC (silica gel, CH_2Cl_2) and when $\mathbf{2_M}$ was no longer observed (usually within 1—2 hours) the orange-brown mixtures were dried under reduced pressure, extracted into CH_2Cl_2 and filtered through diatomaceous earth. The filtrate was transferred to a column of silica gel (25 x 5 cm) made up in CH_2Cl_2 and eluted with the same solvent under gravity. All $\mathbf{3_M}$ products elute as orange bands which were collected (for $\mathbf{3_{Mo}}$ and $\mathbf{3_W}$, under a gentle stream of nitrogen) and dried *in vacuo*. Re-crystallisation from the minimum volume of CH_2Cl_2/*n*-hexane at 0 °C ($\mathbf{3_{Cr}}$, $\mathbf{3_{Mo}}$) or toluene/*n*-hexane ($\mathbf{3_W}$) at -30 °C deposited large orange needles. All $\mathbf{3_M}$ are readily soluble in polar organic and aromatic solvents and sparingly soluble in aliphatic hydrocarbons; $\mathbf{3_{Cr}}$ is reasonably air stable, whilst $\mathbf{3_{Mo}}$ and $\mathbf{32_W}$ are moderately air sensitive.

During this work, it was noted that the use of other strong bases (Na[N(SiMe$_3$)$_2$], K[N(SiMe$_3$)$_2$], Li[N^{i}Pr$_2$], *n*-BuLi, NaH) for Ph$_3$P=CH$_2$ formation resulted in poorer isolated yields of $\mathbf{3_M}$, with $\mathbf{2_M}$ always recovered. We suspect that the conjugate acid of the base plays a role during the reaction, possibly as a proton-source; the increased Brønsted acidity of alcohols (^{t}BuOH) *vs* amines (HN(SiMe$_3$)$_2$, HN^{i}Pr$_2$) would be circumstantial evidence for this inference.

5.2 [Cr(CNHP^{t}Bu$_2$CRCRCH)(CO)$_5$] (R = CO_2Me) ($\mathbf{3_{Cr}}$)

Quantities used: 0.445 g ^{t}BuOK (3.96 mmol, 4 equiv.), 1.60 g [Ph$_3$P-CH$_3$]I (3.96 mmol, 4 equiv.), 0.50 g $\mathbf{1_{Cr}}$ (0.99 mmol). Isolated yield: 0.20 g (0.37 mmol, 38%).

NMR: ^{1}H (C_6D_6, 400 MHz, 25 °C) δ_H = 7.01 (s.br., 1H, N*H*), 6.67 (s, 1H, 6-C*H*), 3.41 (s, 3H, OCH_3), 3.22 (s, 3H, OCH_3), 0.90 (d, $^3J_{PH}$ = 16.5 Hz, 18H, CCH_3) ppm; $^{13}C\{^1H\}$ (C_6D_6, 201 MHz, 25 °C) δ_C = 244.9 (d, $^2J_{PC}$ = 18.5 Hz, Cr=*C*), 223.6 (*CO*$_{ax}$), 219.3 (*CO*$_{eq}$), 168.3 (d, J_{PC} = 14.1 Hz, *C*O$_2$CH$_3$), 167.1 (d, J_{PC} = 19.6 Hz, *C*O$_2$CH$_3$), 143.9 (5-*C*$_{allyl}$), 117.6 (d, J_{PC} = 12.9 Hz, 6-*C*H), 73.4 (d, J_{PC} = 99.1 Hz, 5-*C*$_{allyl}$), 52.2 OCH$_3$), 51.4 (OCH$_3$), 41.5 (d, J_{PC} = 41.3 Hz, *C*Me$_3$), 25.7 (C*C*H$_3$) ppm; $^{31}P\{^1H\}$ (C_6D_6, 162 MHz, 25 °C) δ_P = 52.6 ppm. IR (CH_2Cl_2, 25 °C) ν_{CO} 2049(s), 1970(w), 1925(vs), 1736(w), 1703(w) cm^{-1}; IR (ATR, 25 °C) ν_{CO} 2044(s), 1966(w), 1915(s), 1881 (vs, br), 1720(s), 1697(s) cm^{-1}. HR-MS (ESI, MeCN, +ve ion) found *m*/*z* 520.0836 (calc. for $C_{21}H_{27}NO_9P^{52}Cr$ [*M* + H]$^+$: 520.0823). Analysis found: C, 47.89; H, 5.06; N, 2.53%. Calc. for $C_{21}H_{26}CrNO_9P$: C, 48.56; H, 5.05; N, 2.70%.

Single crystals were grown from CH_2Cl_2/*n*-hexane at -30 °C. *Crystal data for* $C_{21}H_{26}NO_9PCr$ (M_w = 519.40 gmol^{-1}): orange needle 0.179 × 0.089 × 0.047 mm, monoclinic, space group $P2_1/c$ (no. 14), a = 10.39060(10) Å, b = 17.0232(2) Å, c = 14.0859(2) Å, β = 103.8840(10)°, V = 2418.74(5) Å^3, Z = 4, multi-scan correction T_{min}/T_{max} = 0.880/1.000, μ(Cu-Kα) = 4.960 mm^{-1}, ρ_{calc} = 1.426 Mgm^{-3}, 26150 reflections measured (8.294° ≤ 2Θ ≤ 155.884°), 5086 unique (R_{int} = 0.0447, R_{sigma} = 0.0347) which were used in all calculations against 306 refined parameters. The final R_1 was 0.0422 (I > 2σ(I)) and wR_2 was 0.1256 (all data), *GOF*(F^2) = 1.082, D_{min}/D_{max} = -0.50/1.65 eÅ^{-3}. CCDC 2426018.

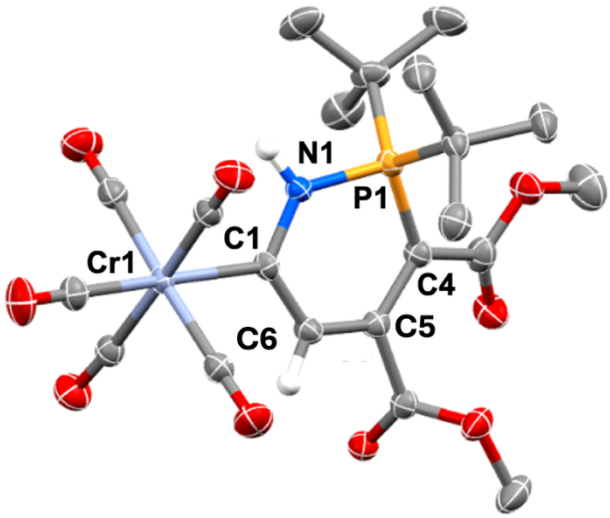

Figure S1. The molecular structures of $\mathbf{3_{Cr}}$ in a crystal (most hydrogen atoms omitted, 50% displacement ellipsoids). Selected distances (Å) and angles (°): 3Cr Cr1-C1 2.103(2), C1-C6 1.394(3), C6-C5 1.395(3), C5-C4 1.399(3), C4-P1 1.768(2), P1-N1 1.690(2), N1-C1 1.390(2), N1-C1-C6 116.2(2), C1-C6-C5 125.6(2), C6-C5-C4 126.7(2), C5-C4-P1 117.3(2), C4-P1-N1 102.1(1), P1-N1-C1 129.0(1).

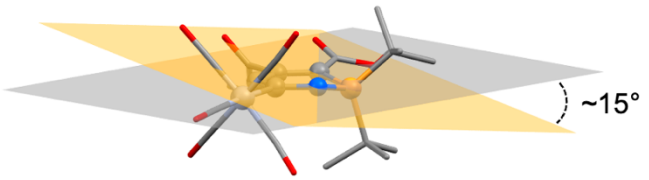

Figure S2. Simplified view of $\mathbf{3_{Cr}}$ highlighting P1 envelope folding (yellow) from the {C1,C4,C5,C6,N1} mean plane (grey).

5.3 *In-situ* reaction between 2_{Cr} and $Ph_3P{=}CH_2$

Within an argon-filled glovebox, a J. Young's NMR tube was charged with 0.040 g $\mathbf{2_{Cr}}$ (0.079 mmol) and 0.022 g $Ph_3P{=}CH_2$ (0.079 mmol); ~0.5 mL C_6D_6 was admitted and the contents shaken to dissolve. After standing overnight at ambient temperature, the $^{31}P\{^1H\}$ NMR spectrum showed signals corresponding to $\mathbf{2_{Cr}}$ (δ_P = 101.3), $\mathbf{3_{Cr}}$ (δ_P = 52.6), and Ph_3P (δ_P = -5.3) in a ~4:1:1.5 ratio by area integration (noting that the sensitivity of the respective P atoms may not necessarily be equivalent due to different coordination environments). No remaining $Ph_3P{=}CH_2$ (δ_P 20.6) was observed.

5.4 $[Mo(CNHP^tBu_2CRCRCH)(CO)_5]$ (R = CO_2Me) ($\mathbf{3_{Mo}}$)

Quantities used: 0.41 g ^{t}BuOK (3.6 mmol, 4 equiv.), 1.47 g $[Ph_3P\text{-}CH_3]I$ (3.64 mmol, 4 equiv.), 0.50 g $\mathbf{2_{Mo}}$ (0.91 mmol). Isolated yield: 0.095 g (0.17 mmol, 19%).

We observed $\mathbf{3_{Mo}}$ to slowly degrade (orange → yellow/brown) in solution over time to $[Mo(CO)_6]$ (*inter alia* unidentified materials), precluding acquisition of analytically pure NMR spectra, although data are not sufficiently comprised so as to preclude assignment.

NMR: ^1H (C_6D_6, 400 MHz, 25 °C) δ_H = 6.91 (s.br., 1H, N*H*), 6.64 (J_{PH} unresolved, 6-C*H*), 3.42 (s, 3H, OCH_3), 3.24 (s, 3H, OCH_3), 0.89 (d, $^3J_{PH}$ = 16.5 Hz, 18H, CCH_3) ppm; $^{13}C\{^1H\}$ (C_6D_6, 201 MHz, 25 °C) δ_C = 236.1 (d, $^2J_{PC}$ = 18.1 Hz, Mo=*C*), 213.6 (*C*O$_{ax}$), 208.1 (*C*O$_{eq}$), 168.4 (d, J_{PC} = 13.1 Hz, CO_2), 167.1 (d, J_{PC} = 19.5 Hz, CO_2), 145.0 (5-*C*$_{allyl}$), 118.0 (d, $^3J_{PC}$ = 14.0 Hz, 6-*C*H), 73.6 (d, $^1J_{PC}$ = 98.5 Hz, 4-*C*$_{allyl}$), 52.1 (OCH_3), 51.5 (OCH_3), 41.4 (*C*Me$_3$), 25.7 (C*C*H$_3$) ppm; $^{31}P\{^1H\}$ (C_6D_6, 162 MHz, 25 °C) δ_P = 51.5 ppm. IR (CH_2Cl_2, 25 °C) ν_{CO} 2059(s), 1982(w), 1940(vs), 1732(w), 1700(w) cm^{-1}; IR (ATR, 25 °C) ν_{CO} 2053(s), 1960(w), 1882(vs, br), 1720(s), 1697(s) cm^{-1}. HR-MS (ESI, MeCN, +ve ion) found *m/z* 566.0472. Calc. for $C_{21}H_{27}NO_9P^{98}Mo$ [*M* + H]$^+$: 566.0472). Satisfactory elemental microanalytical data were not obtained due to instability.

Single crystals were grown from CH_2Cl_2/*n*-hexane at 0 °C. *Crystal data for* $C_{21}H_{26}NO_9PMo$ (M_w = 563.34 gmol^{-1}): orange needle 0.73 × 0.11 × 0.05 mm, monoclinic, space group $P2_1/c$ (no. 14), a = 10.5209(5) Å, b = 17.2503(9) Å, c = 14.0286(7) Å, β = 103.537(5)°, V = 2475.3(2) Å^3, Z = 4, multi-scan correction T_{min}/T_{max} = 0.727/1.000, μ(Mo-Kα) = 0.643 mm^{-1}, ρ_{calc} = 1.512 Mgm^{-3}, 15863 reflections measured (4.722° ≤ 2Θ ≤ 61.466°), 5775 unique (R_{int} = 0.0574, R_{sigma} = 0.0634) which were used in all calculations against 306 refined parameters. The final R_1 was 0.0445 (I > 2σ(I)) and wR_2 was 0.1174 (all data), $GOF(F^2)$ = 1.037, D_{min}/D_{max} = -0.79/2.26 eÅ^{-3}. CCDC 2426019.

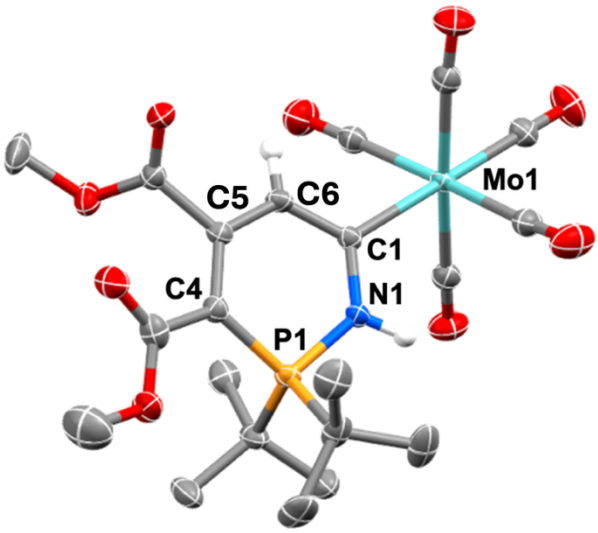

Figure S3. The molecular structures of $\mathbf{3_{Mo}}$ in a crystal (most hydrogen atoms omitted, 50% displacement ellipsoids). Selected distances (Å) and angles (°): Mo1-C1 2.237(3), C1-C6 1.391(4), C6-C5 1.397(5), C5-C4 1.396(4), C4-P1 1.786(3), P1-N1 1.694(3), N1-C1 1.383(3), N1-C1-C6 116.3(3), C1-C6-C5 125.5(3), C6-C5-C4 126.9(3), C5-C4-P1 116.9(2), C4-P1-N1 102.1(1), P1-N1-C1 128.9(2).

5.5 $[W(CNHP^tBu_2CRCRCH)(CO)_5]$ (R = CO_2Me) ($\mathbf{3_W}$)

Quantities used: 0.35 g ^{t}BuOK (3.1 mmol, 4 equiv.), 1.26 g $[Ph_3P\text{-}CH_3]I$ (3.12 mmol, 4 equiv.), 0.50 g $\mathbf{2_W}$ (0.78 mmol). Isolated yield: 0.13 g (0.20 mmol, 26%).

NMR: ^1H (C_6D_6, 400 MHz, 25 °C) δ_H = 6.74 (s.br, 1H, NH), 6.71 (s, 1H, 6-CH), 3.42 (s, 3H, OCH_3), 3.24 (s, 3H, OCH_3), 0.89 (d, $^3J_{PH}$ = 16.5 Hz, 18H, CCH_3) ppm; $^{13}C\{^1H\}$ (C_6D_6, 201 MHz, 25 °C) δ_C = 222.1 (d, $^1J_{WC}$ = 90.3 Hz, $^2J_{PC}$ = 16.8 Hz, W=C), 203.7 ($^1J_{WC}$ = 127.7 Hz, CO_{ax}), 200.1 ($^1J_{WC}$ = 126.2 Hz, CO_{eq}), 168.3 (d, J_{PC} = 14.0 Hz, CO_2), 167.0 (d, J_{PC} = 19.3 Hz, CO_2), 146.7 (5-Callyl), 119.8 (d, $^3J_{PC}$ = 12.4 Hz, 6-CH), 73.8 (d, $^1J_{PC}$ = 98.2 Hz, 4-Callyl), 52.2 (OCH_3), 51.6 (OCH_3), 41.4 (d, $^1J_{PC}$ = 40.6 Hz, CCH_3), 25.5 (CCH_3) ppm; $^{31}P\{^1H\}$ (C_6D_6, 162 MHz, 25 °C) δ_P = 53.5 ppm. IR (CH_2Cl_2, 25 °C) νCO 2057(s), 1968(w), 1921(vs), 1736(w), 1702(w) cm^{-1}; IR (ATR, 25 °C) νCO 2053(s), 1962(w), 1876(vs, br), 1737(s), 1712(s) cm^{-1}. HR-MS (ESI, MeCN, +ve ion) found *m/z* 652.0930. Calc. for $C_{21}H_{27}NO_9P^{184}W$ [M + H]$^+$: 652.0927. Analysis found C, 38.16; H, 4.05; N, 2.19%. Calc. for $C_{21}H_{26}NO_9PW$: C, 38.73; H, 4.02; N, 2.15%.

Single crystals were grown from toluene/n-hexane at -30 °C. *Crystal data for* $C_{21}H_{26}NO_9PW$ (M_w = 651.25 gmol^{-1}): orange needle 0.779 × 0.119 × 0.091 mm, monoclinic, space group $P2_1/c$ (no. 14), a = 10.5058(8) Å, b = 17.2378(13) Å, c = 14.0587(9) Å, β = 103.445(7)°, V = 2476.2(3) Å^3, Z = 4, Gaussian correction T_{min}/T_{max} = 0.308/0.676, μ(Mo-Kα) = 4.778 mm-1, ρ_{calc} = 1.747 Mgm^{-3}, 11843 reflections measured (7.258° ≤ 2Θ ≤ 58.18°), 5367 unique (R_{int} = 0.0398, R_{sigma} = 0.0663) which were used in all calculations against 306 refined parameters. The final R_1 was 0.0408 (I > 2σ(I)) and wR_2 was 0.1010 (all data), $GOF(F^2)$ = 1.074, D_{min}/D_{max} = -1.61/2.07 eÅ^{-3}. CCDC 2426020.

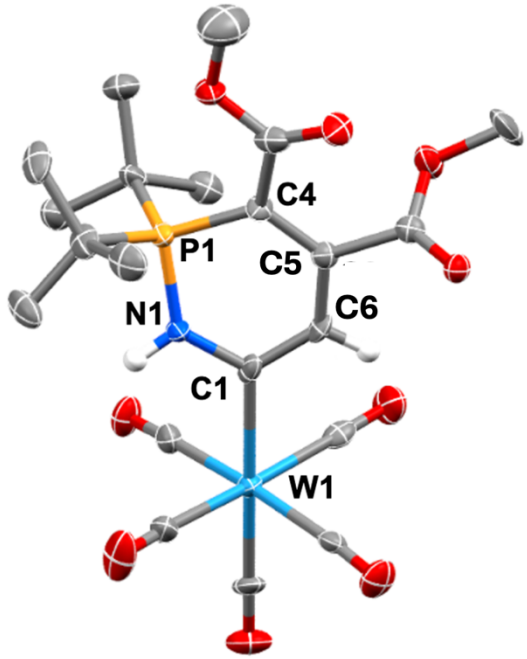

Figure S4. The molecular structures of $\mathbf{3_W}$ in a crystal (most hydrogen atoms omitted, 50% displacement ellipsoids). Selected distances (Å) and angles (°): $\mathbf{3_W}$ W1-C1 2.236(7), C1-C6 1.377(9), C6-C5 1.409(9), C5-C4 1.393(8), C4-P1 1.766(6), P1-N1 1.681(5), N1-C1 1.394(7), N1-C1-C6 115.7(6), C1-C6-C5 126.2(6), C6-C5-C4 125.8(6), C5-C4-P1 117.7(5), C4-P1-N1 101.8(3), P1-N1-C1 129.4(5).

5.6 Synthesis of $\mathbf{3_{Cr}}$ *via* $Ph_3P{=}CHLi$

A solution of $Ph_3P{=}CHLi$ in THF was prepared according to Corey:[10] A 250 mL Schlenk tube was charged with 0.11 g ^{t}BuOK (1.05 mmol) and 0.43 g $[Ph_3P\text{-}CH_2Br]Br$ (1.05 mmol) and cooled to -78 °C. To this was admitted ~60 mL THF resulting in a yellow suspension which was stirred at low temperature for 60 minutes. After this time, 1.8 mL of ^{t}BuLi solution (1.7 M in pentane, 3.2 mmol, 3 equiv.) was added dropwise affording an orange solution and stirring was continued for a further 60 minutes. To this, 0.50 g solid $\mathbf{2_{Cr}}$ (0.99 mmol) was added and the mixture allowed to gradually warm to ambient temperature overnight. After this time, TLC (silica gel, CH_2Cl_2) showed no $\mathbf{2_{Cr}}$ to be present and the orange-brown mixture was freed of volatiles in vacuo. The residue was extracted with CH_2Cl_2 and filtered, and the filtrate purified by column chromatography on silica gel (25 x 5 cm) with CH_2Cl_2 eluent under gravity. A fast-moving light-yellow band of $[Cr(PPh_3)(CO)_5]$ was collected and dried by rotary evaporation (0.04 g, 0.09 mmol, 9%: $^{31}P\{^1H\}$ ($CDCl_3$, 162 MHz, 25 °C) δ 56.0 ppm). A bright orange band of $\mathbf{3_{Cr}}$ was then collected and dried by rotary evaporation. Isolated yield: 0.16 g (0.30 mmol, 29%). Eluting with neat EtOAc developed a blue-brown band which was collected and re-subjected to column chromatography on silica gel (15 x 5 cm) with 1:2 petroleum ether/EtOAc under gravity. A blue band was collected and dried by rotary evaporation, and re-crystallised from EtOAc/*n*-heptane at 0 °C to give dimethyl 5,5'-oxalylbis(2,2-di-*tert*-butyl-4-pivaloyl-1*H*-1,2λ^5-azaphosphole-3-carboxylate) (**G**). Isolated yield: ~0.02 g (~0.027 mmol, ~5% w.r.t. $\mathbf{2_{Cr}}$. The formation of this unusual side product is clearly the result of adventitious ^{t}BuLi which according to the Corey protocol is employed in excess. Given the vanishingly low yields, the formation of **G** was not further studied here but it is noted in passing that the skeleton is without precedent.

NMR: ^1H ($CDCl_3$, 400 MHz, 25 °C) δ_H = 9.06 (d, J_{PH} = 19.7 Hz, 1H, NH), 3.63 (s, 3H, OCH_3), 1.40 (d, J_{PH} = 16.1 Hz, 9H, CCH_3), 1.34 (d, J_{PH} = 15.9 Hz, 9H, CCH_3), 1.26 (d, J_{PH} = 9.2 Hz, 9H, CCH_3) ppm; $^{31}P\{^1H\}$ ($CDCl_3$, 162 MHz, 25 °C) δ_P = 78.9 ppm. IR (ATR, 25 °C) ν_{CO} 1688(vs), 1651(s) cm^{-1}. HR-MS (ESI, MeCN, +ve ion) found *m/z* 737.4056. Calc. for $C_{38}H_{62}N_2O_8P_2$ $[M + H]^+$: 737.4059. Insufficient material was acquired for the obtention of satisfactory $^{13}C\{^1H\}$ NMR and elemental microanalytical data.

Single crystals were grown from EtOAc/*n*-heptane at 0 °C. The asymmetric unit comprises one-half of a molecule, the remainder generated by a crystallographic inversion centre at the C1-C1 midpoint. One-half of an *n*-heptane molecule was found within the asymmetric unit, however was badly disordered and could not be modelled satisfactorily. A solvent mask was calculated and 230 electrons were found in a volume of 1168 Å^3 in one void per unit cell. This is consistent with the presence of $0.5{\cdot}C_7H_{16}$ per asymmetric unit which account for 232 electrons per unit cell. *Crystal data for* $C_{45}H_{78}N_2O_8P_2$ (M_w = 837.03 gmol^{-1}): blue needle 0.405 × 0.053 × 0.051 mm, monoclinic, space group *I*2/a (no. 15), *a* = 19.4536(3) Å, *b* = 15.0266(2) Å, *c* = 16.2751(2) Å, β = 91.7420(10)°, *V* = 4755.36(11) Å^3, *Z* = 4, multi-scan correction T_{min}/T_{max} = 0.809/1.000, μ(Cu-Kα) = 1.231 mm^{-1}, ρ_{calc} = 1.169 Mgm^{-3}, 15499 reflections measured (7.436° ≤ 2Θ ≤ 157.534°), 4928 unique (R_{int} = 0.0418, R_{sigma} = 0.0423) which were used in all calculations against 240 refined parameters. The final R_1 was 0.1016 ($I > 2\sigma(I)$) and wR_2 was 0.2251 (all data), $GOF(F^2)$ = 1.115, D_{min}/D_{max} = -0.57/0.61 eÅ^{-3}. CCDC 2516364.

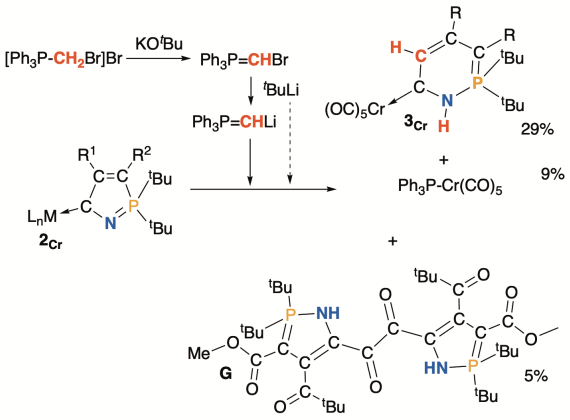

dimethyl 5,5'-oxalylbis(2,2-di-*tert*-butyl-4-pivaloyl-1*H*-1,2λ^5-azaphosphole-3-carboxylate)

Scheme S1. Formation of $\mathbf{3_{Cr}}$ from $\mathbf{2_{Cr}}$ (R = CO_2Me) and $Ph_3P{=}CHLi$ (^{t}BuLi) accompanied by an unusual blue glyoxal derivative **G** = dimethyl 5,5'-oxalylbis(2,2-di-*tert*-butyl-4-pivaloyl-1*H*-1,2λ^5-azaphosphole-3-carboxylate)).

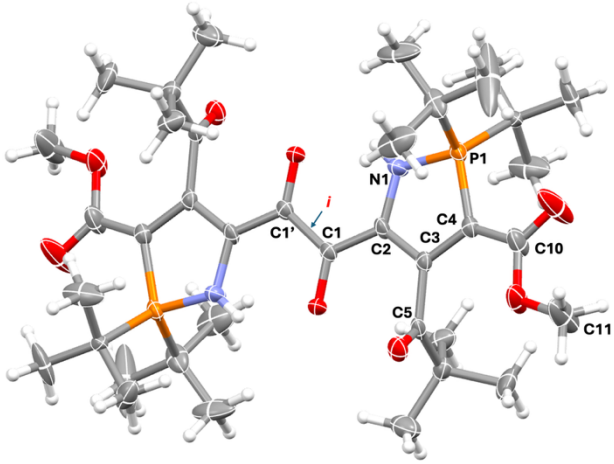

Figure S5. The molecular structure of centrosymmetric **G** in a crystal of $\mathbf{G}_2.C_7H_{16}$ (50% displacement ellipsoids, solvent omitted). Only one half of the molecule is unique in I_2/a due to the presence of a crystallographic inversion centre at the C1-C1' midpoint. Selected distances (Å) and angles (°): C1-C1 1.513(6), C1-O1 1.261(5), C1-C2 1.427(5), C2-C3 1.399(6), C3-C4 1.407(5), C4-P1 1.771(5), P1-N1 1.644(4), N1-C2 1.407(5), O1···H-N1 2.00(6), O1-N1 2.605(5), O1-C1-C2 121.1(4), N1-C2-C3 111.9(3), C2-C3-C4 113.0(3), C3 C4 P1 108.8(3), C4-P1-N1 92.7(2), P1-N1-C2 113.5(3).

The intense blue colouration of the compound may be traced to the symmetry-allowed HOMO→LUMO transition identified by TD-DFT analysis.

Table S1. Calculated[a] electronic transitions for dimethyl 5,5'-oxalylbis(2,2-dimethyl-4-pivaloyl-1*H*-1,2λ⁵-azaphosphole-3-carboxylate).

λ (nm)	strength	MO Component	%
275.02	0.0000	HOMO → LUMO+1	32%
		HOMO-3 → LUMO	27%
		HOMO → LUMO+2	14%
		HOMO-1 → LUMO+3	12%
278.01	0.0071	HOMO-4 → LUMO	39%
		HOMO-4 → LUMO+3	15%
		HOMO-3 → LUMO+2	14%
		HOMO-3 → LUMO+1	11%
278.71	0.0000	HOMO-3 → LUMO	31%
		HOMO-3 → LUMO+3	14%
		HOMO-4 → LUMO+2	13%
372.66	0.0000	HOMO-1 → LUMO	96%
388.64	0.0036	HOMO-2 → LUMO	93%
434.61	0.8451	HOMO → LUMO	95%

[a] TD-DFT: ωB97X-D/6-31G*/gas phase.

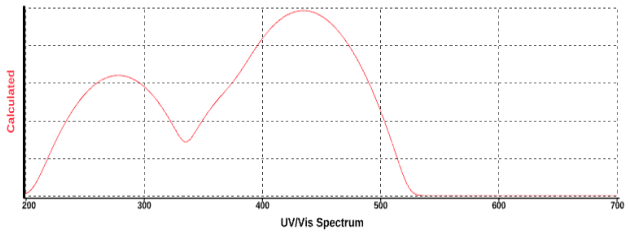

Figure S6. Calculated[a] electronic spectrum for dimethyl 5,5'-oxalylbis(2,2-dimethyl-4-pivaloyl-1*H*-1,2λ⁵-azaphosphole-3-carboxylate) (TD-DFT: ωB97X-D/6-31G*/gas phase).

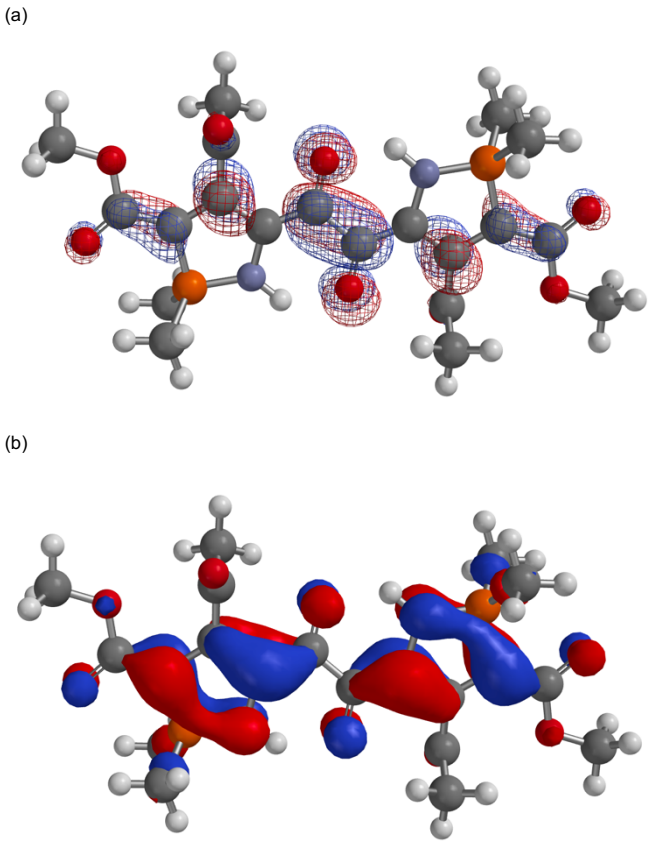

Figure S7. (a) LUMO and (b) HOMO associated with the Laporte-allowed (*g*→*u*) transition (434 nm) calculated for dimethyl 5,5'-oxalylbis(2,2-dimethyl-4-pivaloyl-1*H*-1,2λ⁵-azaphosphole-3-carboxylate).

5.7 [AuCl(CNHP^{t}Bu$_2$CRCRCH)] (R = CO$_2$Me) (**4**)

A 25 mL Schlenk tube was charged with **3$_{Cr}$** (0.050 g, 0.1 mmol) and [AuCl(SMe$_2$)] (0.03 g , 0.1 mmol). To this was added CH_2Cl_2 (5 mL) and the mixture stirred for 2 hours whilst shielded from laboratory lighting, to provide a yellow-brown suspension. The mixture was then filtered through a short plug of oven-dried diatomaceous earth (2.5 x 2.5 cm) and the yellow-orange filtrate was dried under reduced pressure. Attempts to isolate 4 completely free of the side product [Cr(SMe$_2$)(CO)$_5$] resulted in sample degradation.

NMR: ^{1}H (CD_2Cl_2, 400 MHz, 25 °C) δ_H = 8.49 (d, $^2J_{PH}$ = 15.6 Hz, 1H, NH), 5.61 (s, 1H, 6-CH), 3.81 (s, 3H, OCH_3), 3.74 (s, 3H, OCH_3), 2.33 ([Cr(SMe$_2$)(CO)$_5$]: s, 6H, SCH_3), 1.47 (d, $^1J_{PH}$ = 17.0 Hz, 18H, CCH_3) ppm; $^{13}C\{^1H\}$ (CD_2Cl_2, 201 MHz, 25 °C) δ_C = 221.6 ([Cr(SMe$_2$)(CO)$_5$]: CO_{ax}), 215.3 ([Cr(SMe$_2$)(CO)$_5$]: CO_{eq}), 212.1 ([Cr(CO)$_6$]), 189.8 (d, $^2J_{PC}$ = 15.4 Hz, Au=C), 168.5 (d, J_{PC} = 13.6 Hz, CO_2), 165.7 (d, J_{PC} = 17.9 Hz, CO_2), 153.0 (5-Callyl), 111.2 (d, J_{PC} = 13.3 Hz, 6-CH), 79.6 (d, $^1J_{PC}$ = 89.8 Hz, 4-Callyl), 53.0 (OCH_3), 52.5 (OCH_3), 42.5 (d, $^1J_{PC}$ = 39.6 Hz, CMe_3), 27.4 ([Cr(SMe$_2$)(CO)$_5$]: SCH_3), 26.7 (CCH_3) ppm; $^{31}P\{^1H\}$ (CD_2Cl_2, 162 MHz, 25 °C) δ_H = 61.7 ppm. Satisfactory elemental microanalytical data were not acquired due to solution light sensitivity.

Single crystals were grown by vapour diffusion of Et_2O into CH_2Cl_2 solution at -30 °C. The complex is dimeric in the solid state with the asymmetric unit comprised of two crystallographically independent molecules associating in a C2-symmetric (chiral) dimer *via* one aurophilic Au···Au interaction and a pair of N-H···Cl-Au hydrogen bonds. The alternative enantiomer is generated by crystal symmetry. One dichloromethane solvate molecule was also found within the asymmetric unit. *Crystal data for* $C_{32}H_{52}Au_2Cl_2N_2O_8P_2 \cdot CH_2Cl_2$ (M_w = 1204.45 gmol^{-1}): yellow plate 0.453 × 0.217 × 0.063 mm, monoclinic, space group $P2_1/n$ (no. 14), a = 16.5200(2) Å, b = 15.33010(10) Å, c = 18.6177(2) Å, β = 112.3550(10)°, V = 4360.64(8) Å^3, Z = 4, analytical correction T_{min}/T_{max} = 0.058/0.444, μ(Cu-Kα) = 15.805 mm^{-1}, ρ_{calc} = 1.835 Mgm^{-3}, 31535 reflections measured (6.102° ≤ 2Θ ≤ 157.18°), 9136 unique (R_{int} = 0.0691, R_{sigma} = 0.0489) which were used in all calculations against 476 refined parameters. The final R_1 was 0.0686 ($I > 2\sigma(I)$) and wR_2 was 0.2101 (all data), $GOF(F^2)$ = 1.048, D_{min}/D_{max} = -3.42/2.23 eÅ^{-3}. CCDC 2430693.

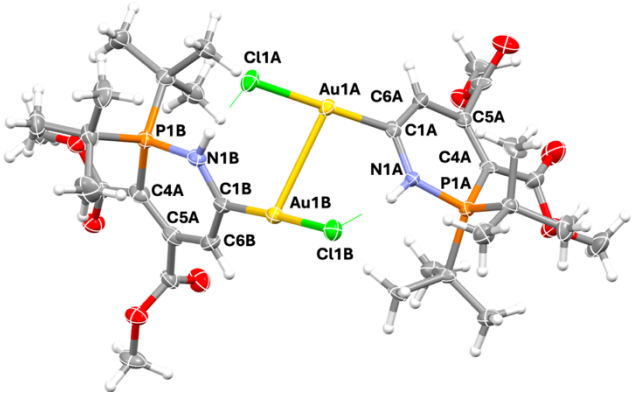

Figure S8. The molecular structure of [**4**]$_2$ in a crystal of [**4**]$_2$·CH_2Cl_2 (solvent omitted, 50% displacement ellipsoids).

5.8 *E*-(CNHP^{t}Bu$_2$CRCRCH)$_2$ (R = CO_2Me) (**7**)

A 25 mL Schlenk tube was charged with **3$_{Cr}$** (0.150 g, 0.28 mmol) and [AuCl(SMe$_2$)] (0.100 g , 0.34 mmol, ~1.2 equiv.). To this was added CH_2Cl_2 (10 mL) and the mixture stirred for 2 hours (shielded with foil from ambient lighting) forming a yellow-brown suspension. Exposing the reaction mixture to a gentle stream of compressed air resulted in a rapid (<< 30 seconds) colour change to a reddish-brown with deposition of purple nanoparticulate gold. After 5 minutes all volatiles were removed by rotary evaporation and the residue was purified by column chromatography on silica gel (30 x 2.5 cm). Eluting with 4:1 petroleum ether/EtOAc afforded a yellow band of [Cr(SMe$_2$)(CO)$_5$] (IR (CH_2Cl_2): ν_{CO} 2069(s), 1980(s), 1940(vs) cm^{-1}), which was discarded. Further elution with 1:1 petroleum ether/EtOAc afforded a reddish-pink band which was collected and dried. Isolated yield: 0.09 g (0.13 mmol, 92% *w.r.t.* **3$_{Cr}$**). The product is air-stable and is readily soluble in polar organic and aromatic solvents. At present, an analytically pure specimen has not been forthcoming, however quality was sufficient for characterisation.

NMR: ^{1}H ($CDCl_3$, 400 MHz, 25 °C) δ 6.17 (s, 1H, C*H*), 3.84 (s, 3H, CO_2CH_3), 3.69 (s, 3H, CO_2CH_3), 1.30 (d, $^3J_{PH}$ = 15.5 Hz, 18H, C(CH_3)$_3$) ppm (the NH hydrogen was not observed); ^{13}C{^{1}H} ($CDCl_3$, 176 MHz, 25 °C) δ 171.1 (d, J_{PC} = 12.8 Hz, CO_2CH_3), 167.9 (d, J_{PC} = 17.4 Hz, CO_2CH_3), 154.7 (d, J_{PC} = 3.6 Hz, 3-*C*), 96.9 (d, J_{PC} = 18.6 Hz, 2-*C*H), 69.3 (d, J_{PC} = 72.7 Hz, 4-*C*), 52.5 (CO_2CH_3), 51.1 (CO_2CH_3), 41.5 (d, J_{PC} = 59.0 Hz, *C*(CH$_3$)$_3$), 26.5 (C(*C*H$_3$)$_3$) ppm (the C1 carbon could not be reliably assigned, even with the aid of ^{1}H,^{13}C-HSQC and -HMBC spectra); ^{31}P{^{1}H} ($CDCl_3$, 162 MHz, 25 °C) δ 53.3 ppm. IR (CH_2Cl_2, 25 °C) ν_{CO} 1733(s), 1675(s) cm^{-1}. IR (ATR, 25 °C) ν_{CO} 1762(vs), 1692(s) cm^{-1}. HR-MS (ESI, MeCN, +ve ion) found *m*/*z* 653.3096. Calc. for $C_{32}H_{53}N_2O_8P_2$ [*M* + H]$^+$: 653.3115.

Single crystals were obtained by layering a CH_2Cl_2 solution with *n*-hexane at 0 °C. The asymmetric unit comprises one-half of a molecule with a crystallographic inversion centre situated at the C1-C1' midpoint. *Crystal data for* $C_{32}H_{52}N_2O_8P_2$ (M_w = 654.69 gmol^{-1}): red plate 0.17 × 0.1 × 0.03 mm, triclinic, space group *P*-1 (no. 2), a = 7.8049(4) Å, b = 8.2345(4) Å, c = 13.8840(6) Å, α = 85.907(4)°, β = 77.024(4)°, γ = 78.055(4)°, V = 850.41(7) Å^3, Z = 1, multi-scan correction T_{min}/T_{max} = 0.947/1.000, μ(Cu-Kα) = 1.581 mm^{-1}, ρ_{calc} = 1.278 Mgm^{-3}, 11047 reflections measured (6.536° ≤ 2Θ ≤ 148.85°), 3443 unique (R_{int} = 0.0529, R_{sigma} = 0.0546) which were used in all calculations against 207 refined parameters. The final R_1 was 0.0777 ($I > 2\sigma(I)$) and wR_2 was 0.2577 (all data), $GOF(F^2)$ = 1.081, D_{min}/D_{max} = -0.49/1.19 eÅ^{-3}. CCDC 2430695

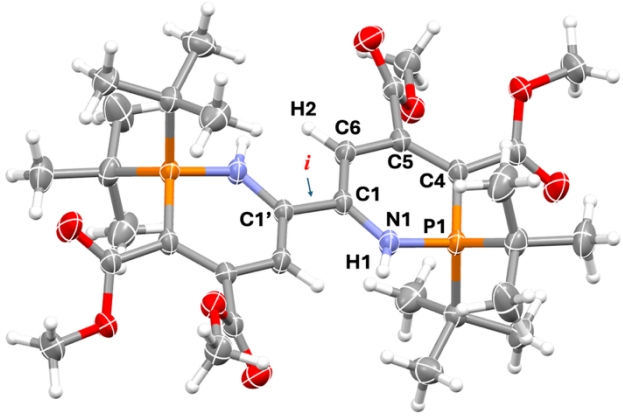

Figure S9. The molecular structure of **7** in a crystal (50% displacement ellipsoids).

5.9 [Au(CNHP^{t}Bu$_2$CRCRCH)$_2$][Au(C$_6$F$_5$)$_2$] (**5**) and [Au(C$_6$F$_5$)(CNHP^{t}Bu$_2$CRCRCH)] (**6**)

A 25 mL Schlenk tube was charged with **3$_{Cr}$** (0.115 g, 0.22 mmol) and [Au(C$_6$F$_5$)(THT)] (0.100 g, 0.22 mmol). To this was admitted 10 mL CH_2Cl_2 and the mixture stirred overnight, becoming dark yellow. The mixture was filtered through a short plug of oven-dried diatomaceous earth (2.5 x 2.5 cm) and the yellow filtrate dried under reduced pressure. The residue was then triturated in 3 x 5 mL portions of *n*-hexane (the pale-yellow supernatant containing [Cr(THT)(CO)$_5$] was discarded) and the yellow, *n*-hexane insoluble material afforded was dried under vacuum.

Analysis of the reaction material revealed two complexes which were identified as the salt $[Au(CNHP^tBu_2CRCRCH\}_2][Au(C_6F_5)_2]$ (**5**, R = CO_2Me) and the neutral complex $[Au(C_6F_5)(CNHP^tBu_2CRCRNH)]$ (**6**). In CD_2Cl_2 at 25 °C, their relative ratio was estimated to be ~1:1 by area integration of ^1H and ^{31}P NMR spectra; this ratio did not change upon dissolution in non-polar C_6D_6 at 25 °C, suggesting these species are not in dynamic equilibrium. The formation of these two products (in a ~1:1 ratio) was reproducible in a repeat experiment.

5.9.1 $[Au(C_6F_5)(CNHP^tBu_2CRCRNH]$ (**6**, R = CO_2Me)

NMR: ^1H (CD_2Cl_2, 400 MHz, 25 °C) δ_H = 7.33 (d, $^2J_{PH}$ = 16.3 Hz, 1H, N*H*), 5.68 (s, 1H, C*H*), 3.83 (s, 3H, OCH_3), 3.76 (s, 3H, OCH_3), 1.34 (d, $^3J_{PH}$ = 17.0 Hz, 18H, CCH_3) ppm; $^{13}C\{^1H\}$ (CD_2Cl_2, 201 MHz, 25 °C) δ_C = 205.1 (dd, $^2J_{PC}$ = 16.2 Hz, $^4J_{FC}$ = 5.0 Hz, Au=*C*), 168.2 (d, J_{PC} = 13.6 Hz, CO_2), 165.3 (d, J_{PC} = 17.8 Hz, CO_2), 152.7 (5-C_{allyl}), 112.5 (d, J_{PC} = 14.5 Hz, 6-CH), 82.3 (d, J_{PC} = 90.7 Hz, 4-C_{allyl}), 53.2 (OCH_3), 53.0 (OCH_3), 42.3 (d, $^1J_{PC}$ = 39.2 Hz, *C*CH_3), 26.3 (CCH_3) ppm; $^{19}F\{^1H\}$ (CD_2Cl_2, 376 MHz, 25 °C) δ_F = -112.6 (m, 2F, 2,6-C_6F_5), -161.5 (t, $^3J_{FF}$ = 20.3 Hz, 1F, 4-C_6F_5), -163.0 (m, 2F, 3,5-C_6F_5); $^{31}P\{^1H\}$ (CD_2Cl_2, 162 MHz, 25 °C) δ_P = 57.8 ppm.

5.9.2 $[Au(CNHP^tBu_2CRCRCH)_2][Au(C_6F_5)_2]$ (**5**, R = CO_2Me)

NMR: ^1H (CD_2Cl_2, 400 MHz, 25 °C) δ_H = 7.18 (d, $^2J_{PH}$ = 16.2 Hz, NH), 5.80 (s, 1H, CH), 3.83 (s, 3H, OCH_3), 3.77 (s, 3H, OCH_3), 1.46 (d, $^3J_{PH}$ = 16.9 Hz, 18H, CCH_3) ppm; $^{13}C\{^1H\}$ (CD_2Cl_2, 201 MHz, 25 °C): δ_C = 209.7 (d, $^2J_{PC}$ = 16.4 Hz, Au=C), 168.4 (d, J_{PC} = 13.1 Hz, CO_2), 165.6 (d, J_{PC} = 18.4 Hz, CO_2), 152.9 (5-C_{allyl}), 111.8 (d, J_{PC} = 14.6 Hz, 6-CH), 80.5 (d, J_{PC} = 91.8 Hz, 4-C_{allyl}), 53.1 (OCH_3), 52.8 (OCH_3), 42.4 (d, $^1J_{PC}$ = 39.6 Hz, *C*CH_3), 26.5 (CCH_3) ppm; $^{19}F\{^1H\}$ (CD_2Cl_2, 376 MHz, 25 °C) δ_F = -114.7 (m, 2F, 2,6-C_6F_5), -160.4 (t, $^3J_{FF}$ = 20.1 Hz, 1F, 4-C_6F_5), -162.8 (m, 2F, 3,5-C_6F_5) ppm; $^{31}P\{^1H\}$ (CD_2Cl_2, 162 MHz, 25 °C) δ 58.0 ppm. Multiplet signals in the $^{13}C\{^1H\}$ NMR spectrum corresponding to C_6F_5 residues are measured at 149.6, 149.3, 139.2, 138.6, 137.9, 137.4, 136.7, 133.6 ppm with complex J_{FC} profiles, which could not be unambiguously assigned to either complex.

Single crystals of **5** were obtained by layering a CH_2Cl_2 solution with *n*-hexane at -30 °C; despite repeated efforts using a variety of crystallisation conditions, X-ray quality crystals of **6** have not yet been forthcoming. The asymmetric unit comprises two-half $[Au(CNHP^tBu_2CRCRCH)_2]^+$ cations which are crystallographically independent and one $[Au(C_6F_5)_2]^-$ anion; the remaining halves of each cation and another $[Au(C_6F_5)_2]^-$ counterion are generated by crystallographic inversion symmetry. *Crystal data for* $C_{44}H_{52}N_2O_8F_{10}P_2Au_2$ (M_w = 1382.75 g/mol): yellow plate 0.155 × 0.066 × 0.031 mm, triclinic, space group *P*-1 (no. 2), *a* = 12.1925(4) Å, *b* = 12.2849(4) Å, *c* = 20.2017(7) Å, *α* = 94.082(3)°, *β* = 105.944(3)°, *γ* = 103.852(3)°, *V* = 2794.30(17) Å^3, *Z* = 2, Gaussian correction T_{min}/T_{max} = 0.293/0.885, *μ*(Cu-Kα) = 10.973 mm^{-1}, ρ_{calc} = 1.643 Mgm^{-3}, 32883 reflections measured (7.492° ≤ 2Θ ≤ 157.548°), 11582 unique (R_{int} = 0.0583, R_{sigma} = 0.0641) which were used in all calculations against 632 parameters. The final R_1 was 0.0694 ($I > 2\sigma(I)$) and wR_2 was 0.2000 (all data), $GOF(F^2)$ = 1.046, D_{min}/D_{max} = -2.78/3.12 e/Å^3. CCDC 2516365.

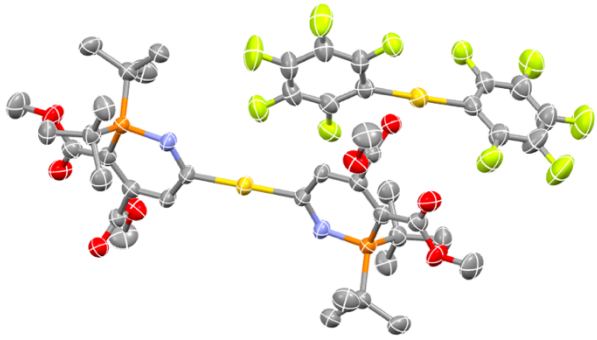

Figure S10. The molecular structure of **6** in a crystal (most hydrogen atoms omitted, 50% displacement ellipsoids).

5.10 $[Cr(CNP^tBu_2CRCRNH)(CO)_5]$ (**8**) (R = CO_2Me) and $[Cr\{CNP^tBu_2C(CN)C(C(O)N{=}AsPh_3)NH\}(CO)_5]$ (**9**)

To a suspension of $[Ph_3As\text{-}NH_2]Br$ (1.60 g, 3.98 mmol, 4 equiv.) in THF (50 mL) cooled to -78 °C was added 8 mL LDA solution (1 M in THF, 7.96 mmol, 8 equiv.). The mixture was warmed and stirred for 2 hours at ambient temperature forming a pale-yellow suspension, which was then re-cooled to -78 °C before solid $\mathbf{2_{Cr}}$ (0.50 g, 1.05 mmol) was added in one portion. The mixture was allowed to warm to ambient temperature and monitored by TLC (silica gel, CH_2Cl_2). When $\mathbf{2_{Cr}}$ was no longer observed (~ 2 hours) the mixture was freed of volatiles under reduced pressure, and the residue was extracted with CH_2Cl_2 and filtered through diatomaceous earth. The orange-brown filtrate was purified by column chromatography on silica gel (25 x 5 cm) eluting with CH_2Cl_2 under gravity. Two yellow-orange bands separated which were collected and dried, and re-crystallised from the minimum volume of CH_2Cl_2/*n*-hexane or CH_2Cl_2/cyclohexane at 0 °C. The products are air stable and readily soluble in polar organic and aromatic solvents.

5.10.1 $[Cr(CNP^tBu_2CRCRNH)(CO)_5]$ (**8**) (R = CO_2Me)

The first yellow band was identified as $[Cr(CNP^tBu_2CRCRNH)(CO)_5]$ (**8**, R = CO_2Me). Isolated yield: 0.07 g (0.12 mmol, 13% *w.r.t.* $\mathbf{2_{Cr}}$).

NMR: ^1H (C_6D_6, 400 MHz, 25 °C) δ_H = 8.96 (s, 1H, NH), 3.23 (s, 3H, OCH_3), 3.05 (s, 3H, OCH_3), 1.03 (d, $^3J_{PH}$ = 16.3 Hz, 18H, CCH_3) ppm; $^{13}C\{^1H\}$ (C_6D_6, 176 MHz, 25 °C) δ_C = 236.9 (d, $^2J_{PC}$ = 28.2 Hz, Cr=C), 223.5 (CO_{ax}), 219.7 (CO_{eq}), 166.1 (d, J_{PC} = 4.5 Hz, CO_2), 161.3 (d, J_{PC} = 7.5 Hz, CO_2), 140.2 (5-C_{allyl}), 85.7 (d, $^1J_{PC}$ = 47.4 Hz, 4-C_{allyl}), 53.4 (OCH_3), 52.3 (OCH_3), 38.8 (d, $^1J_{PC}$ = 57.3 Hz, *C*CH_3), 25.5 (CCH_3) ppm; $^{31}P\{^1H\}$ (C_6D_6, 162 MHz, 25 °C) δ_P = 18.2 ppm. IR (CH_2Cl_2, 25 °C) 2052(s), 1971(w), 1922(vs), 1894(sh), 1747(w), 1719(w) cm^{-1}; IR (ATR, 25 °C) ν_{CO} 2052(s), 1978(s), 1898(vs), 1863(vs), 1735(s), 1714(s) cm^{-1}. HR-

MS (ESI, MeCN, +ve ion) found *m/z* 493.0823. Calc. for $C_{19}H_{25}N_2O_8P^{52}Cr$ $[M–CO]^+$: 493.0832. Low isolated quantities precluded the acquisition of elemental microanalytical data for this compound.

Single crystals were grown from CH_2Cl_2/*n*-hexane at 0 °C. *Crystal data for* $C_{20}H_{25}N_2O_9PCr$ (M_w = 520.39 gmol^{-1}): orange block 0.358 × 0.187 × 0.13 mm, monoclinic, space group *C2/c* (no. 15), *a* = 23.4316(18) Å, *b* = 8.6174(8) Å, *c* = 24.6541(19) Å, *β* = 97.774(7)°, *V* = 4932.4(7) Å^3, *Z* = 8, multi-scan correction T_{min}/T_{max} = 0.525/1.000, *μ*(Mo-Kα) = 0.579 mm^{-1}, ρ_{calc} = 1.402 Mgm^{-3}, 12078 reflections measured (6.936° ≤ 2Θ ≤ 58.246°), 5308 unique (R_{int} = 0.0363, R_{sigma} = 0.0508) which were used in all calculations against 306 refined parameters. The final R_1 was 0.0432 ($I > 2\sigma(I)$) and wR_2 was 0.1072 (all data), $GOF(F^2)$ = 1.038, D_{min}/D_{max} = -0.45/0.35 e/Å^3. CCDC 2516362.

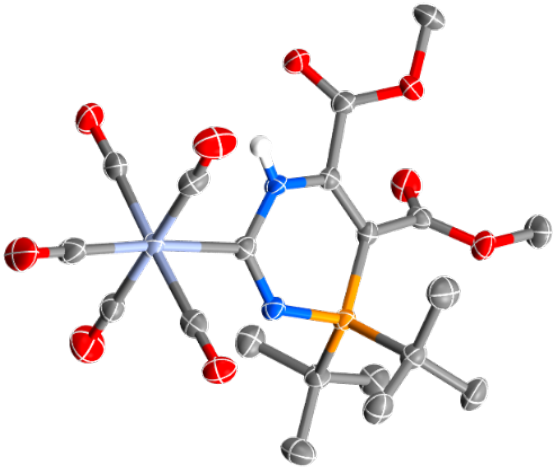

Figure S11. The molecular structure of **8** in a crystal (most hydrogen atoms omitted, 50% displacement ellipsoids).

5.10.2 [Cr{CNP^{t}Bu$_2$C(CN)C(C(O)N=AsPh$_3$)NH}(CO)$_5$] (**9**)

The second yellow band was identified as [Cr{CNP^{t}Bu$_2$C(CN)C(C(O)N=AsPh$_3$)NH}(CO)$_5$] (**9**). Isolated yield: 0.14 mg (0.18 mmol, 19% *w.r.t.* **2$_{Cr}$**).

NMR: ^{1}H (C_6D_6, 400 MHz, 25 °C) δ_H = 11.15 (s, 1H, NH), 7.70-7.67 (m, 6H, C_6H_5), 7.00-6.92 (m, 9H, C_6H_5), 1.03 (d, $^3J_{PH}$ = 16.1 Hz, 18H, CCH_3) ppm; $^{13}C\{^1H\}$ (C_6D_6, 176 MHz, 25 °C) δ_C = 238.3 (d, $^2J_{PC}$ = 28.7 Hz, Cr=C), 224.1 (CO_{ax}), 219.9 (CO_{eq}), 167.2 (d, J_{PC} = 4.8 Hz, C≡N), 149.6 (OCN), 132.9 [$C^{2,6}(C_6H_5)$], 132.8 [$C^4(C_6H_5)$], 129.8 [$C^{3,5}(C_6H_5)$], 128.4 [$C^1(C_6H_5)$], 118.3 (5-C), 60.5 (d, $^1J_{PC}$ = 53.9 Hz, 4-C), 38.8 (d, $^1J_{PC}$ = 57.1 Hz, CCH_3), 25.6 (CCH_3) ppm; $^{31}P\{^1H\}$ (C_6D_6, 162 MHz, 25 °C) δ_P = 21.3 ppm. IR (CH_2Cl_2, 25 °C) ν_{CO} 2051(s), 1970(w), 1921(vs), 1890(sh), 1596(w) cm^{-1}, ν_{CN} 2196(w) cm^{-1}; IR (ATR, 25 °C) ν_{CO} 2048(s), 1966(s), 1902(vs), 1878(vs), 1570(s) cm^{-1}, ν_{CN} 2200(s) cm^{-1}. HR-MS (ESI, MeCN, +ve ion) found *m/z* 777.1061. Calc. for $C_{36}H_{35}N_4O_6P^{52}Cr^{75}As$ $[M + H]^+$: 777.0916. Low isolated quantities precluded the acquisition of elemental microanalytical data for this particular specimen.

Single crystals were grown from CH_2Cl_2/cyclohexane at 0 °C. *Crystal data for* $C_{36}H_{34}N_4O_6PCrAs$ (M_w = 776.56 gmol^{-1}): yellow prism 0.611 × 0.312 × 0.103 mm, monoclinic, space group $P2_1/c$ (no. 14), *a* = 14.4657(8) Å, *b* = 16.3120(9) Å, *c* = 19.1637(10) Å, *β* = 102.840(6)°, *V* = 4408.9(4) Å^3, *Z* = 4, multi-scan correction T_{min}/T_{max} = 0.793/1.000, *μ*(Mo-Kα) = 1.081 mm^{-1}, ρ_{calc} = 1.170 Mgm^{-3}, 24255 reflections measured (6.888° ≤ 2Θ ≤ 58.098°), 9669 unique (R_{int} = 0.0433, R_{sigma} = 0.0726) which were used in all calculations against 448 refined parameters. The final R_1 was 0.0770 ($I > 2\sigma(I)$) and wR_2 was 0.2600 (all data), $GOF(F^2)$ = 1.068, D_{min}/D_{max} = -0.70/2.28 eÅ^{-3}. CCDC 2516361.

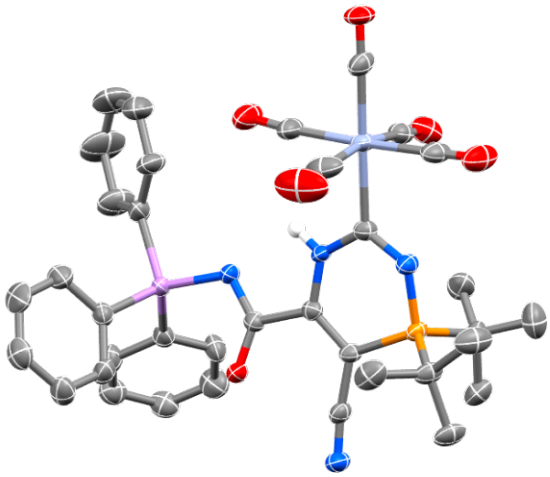

Figure S12. The molecular structure of **9** in a crystal (most hydrogen atoms omitted, 50% displacement ellipsoids).

5.11 Reaction of **2$_{Cr}$** with Ph$_3$P=NLi: [Cr{CNP^{t}Bu$_2$CRC(C(=O)NPPh$_3$)}(CO)$_5$] (**10**, R = CO$_2$Me)

To a stirred suspension of [Ph$_3$P-NH$_2$]Cl (1.24 g , 3.96 mmol, 4 equiv.) in THF (50 mL) cooled to -78 °C was added LDA solution (8.0 mL, 1 M in THF, 8.0 mmol, 8 equiv.). The mixture was warmed to ambient temperature and stirred for 2 hours forming a white suspension, which was then re-cooled to -78 °C before **2$_{Cr}$** (0.50 g , 0.99 mmol) was added in one portion. The mixture was allowed to warm to ambient temperature and monitored by TLC (silica gel, CH_2Cl_2). When **2$_{Cr}$** was no longer observed (~3 hours) the mixture was freed of volatiles and the residue extracted with CH_2Cl_2 and filtered through diatomaceous earth. The dark brown filtrate was purified by column chromatography on silica gel (25 x 2.5 cm) eluting with CH_2Cl_2 under gravity. A purple band was collected and dried, and re-crystallised from the minimum volume of Et_2O/*n*-heptane at 0 °C. The product is air stable and is readily soluble in polar organic and aromatic solvents. Isolated yield: 0.18 g (0.24 mmol, 24%).

^{1}H (C_6D_6, 400 MHz, 25 °C) δ_H = 7.74-7.68 (m, 6H, C_6H_5), 7.07—6.98 (m, 9H, C_6H_5), 3.69 (s, 3H, OCH_3), 1.06 (d, $^3J_{PH}$ = 15.5 Hz, 18H, CCH_3); $^{13}C\{^1H\}$ (C_6D_6, 201 MHz, 25 °C) δ_C = 288.6 (d, $^2J_{PC}$ = 32.7 Hz, Cr=C), 226.8 (CO_{ax}), 220.1 (CO_{eq}), 171.5 (dd, J_{PC} = 16.9, 7.2 Hz, OCN), 167.1 (d, J_{PC} = 23.1 Hz, OCH_3), 156.2 (d, J_{PC} = 52.3 Hz, 5-C_{vinyl}), 134.2 (dd, J_{PC} = 53.1 & 23.6 Hz, 4-C_{vinyl}), 133.4 [d, $^3J_{PC}$ = 10.4 Hz, $C^{3,5}(C_6H_5)$], 132.7 [d, $^4J_{PC}$ = 2.9 Hz, $C^4(C_6H_5)$], 128.9 [d, $^2J_{PC}$ = 12.2 Hz, $C^{2,6}(C_6H_5)$], 128.3 [$C^1(C_6H_5)$, partially obscured by C_6D_6, ambiguous], 52.1 (OCH_3), 35.6 (d, $^1J_{PC}$ = 38.8 Hz, CCH_3), 26.6 (CCH_3); $^{31}P\{^1H\}$ (C_6D_6, 162 MHz,

25 °C) δ_P = 100.5 (d, $^4J_{PP}$ = 8.2 Hz, ring-P), 21.5 (d, $^4J_{PP}$ = 8.2 Hz, OCNP). IR (CH_2Cl_2, 25 °C) ν_{CO} 2047(s), 1965(sh), 1926(vs), 1893(sh), 1750(s), 1717(s), 1631(vs) cm^{-1}; IR (ATR, 25 °C) ν_{CO} 2045(s), 1913(vs), 181(sh), 1749(s), 1715(s), 1626(s) cm^{-1}. HR-MS (ESI, MeCN, +ve ion) found m/z 751.1451. Calc. for $C_{37}H_{37}N_2O_8P_2{}^{52}Cr$ [*M* + H]$^+$: 751.1431). Elemental microanalytical data were not collected for this compound.

Single crystals were grown from Et_2O/*n*-heptane at 0 °C. The asymmetric unit contains one-half of an *n*-heptane solvate molecule, however this was highly disordered and could not be modelled satisfactorily. A solvent mask was calculated, and 232 electrons were found in a volume of 1316 Å^3 in two voids per unit cell. This is consistent with the presence of 0.5·C_7H_{16} per asymmetric unit which account for 232 electrons per unit cell. *Crystal data for* $C_{37}H_{36}CrN_2O_8P_2{\cdot}½C_7H_{16}$ (M_w = 800.71 $gmol^{-1}$): purple plate 0.364 × 0.193 × 0.096 mm, orthorhombic, space group *P*bca (no. 61), *a* = 24.1801(5) Å, *b* = 11.1078(2) Å, *c* = 30.4394(6) Å, *V* = 8175.6(3) Å^3, *Z* = 8, Gaussian correction T_{min}/T_{max} = 0.324/1.000, μ(Cu-Kα) = 3.474 mm^{-1}, ρ_{calc} = 1.301 Mgm^{-3}, 27604 reflections measured (5.806° ≤ 2Θ ≤ 157.318°), 8464 unique (R_{int} = 0.0657, R_{sigma} = 0.0637) which were used in all calculations against 458 refined parameters. The final R_1 was 0.0653 ($I > 2\sigma(I)$) and wR_2 was 0.1690 (all data), *GOF*(F^2) = 1.036, D_{min}/D_{max} = -0.46/0.73 eÅ^{-3}. CCDC 2516363.

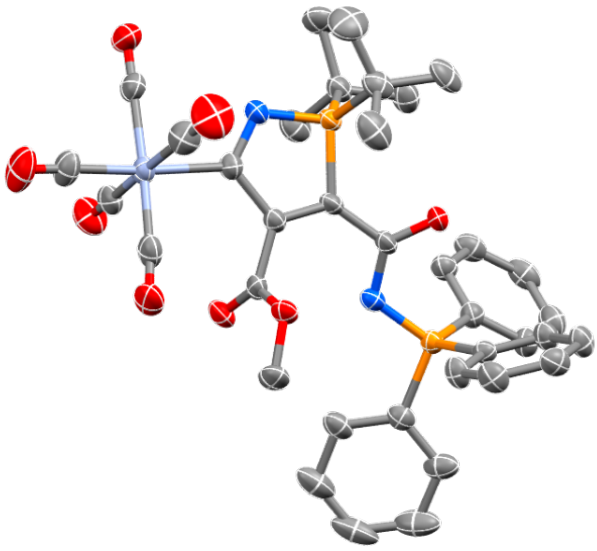

Figure S13. The molecular structure of **10** in a crystal (most hydrogen atoms omitted, 50% displacement ellipsoids).

6 Computational Results

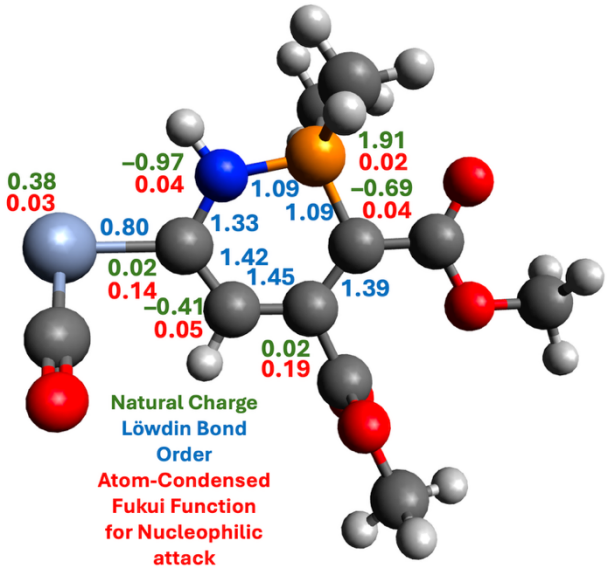

Figure S14. Natural Charges (green), Löwdin Bond Orders (blue) and Atom-Condensed Fukui functions (f^-, red) for the model complex [Cr(=CNHPMe$_2$CRCRCH)(CO)$_5$] (R = CO_2Me).

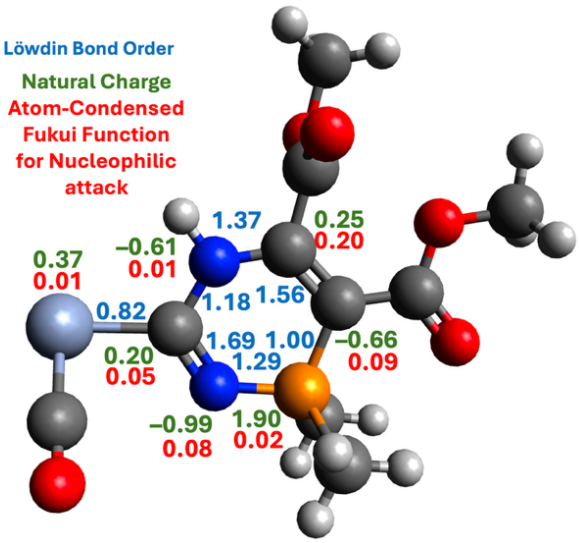

Figure S15. Natural Charges (green), Löwdin Bond Orders (blue) and Atom-Condensed Fukui functions (f^-, red) for the model complex [Cr(=CNHPMe$_2$CRCRN)(CO)$_5$] (R = CO_2Me).

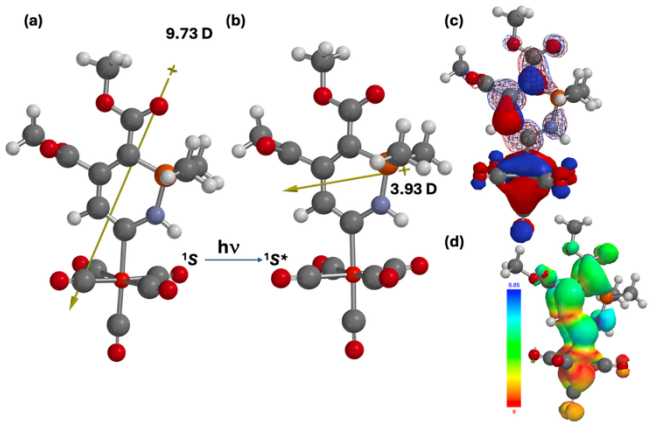

Figure S16. Molecular dipoles for (a) singlet ground state and (b) singlet excited state of **3**$_{Me}$. (c) HOMO (solid) and LUMO (mesh) for **3**$_{Me}$. (d) Spin density for the singlet excited state ($^1\pi\pi^*$) of **3**$_{Me}$ (0.001 e/au^3 isosurface).

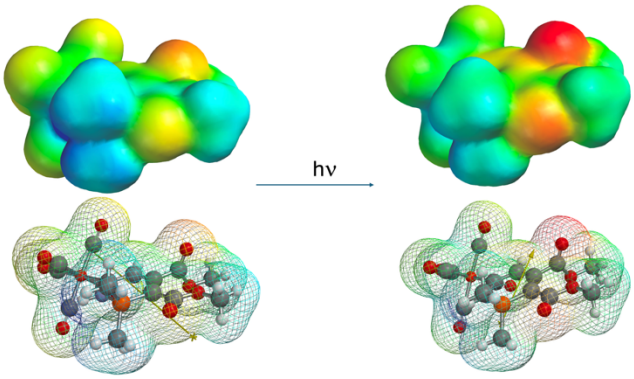

Figure S17. Electrostatic Potential surfaces for ground and excited states indicating change in dipole with metal to ligand charge transfer.

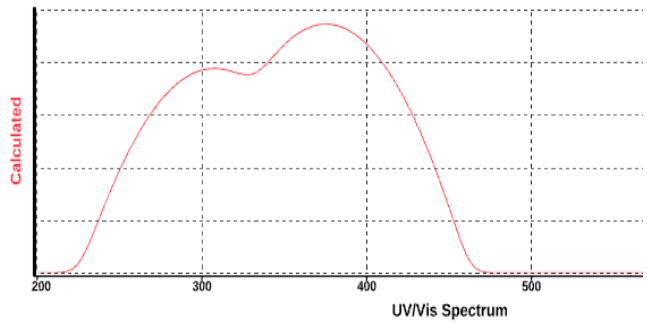

Figure S18. Calculated electronic spectrum for Cr(=CNHPMe$_2$CRCRCH)(CO)$_5$] (R = CO_2Me, TD-DFT: ωB97X-D/6-31G*/LANL2DZ(Cr))

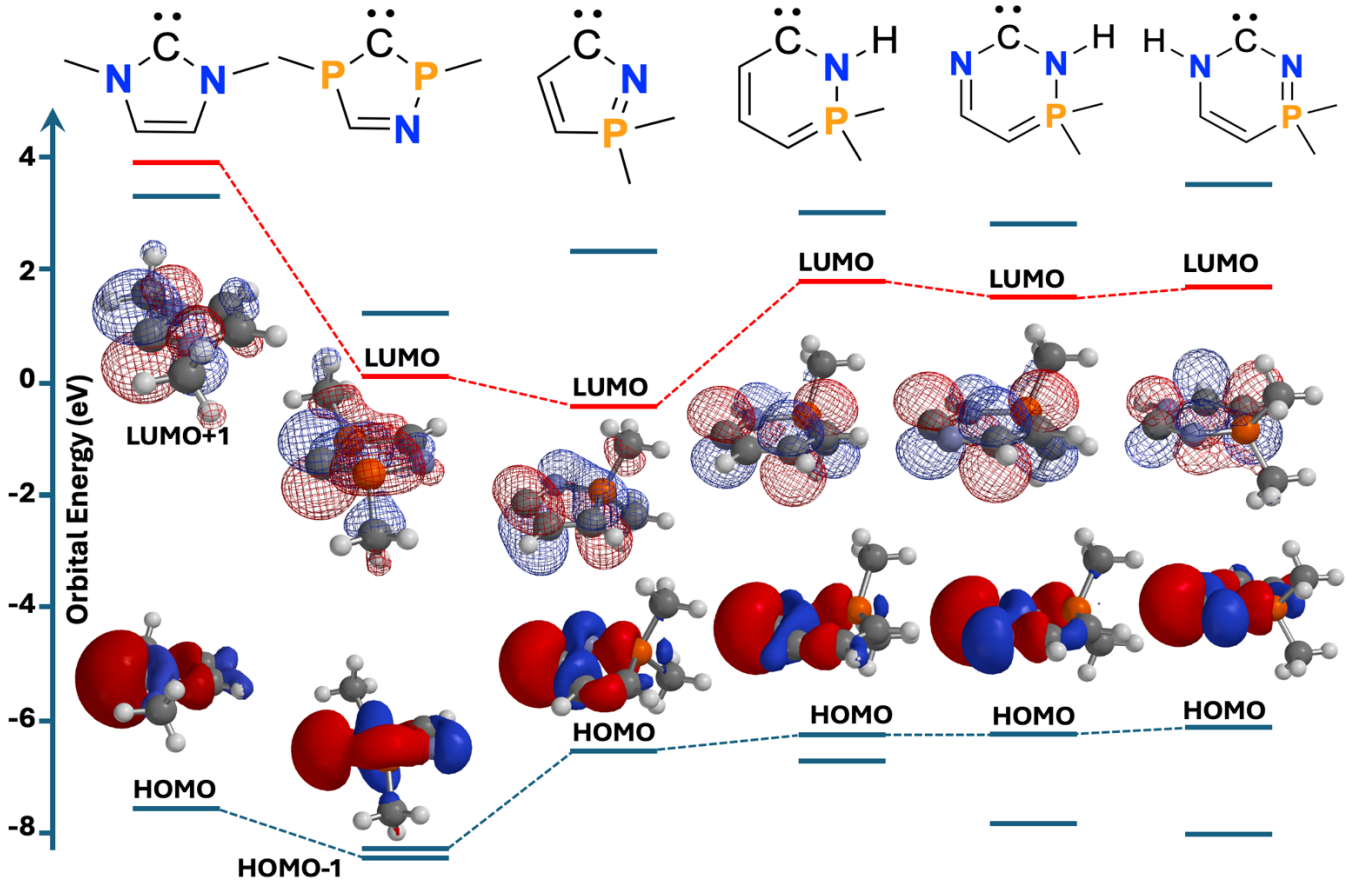

Figure S19. Frontier orbitals of interest for a range of free *N,P*-heterocyclic carbenes in the gas phase (DFT: ωB97X-D/6-31G*)

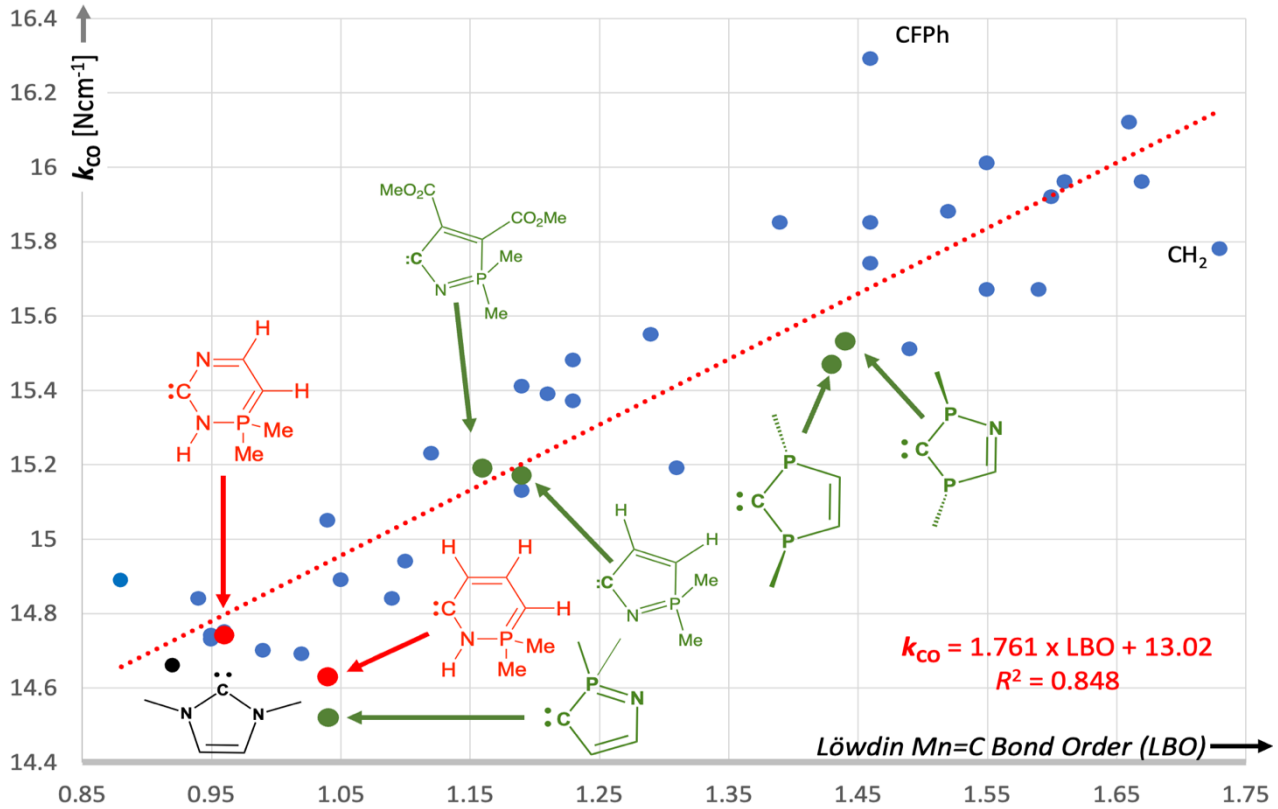

Figure S20. Mapping the distribution of Cotton-Kraihanzel force constats (k_{CO}) and Mn–C Löwdin bond orders (LBO) for a range of carbene ligands bound to the 'Mn(CO)$_2$(η^5-C$_5$H$_5$)' fragment (DFT: ωB97X-D/6-31G*/LANL2DZ(Mn)/gas phase). This is an update of Figure S11 from reference 3 to include models for known and new NPHC ligands.

6.1 Free :CNPMe$_2$CHCH

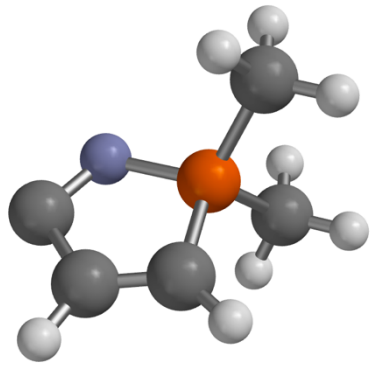

Figure S21. Optimised geometry for :CNPMe$_2$CHCH at the ωB97X-D/6-31Glevel of DFT. Selected distances (Å) and angles (°): C–N 1.333, N–P 1.672, C–C= 1.570, N-C-C 109.3.

Table S2. Cartesian Coordinates :CNPMe$_2$CHCH

Atom	x	y	z
C	-0.082274	-0.145456	2.497451
N	-0.150272	0.841930	1.604133
C	0.089060	-1.514332	1.747564
C	0.137732	-1.489185	0.405671
P	-0.027869	0.251698	0.045038
C	1.403357	0.915309	-0.850458
H	1.310272	2.002553	-0.918065
H	1.477307	0.494474	-1.857265
H	2.306964	0.674082	-0.285487
C	-1.492027	0.619448	-0.961903
H	-1.617879	1.703633	-1.025587
H	-2.368015	0.192033	-0.468083
H	-1.400024	0.204762	-1.969725
H	0.250631	-2.315350	-0.285464
H	0.163036	-2.435601	2.322181

Table S3. Thermodynamic data (298.15 K) :CNPMe$_2$CHCH ωB97X-D/6-31G*

Zero Point Energy :	292.87	kJ/mol (
Temperature Correction :	22.74	kJ/mol
Enthalpy Correction :	315.61	kJ/mol
Enthalpy :	-591.099837	au
Entropy :	356.83	J/mol•K
Gibbs Energy :	-591.140358	au
Cv :	130.39	J/mol•K

Lowest frequency vibrational mode (Uncorrected) 107 cm^{-1}.

6.2 Free :CNHPMe$_2$CHCHCH

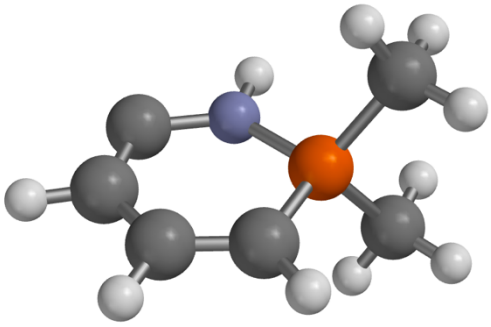

Figure S22. Optimised geometry for :CNHPMe$_2$CHCHCH at the ωB97X-D/6-31Glevel of DFT. Selected distances (Å) and angles (°): C–N 1.405, N–P 1.681, C–C= 1.400, N-C-C 114.1.

Table S4. Cartesian Coordinates :CNHPMe$_2$CHCHCH

Atom	x	y	z
C	-1.047543	1.749270	-1.370058
C	-2.121917	0.854809	-1.290949
H	-3.034928	1.141149	-1.806843
C	-2.135251	-0.367475	-0.606077
C	-1.093259	-0.934445	0.115164
N	0.103256	1.324631	-0.685257
H	0.881822	1.970312	-0.739277
P	0.394235	-0.076376	0.196697
C	1.833674	-0.967596	-0.490726
H	2.737727	-0.351194	-0.440461
H	1.621573	-1.215717	-1.533325
H	2.008542	-1.892654	0.068880
C	0.946183	0.338474	1.888287
H	1.873752	0.920586	1.866415
H	1.121985	-0.576971	2.463265
H	0.162622	0.922282	2.376697
H	-1.194552	-1.889520	0.618295
H	-3.057922	-0.949565	-0.630727

Table S5. Thermodynamic data (298.15 K) :CNHPMe$_2$CHCHCH ωB97X-D/6-31G*

Zero Point Energy :	367.30	kJ/mol
Temperature Correction :	25.12	kJ/mol
Enthalpy Correction :	392.43	kJ/mol
Enthalpy :	-630.389856	au
Entropy :	373.64	J/mol•K
Gibbs Energy :	-630.432286	au
Cv :	150.72	J/mol•K

Lowest frequency vibrational mode (Uncorrected) 43 cm^{-1}.

6.3 Free :CNHPMe$_2$CHCHN

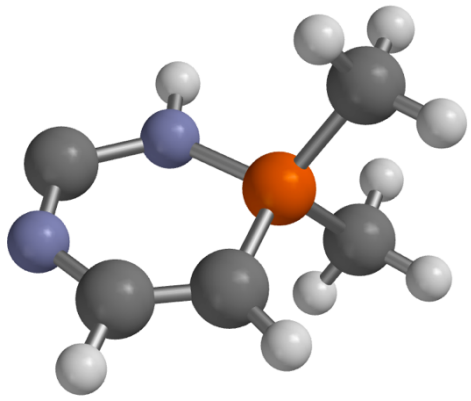

Figure S23. Optimised geometry for :CNHPMe$_2$CHCHN at the ωB97X-D/6-31Glevel of DFT. Selected distances (Å) and angles (°): C–N 1.334, N–P 1.664, C–NH= 1.455, N-C-C 115.9.

Table S6. Cartesian Coordinates :CNHPMe$_2$CHCHN

Atom	x	y	z
C	-1.213636	1.813398	-1.505762
N	-2.271255	1.004778	-1.415930
C	-2.274038	-0.161019	-0.736037
C	-1.280437	-0.784337	-0.013908
N	-0.011249	1.367255	-0.817603
H	0.750168	2.024906	-0.918501
P	0.255301	-0.000251	0.092238
C	1.635064	-1.001706	-0.555610
H	2.580597	-0.453800	-0.489834
H	1.427355	-1.243913	-1.600469
H	1.725521	-1.930936	0.016979
C	0.766393	0.389192	1.797807
H	1.738460	0.892794	1.812115
H	0.838804	-0.530361	2.388663
H	0.013206	1.041845	2.245230
H	-3.229204	-0.691388	-0.775373
H	-1.451053	-1.736457	0.475995

Table S7. Thermodynamic data (298.15 K) :CNHPMe$_2$CHCHN ωB97X-D/6-31G*

Zero Point Energy :	336.39	kJ/mol
Temperature Correction :	25.07	kJ/mol
Enthalpy Correction :	361.46	kJ/mol
Enthalpy :	-646.440964	au
Entropy :	374.34	J/mol•K
Gibbs Energy :	-646.483474	au
Cv :	148.01	J/mol•K

Lowest frequency vibrational mode (Uncorrected) 70 cm^{-1}.

6.4 Free :CNPMe$_2$CHCHNH

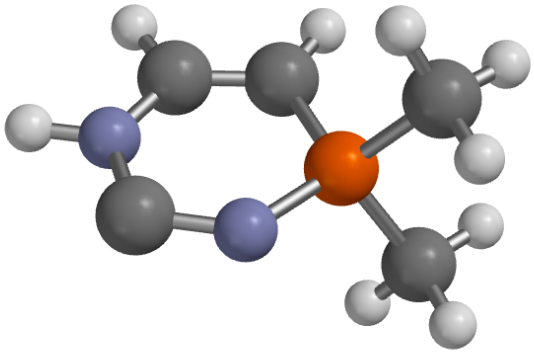

Figure S24. Optimised geometry for :CNPMe$_2$CHCHNH at the ωB97X-D/6-31Glevel of DFT. Selected distances (Å) and angles (°): C–N 1.338, N–P 1.630, C–NH= 1.427, N-C-C 114.5.

Table S8. Cartesian Coordinates :CNPMe$_2$CHCHNH

Atom	x	y	z
C	-0.838612	1.889200	-1.343140
C	-2.057051	-0.210577	-0.626088
C	-1.057349	-0.834644	0.049662
N	0.272279	1.458236	-0.733586
P	0.448539	0.074549	0.109342
C	1.829127	-0.906144	-0.550667
H	2.735047	-0.292849	-0.550833
H	1.598633	-1.195578	-1.578624
H	1.997621	-1.804148	0.052130
C	0.939827	0.429213	1.822268
H	1.841026	1.049716	1.814658
H	1.138347	-0.493715	2.376505
H	0.135829	0.982148	2.313716
H	-3.028938	-0.691509	-0.722984
H	-1.215627	-1.813422	0.489282
N	-1.956375	1.010315	-1.226910
H	-2.782324	1.349208	-1.694733

Table S9. Thermodynamic data (298.15 K) :CNHPMe$_2$CHCHN ωB97X-D/6-31G*

Zero Point Energy :	339.78	kJ/mol
Temperature Correction :	24.70	kJ/mol
Enthalpy Correction :	364.48	kJ/mol
Enthalpy :	-646.464281	au
Entropy :	371.17	J/mol•K
Gibbs Energy :	-646.506431	au
Cv :	145.67	J/mol•K

Lowest frequency vibrational mode (Uncorrected) 36 cm^{-1}.

6.5 Free :C(PMe)$_2$NCH

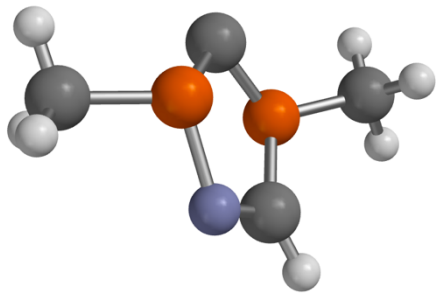

Figure S25. Optimised geometry for :C(PMe)$_2$NCH at the ωB97X-D/6-31Glevel of DFT. Selected distances (Å) and angles (°): C–P 1.712, 1.694, N–P 1.739, P–CH= 1.823, P-C-P 100.4.

Table S10. Cartesian Coordinates :C(PMe)$_2$NCH

Atom	x	y	z
C	0.058014	-0.265247	-1.246242
P	-0.752528	0.873198	-0.289167
P	0.793015	-1.221886	-0.031824
C	2.601239	-1.463160	-0.175184
H	2.938098	-2.135934	0.616576
H	3.131827	-0.511981	-0.095497
H	2.808241	-1.914329	-1.148007
N	0.515196	-0.515572	1.532968
C	-0.400706	0.384195	1.431120
H	-0.790040	0.893808	2.311737
C	-2.470544	1.385738	-0.661465
H	-2.514648	1.670534	-1.715166
H	-2.742288	2.249517	-0.049330
H	-3.174877	0.571121	-0.480518

Table S11. Thermodynamic data (298.15 K) :CNHPMe$_2$CHCHN ωB97X-D/6-31G*

Zero Point Energy :	257.58	kJ/mol
Temperature Correction :	23.09	kJ/mol
Enthalpy Correction :	280.68	kJ/mol
Enthalpy :	-893.766194	au
Entropy :	364.05	J/mol•K
Gibbs Energy :	-893.807535	au
Cv :	131.56	J/mol•K

Lowest frequency vibrational mode (Uncorrected) 48cm^{-1}.

6.6 Free :C(NMe)$_2$CHCH

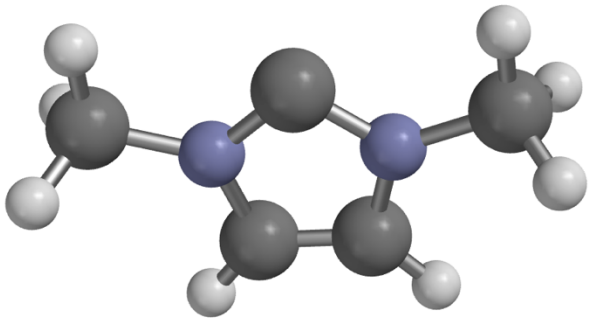

Figure S26. Optimised geometry for :C(NMe)$_2$CHCH at the ωB97X-D/6-31Glevel of DFT. Selected distances (Å) and angles (°): C–N 1.367, N-C-N 101.4.

Table S12. Cartesian Coordinates :C(NMe)$_2$CHCH

Atom	x	y	z
C	-0.000737	0.003182	-0.982787
N	0.176910	1.043269	-0.113760
N	-0.173834	-1.043077	-0.120327
C	0.116082	0.662072	1.217875
H	0.234588	1.357473	2.035429
C	-0.107311	-0.671040	1.213604
H	-0.224998	-1.371473	2.026931
C	0.401845	2.401999	-0.558118
H	0.391331	2.393178	-1.647928
H	1.371200	2.771342	-0.207464
H	-0.386477	3.068304	-0.192723
C	-0.405849	-2.397882	-0.572852
H	-1.374335	-2.767024	-0.219424
H	0.382583	-3.068568	-0.215853
H	-0.400999	-2.381756	-1.662603

Table S13. Thermodynamic data (298.15 K) :C(NMe)$_2$CHCH ωB97X-D/6-31G*

Zero Point Energy :	318.45	kJ/mol
Temperature Correction :	19.79	kJ/mol
Enthalpy Correction :	338.25	kJ/mol
Enthalpy :	-304.564366	au
Entropy :	333.74	J/mol•K
Gibbs Energy :	-304.602266	au (
Cv :	108.23	J/mol•K

Lowest frequency vibrational mode (Uncorrected) 112 cm^{-1}.

6.7 Free :CNHPMe$_2$CRCRCH (R = CO$_2$Me)

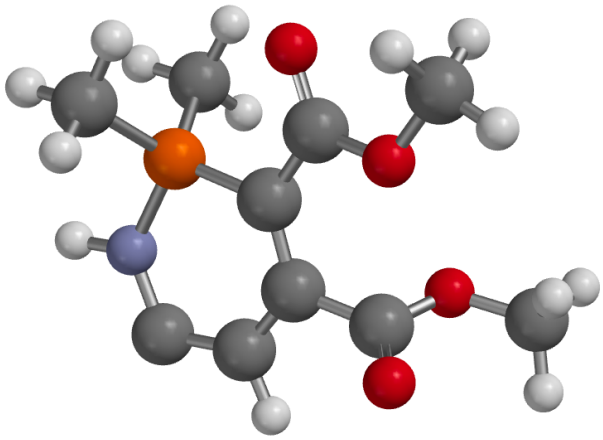

Figure S27. Optimised geometry for :CNHPMe$_2$CRCRCH (R = CO$_2$Me) at the ωB97X-D/6-31Glevel of DFT. Selected distances (Å) and angles (°): C–N 1.379, N–P 1.696, C–C= 1.419, N-C-C 114.9.

Table S14. Cartesian Coordinates :CNHPMe$_2$CHCHCH (R = CO$_2$Me)

Atom	x	y	z
P	-1.268065	-0.853560	1.391859
O	2.587291	0.491637	-0.742535
O	-0.001193	0.769906	-1.909093
O	1.969436	2.586539	-0.188521
O	-1.631801	-0.702905	-1.421095

Atom	x	y	z
C	1.843475	1.392595	-0.087332
C	0.884990	0.708352	0.854240
C	-0.682696	-0.011548	-1.059521
C	-0.238868	0.043000	0.316328
C	1.211310	0.782371	2.198139
H	2.107156	1.339495	2.456817
C	-3.023103	-0.389601	1.358460
C	-1.240561	-2.655009	1.154593
C	3.491512	1.044513	-1.695252
H	4.207862	1.709334	-1.206920
H	4.002065	0.193636	-2.145578
H	2.943672	1.607624	-2.455901
C	-0.429657	0.732273	-3.266504
H	-1.480074	1.021399	-3.349047
H	0.203233	1.447990	-3.790597
H	-0.302006	-0.269994	-3.682927
H	-0.211169	-3.005007	1.262333
H	-1.600563	-2.877859	0.147029
H	-1.876170	-3.152956	1.893816
H	-3.438225	-0.625103	0.376552
H	-3.571454	-0.936594	2.132383
H	-3.104442	0.683653	1.544905
N	-0.644002	-0.478447	2.924129
H	-1.177521	-0.846014	3.704667
C	0.469568	0.250282	3.284572

Table S15. Thermodynamic data (298.15 K) :CNHPMe$_2$CHCHCH (R = CO$_2$Me) ωB97X-D/6-31G*

Zero Point Energy :	584.67	kJ/mol
Temperature Correction :	43.32	kJ/mol
Enthalpy Correction :	628.00	kJ/mol
Enthalpy :	-1085.927711	au
Entropy :	512.31	J/mol•K
Gibbs Energy :	-1085.985888	au
Cv :	279.77	J/mol•K

Lowest frequency vibrational mode (Uncorrected) 10 cm^{-1}.

6.8 1,2λ^5-azaphosphinine Isomer of 6.6, HCNPMe$_2$CRCRCH

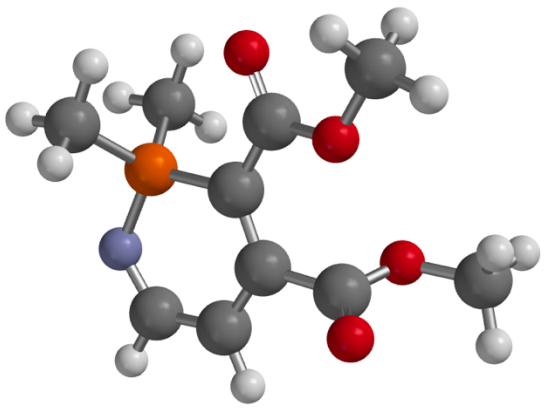

Figure S28. Optimised geometry for HCNPMe$_2$CRCRCH (R = CO$_2$Me) at the ωB97X-D/6-31Glevel of DFT. Selected distances (Å) and angles (°): C–N 1.319, N–P 1.644, C–C= 1.403, 1.393, 1.400.

Table S16. Cartesian Coordinates HCNPMe$_2$CHCHCH (R = CO$_2$Me)

Atom	x	y	z
P	-1.301342	-0.920559	1.440858
O	2.520279	0.488392	-0.786189
O	-0.055586	0.726383	-1.922557
O	1.899532	2.563950	-0.167271
N	-0.720706	-0.656879	2.956041
O	-1.650328	-0.793274	-1.474443
C	0.346415	0.097413	3.138038
C	1.772071	1.366792	-0.109852
C	0.811025	0.656664	0.810739
C	-0.723477	-0.091145	-1.091097
C	-0.288375	-0.039922	0.294760
C	1.123661	0.744206	2.165441
H	1.982804	1.324110	2.478457
C	-3.039749	-0.401079	1.385091
C	-1.343216	-2.706216	1.120200
C	3.429719	1.068310	-1.718086
H	4.127397	1.741001	-1.213880
H	3.964602	0.231733	-2.166254
H	2.881043	1.626884	-2.480718
C	-0.477726	0.701338	-3.282266
H	-1.531835	0.976335	-3.363444
H	0.146696	1.432976	-3.794209
H	-0.334745	-0.292966	-3.712406
H	0.648711	0.216151	4.180916
H	-0.324348	-3.098270	1.164325
H	-1.761913	-2.880748	0.126422
H	-1.952971	-3.200396	1.882147
H	-3.459742	-0.629845	0.403424
H	-3.594290	-0.926144	2.168242
H	-3.093606	0.674804	1.567571

Table S17. Thermodynamic data (298.15 K) HCNPMe$_2$CHCHCH (R = CO$_2$Me) ωB97X-D/6-31G*

Zero Point Energy :	587.40	kJ/mol
Temperature Correction :	42.80	kJ/mol
Enthalpy Correction :	630.19	kJ/mol
Enthalpy :	-1086.007627	au
Entropy :	508.77	J/mol•K
Gibbs Energy :	-1086.065403	au
Cv :	275.91	J/mol•K

Lowest frequency vibrational mode (Uncorrected) 27 cm^{-1}.

6.9 Dimer of 6.6, *E*-(CNHPMe$_2$CRCRCH)$_2$

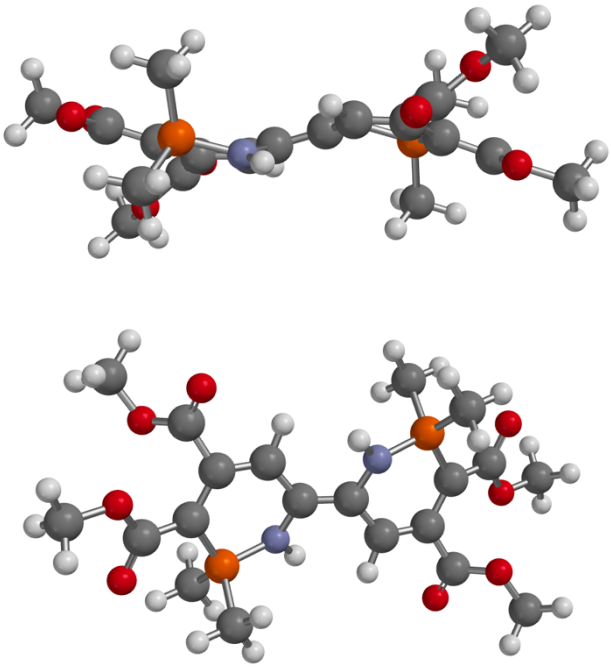

Figure S29. Optimised geometry (two views) for *E*-(CNHPMe$_2$CRCRCH)$_2$ (R = CO_2Me) at the ωB97X-D/6-31Glevel of DFT. Selected distances (Å) and angles (°): C=C 1.359, C–N 1.423, 1.424, N–P 1.668, 1.669, C–CH= 1.452, 1.452, N-C-C 115.9, 115.8.

Table S18. Cartesian Coordinates *E*-(CNHPMe$_2$CRCRCH)$_2$ (R = CO_2Me)

Atom	x	y	z
P	-0.537404	1.922885	2.588220
O	-1.117147	-1.849875	4.823252
O	0.834556	-0.042128	5.618875
O	0.407659	-3.002045	3.641023
N	-0.851440	1.262870	1.088328
H	-1.278913	1.840147	0.377356
O	0.163923	2.093185	5.320928
C	-0.248363	0.049188	0.650198
C	-0.214640	-1.983301	3.842297
C	-0.143190	-0.758135	2.980245
C	0.268623	0.941732	4.886282
C	-0.144404	0.559718	3.573271
C	-0.149843	-1.002074	1.646194
H	-0.154535	-2.034161	1.311080
C	0.787159	3.161473	2.459090
C	-2.028889	2.848617	3.038142
C	-1.194124	-2.949760	5.721402
H	-1.464620	-3.868074	5.193850
H	-1.964483	-2.686100	6.445878
H	-0.234616	-3.098666	6.224037
C	1.204592	0.318291	6.942255
H	1.934936	1.131424	6.935925
H	1.642188	-0.580335	7.378576
H	0.330909	0.633827	7.519437
P	0.491594	-1.934900	-2.591847
O	1.130501	1.869893	-4.763702
O	-0.754947	0.053137	-5.662138
O	-0.452234	2.991965	-3.628971
N	0.754680	-1.290860	-1.075657
H	1.174839	-1.869657	-0.361601
O	-0.093872	-2.082385	-5.349152
C	0.152512	-0.076159	-0.641945
C	0.189685	1.982994	-3.816861
C	0.102010	0.747617	-2.970782
C	-0.220187	-0.933970	-4.911595
C	0.134925	-0.562588	-3.578627
C	0.065591	0.978336	-1.634609
H	0.048256	2.007572	-1.291750
C	-0.840219	-3.169753	-2.523625
C	1.997101	-2.859902	-2.994857
C	1.228108	2.977258	-5.651192
H	1.471820	3.893167	-5.106710
H	2.024740	2.724795	-6.350830
H	0.284361	3.120246	-6.184271
C	-1.060022	-0.299052	-7.003419
H	-1.786754	-1.114628	-7.040366
H	-1.480110	0.600510	-7.454858
H	-0.160074	-0.606809	-7.543253
H	1.877764	-3.255277	-4.006422
H	2.848069	-2.176006	-2.967193
H	2.156131	-3.684329	-2.292476
H	-1.059015	-3.509521	-3.538350
H	-0.547265	-4.019529	-1.899286
H	-1.726230	-2.692506	-2.096979
H	-2.880339	2.164760	3.039507
H	-2.211284	3.672537	2.340908
H	-1.876024	3.245109	4.044864
H	0.468147	4.001189	1.833875
H	1.040360	3.516187	3.460544
H	1.659450	2.681857	2.007487

Table S19. Thermodynamic data (298.15 K) *E*-(CNHPMe$_2$CRCRCH)$_2$ (R = CO_2Me) ωB97X-D/6-31G*

Zero Point Energy :	1183.54	kJ/mol
Temperature Correction :	83.12	kJ/mol
Enthalpy Correction :	1266.66	kJ/mol
Enthalpy :	-2172.010635	au
Entropy :	779.80	J/mol•K
Gibbs Energy :	-2172.099189	au
Cv :	575.74	J/mol•K

Lowest frequency vibrational mode (Uncorrected) 24 cm^{-1}.

6.10 Thermodynamics of Carbene-azaphosphinine isomerism *vs* dimerization.

The formation of the dimer E-{CNHP^{t}Bu$_2$CRCRCH)$_2$ (R = CO_2Me) (**7**) from decomposition of [AuCl({CNHP^{t}Bu$_2$CRCRCH)] would appear to NOT proceed via the free carbene as the dimer as the kinetic barrier for 1,2-hydrogen shift to generate the more stable *pseudo*-aromatic azaphosphinine is likely to be extremely low. Similarly, for the simpler dimethyl derivative (:CNHPMe$_2$CRCRCH), the energy needed for the Wanzlick equilibrium to operate (ca 80 kcalmol-1), albeit exergonic (ca -19.8 kcalmol-1), allowing conversion of the dimer to the azaphosphinine to the would appear to be prohibitively high.

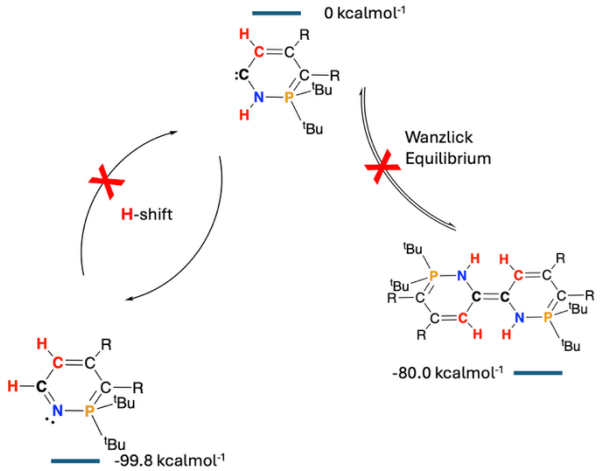

Scheme S2: Thermodynamic relationship of **6.6**, **6.7** and **6.8** (DFT: ωB97X-D/6-31G*/gas phase; 298.15 K)

6.11 [Cr{C(PMe)$_2$NCH)(CO)$_5$]

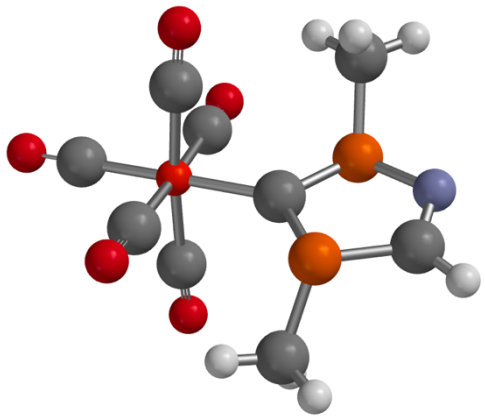

Figure S30. Optimised geometry for [Cr{C(PMe)$_2$NCH)(CO)$_5$] at the ωB97X-D/6-31G/LANL2Dζ level of DFT. Selected distances (Å) and angles (°): Cr-C 2.050, C–P 1.696, C–C= 1.764, 1.746, , P-C-P 104.2.

Table S20. Cartesian Coordinates [Cr{C(PMe)$_2$NCH)(CO)$_5$]

Atom	x	y	z
Cr	-0.059850	0.008897	-1.666676
C	-0.074265	-0.017749	-3.539473
O	-0.077017	-0.033324	-4.690807
C	1.484574	1.103013	-1.602695
O	2.422919	1.760098	-1.508311
C	1.021533	-1.532244	-1.686544
O	1.684815	-2.473404	-1.714955
C	-1.161285	1.542650	-1.719107
O	-1.846157	2.464807	-1.784541
C	-1.602521	-1.085751	-1.545355
O	-2.536529	-1.744993	-1.430431
C	-0.027610	0.045434	0.383160
P	-1.020561	1.046737	1.442255
P	0.997377	-0.848326	1.478326
N	-0.603650	0.572056	3.052319
C	0.467581	-0.129275	3.071980
H	0.923154	-0.418609	4.019925
C	-2.803751	0.648297	1.263038
H	-3.146316	0.987083	0.283167
H	-3.352634	1.192835	2.034753
H	-2.986335	-0.423007	1.368030
C	2.802721	-0.678455	1.169273
H	3.345574	-1.152133	1.991376
H	3.096168	0.369431	1.085886
H	3.052066	-1.204071	0.245407

Table S21. Thermodynamic data (298.15 K) [Cr{C(PMe)$_2$NCH)(CO)$_5$] (ωB97X-D/6-31G/LANL2Dζ)

Zero Point Energy :	368.65	kJ/mol
Temperature Correction :	48.77	kJ/mol
Enthalpy Correction :	417.42	kJ/mol
Enthalpy :	-2504.682299	au
Entropy :	550.94	J/mol•K
Gibbs Energy :	-2504.744863	au
Cv :	317.69	J/mol•K

Lowest frequency vibrational mode (Uncorrected) 32 cm^{-1}.

6.12 [Cr(CNPMe$_2$CHCH)(CO)$_5$]

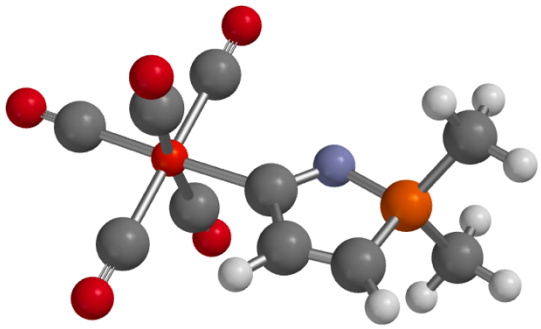

Figure S31. Optimised geometry for [Cr(CNPMe$_2$CHCH)(CO)$_5$] at the ωB97X-D/6-31G/LANL2Dζ level of DFT. Selected distances (Å) and angles (°): Cr-C 2.033, C–N 1.333, N–P 1.647, C–C= 1.535, N-C-C 111.7.

Table S22. Cartesian Coordinates [Cr{C(PMe)$_2$NCH)(CO)$_5$]

Atom	x	y	z
Cr	-0.106192	0.003247	2.420394
C	-0.193053	0.248990	4.277000
O	-0.247490	0.404207	5.418438
C	-0.628389	-1.780925	2.646464
O	-0.936626	-2.884076	2.793332
C	1.699606	-0.523162	2.439671
O	2.802462	-0.856529	2.394330
C	-1.901721	0.504365	2.127464
O	-2.987094	0.794549	1.877236
C	0.416494	1.814733	2.187940
O	0.730925	2.911399	2.057437
C	0.002987	-0.202687	0.401090
N	-0.061541	0.797423	-0.478528
C	0.184074	-1.558425	-0.294735
C	0.227166	-1.531088	-1.634370
P	0.059128	0.208305	-2.011967
C	1.498084	0.873423	-2.884182
H	1.404764	1.960823	-2.948709
H	1.575997	0.453184	-3.890741
H	2.396529	0.628849	-2.312338
C	-1.409244	0.581685	-2.998323
H	-1.526627	1.666541	-3.066025

Atom	x	y	z
H	-2.283695	0.162844	-2.494742
H	-1.325243	0.160480	-4.003985
H	0.344370	-2.367812	-2.310590
H	0.264328	-2.470342	0.288438

Table S23. Thermodynamic data (298.15 K) [Cr{C(PMe)$_2$NCH)(CO)$_5$] (ωB97X-D/6-31G/LANL2Dζ)

Zero Point Energy :	408.56	kJ/mol
Temperature Correction :	47.72	kJ/mol
Enthalpy Correction :	456.28	kJ/mol
Enthalpy :	-2202.041566	au
Entropy :	542.09	J/mol•K
Gibbs Energy :	-2202.103125	au
Cv :	310.75	J/mol•K

Lowest frequency vibrational mode (Uncorrected) 10 cm^{-1}.

6.13 [Cr(CNHPMe$_2$CHCHCH)(CO)$_5$]

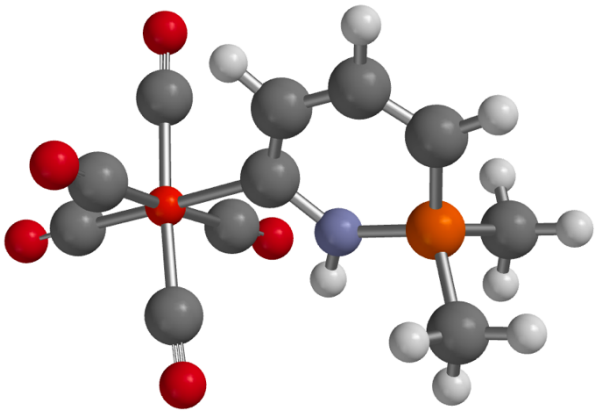

Figure S32. Optimised geometry for [Cr(CNHPMe$_2$CHCHCH)(CO)$_5$] at the ωB97X-D/6-31G/LANL2Dζ level of DFT. Selected distances (Å) and angles (°): Cr-C 2.110, C–N 1.405, N–P 1.668, C–C= 1.387, N-C-C 115.7.

Table S24. Cartesian Coordinates [Cr(CNHPMe$_2$CHCHCH)(CO)$_5$]

Atom	x	y	z
Cr	-0.589708	2.092684	-1.406970
C	1.079959	1.584847	-2.083747
O	2.118804	1.239692	-2.454456
C	-0.552164	3.710650	-2.325658
O	-0.520713	4.715589	-2.894132
C	0.229066	2.856002	0.093321
O	0.753494	3.284353	1.029814
C	-2.281288	2.468009	-0.651109
O	-3.311991	2.667981	-0.180979
C	-1.429366	1.218513	-2.857375
O	-1.944109	0.667161	-3.726037
C	-0.670379	0.247971	-0.385617
C	-1.749126	-0.621204	-0.328621
H	-2.653344	-0.337919	-0.853607
C	-1.767092	-1.845564	0.367840
C	-0.741450	-2.409970	1.094328
N	0.478506	-0.160124	0.313275
H	1.255766	0.487208	0.264735
P	0.757526	-1.558547	1.179460
C	2.178752	-2.437741	0.462158
H	3.077119	-1.812594	0.494191
H	1.948051	-2.685122	-0.576695
H	2.370927	-3.360387	1.019437
C	1.297191	-1.124744	2.860336
H	2.213326	-0.525950	2.829439
H	1.491738	-2.033887	3.438507
H	0.505267	-0.549985	3.345896
H	-0.849500	-3.362530	1.599999
H	-2.695259	-2.414392	0.332264

Table S25. Thermodynamic data (298.15 K) [Cr(CNHPMe$_2$CHCHCH)(CO)$_5$] (ωB97X-D/6-31G/LANL2Dζ)

Zero Point Energy :	481.88	kJ/mol
Temperature Correction :	50.23	kJ/mol
Enthalpy Correction :	532.11	kJ/mol
Enthalpy :	-2241.326249	au
Entropy :	557.86	J/mol•K
Gibbs Energy :	-2241.389599	au
Cv :	333.03	J/mol•K

Lowest frequency vibrational mode (Uncorrected) 16 cm^{-1}.

6.14 [Cr(CNHPMe$_2$CHCHN)(CO)$_5$]

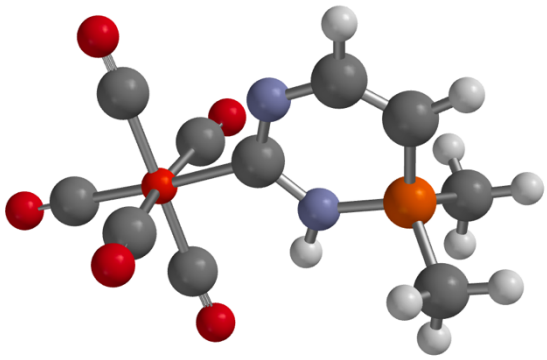

Figure S33. Optimised geometry for [Cr(CNHPMe$_2$CHCHN)(CO)$_5$] at the ωB97X-D/6-31G/LANL2Dζ level of DFT. Selected distances (Å) and angles (°): Cr-C 2.083, C–NH 1.419, C-N 1.326, N–P 1.663, HN–C 1.351, N-C-C 118.4.

Table S26. Cartesian Coordinates [Cr(CNHPMe$_2$CHCHN)(CO)$_5$]

Atom	x	y	z
Cr	-0.675910	2.059542	-1.432198
C	1.145113	2.284619	-1.180852
O	2.286283	2.377677	-0.985710
C	-0.757410	3.673803	-2.367613
O	-0.798051	4.673017	-2.943813
C	-0.987906	2.843934	0.246871
O	-1.145539	3.269244	1.306921
C	-2.563354	1.837932	-1.696942
O	-3.691821	1.754470	-1.876724
C	-0.325478	1.019035	-2.963609
O	-0.091066	0.338261	-3.862406
C	-0.717413	0.244040	-0.412842
N	-1.799011	-0.519962	-0.346227
C	-1.828872	-1.697031	0.315266
C	-0.849698	-2.340921	1.031813
N	0.461305	-0.194757	0.244176
H	1.252575	0.428932	0.140551
P	0.692192	-1.571118	1.149108

Atom	x	y	z
C	2.077443	-2.529188	0.474080
H	3.002358	-1.944692	0.510146
H	1.851733	-2.787974	-0.563018
H	2.217179	-3.446818	1.054348
C	1.195103	-1.135286	2.837898
H	2.147082	-0.594906	2.831181
H	1.308689	-2.042685	3.439896
H	0.422149	-0.503013	3.281127
H	-2.794018	-2.201353	0.256927
H	-1.033657	-3.294800	1.511643

Table S27. Thermodynamic data (298.15 K) [Cr(CNHPMe$_2$CHCHN)(CO)$_5$] (ωB97X-D/6-31G/LANL2Dζ)

Zero Point Energy :	451.87	kJ/mol
Temperature Correction :	49.90	kJ/mol
Enthalpy Correction :	501.77	kJ/mol
Enthalpy :	-2257.377471	au
Entropy :	556.51	J/mol•K
Gibbs Energy :	-2257.440669	au
Cv :	328.64	J/mol•K

Lowest frequency vibrational mode (Uncorrected) 12 cm^{-1}.

6.15 [Cr(CNHPMe$_2$CRCRCH)(CO)$_5$] (R = CO$_2$Me)

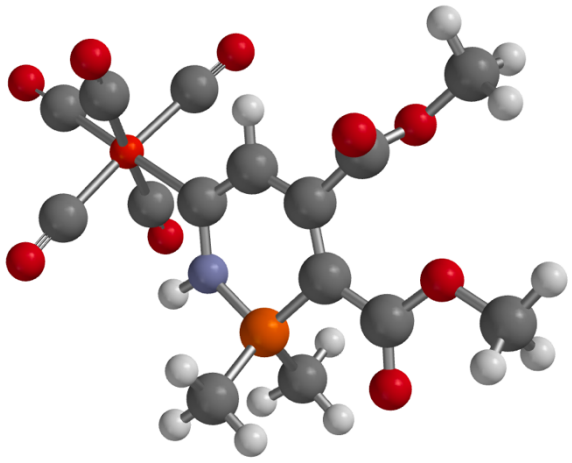

Figure S34. Optimised geometry for [Cr(CNHPMe$_2$CRCRCH)(CO)$_5$] (R = CO$_2$Me) at the ωB97X-D/6-31G/LANL2Dζ level of DFT. Selected distances (Å) and angles (°): Cr-C 2.090, C–N 1.387, N–P 1.683, C–C= 1.405, N-C-C 115.9.

Table S28. Cartesian Coordinates [Cr(CNHPMe$_2$CRCRCH)(CO)$_5$] (R = CO$_2$Me)

Atom	x	y	z
Cr	0.372723	3.271588	-1.892090
C	2.055079	2.795915	-2.569815
O	3.098449	2.469456	-2.940772
C	0.392223	4.902358	-2.800349
O	0.415281	5.910920	-3.359647
C	1.176490	4.044654	-0.386366
O	1.688423	4.478794	0.553315
C	-1.330131	3.624957	-1.145679
O	-2.366757	3.813100	-0.685244
C	-0.453215	2.410947	-3.361531
O	-0.961049	1.874699	-4.242056
C	0.322518	1.438162	-0.890390
C	-0.772391	0.557827	-0.864281
H	-1.650584	0.844580	-1.429936
C	-0.842308	-0.634903	-0.150988
C	0.177430	-1.185875	0.632922
N	1.438452	1.038854	-0.170162
H	2.216118	1.688322	-0.196924
P	1.716406	-0.373098	0.701718
C	3.092925	-1.263943	-0.068355
H	3.998265	-0.648433	-0.059102
H	2.824371	-1.497707	-1.101334
H	3.267471	-2.188621	0.486379
C	2.277478	0.113529	2.353402
H	3.174646	0.735778	2.273889
H	2.500908	-0.782953	2.935331
H	1.483390	0.684054	2.840465
C	-2.142111	-1.393415	-0.289359
C	0.169990	-2.413990	1.406874
O	-0.996599	-3.060405	1.437991
O	-3.022574	-0.992360	0.627410
O	1.172980	-2.812669	1.990560
O	-2.351685	-2.209338	-1.149777
C	-4.281754	-1.667645	0.590652
H	-4.870864	-1.230720	1.395755
H	-4.136996	-2.738556	0.753140
H	-4.771655	-1.514053	-0.373686
C	-1.008022	-4.293314	2.157287
H	-0.783150	-4.121838	3.212608
H	-0.274251	-4.986415	1.740235
H	-2.015921	-4.688243	2.037909

Table S29. Thermodynamic data (298.15 K) [Cr(CNHPMe$_2$CRCRCH)(CO)$_5$] (R = CO$_2$Me) (ωB97X-D/6-31G/LANL2Dζ)

Zero Point Energy :	698.69	kJ/mol
Temperature Correction :	68.47	kJ/mol
Enthalpy Correction :	767.16	kJ/mol
Enthalpy :	-2696.859267	au
Entropy :	683.99	J/mol•K
Gibbs Energy :	-2696.936941	au
Cv :	462.55	J/mol•K

Lowest frequency vibrational mode (Uncorrected) 13 cm^{-1}.

6.16 [Cr(CNPMe$_2$CRCRNH)(CO)$_5$] (R = CO$_2$Me)

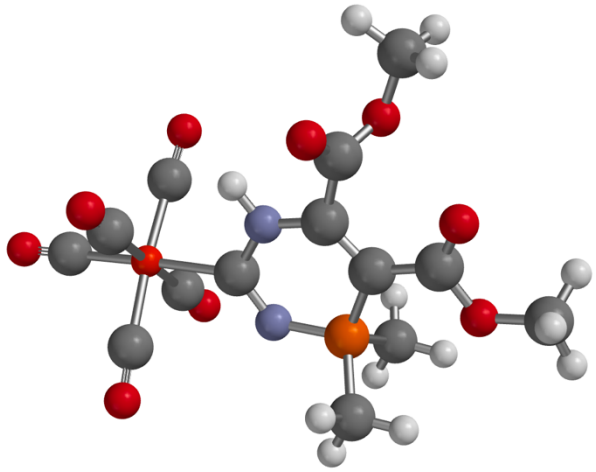

Figure S35. Optimised geometry for [Cr(CNPMe$_2$CRCRNH)(CO)$_5$] (R = CO$_2$Me) at the ωB97X-D/6-31G/LANL2Dζ level of DFT. Selected distances (Å) and angles (°): Cr-C 2.073, C–NH 1.420, C-N 1.317, N–P 1.627, HN–C 1.353, N-C-C 116.8.

Table S30. Cartesian Coordinates [Cr(CNPMe$_2$CRCRNH)(CO)$_5$] (R = CO$_2$Me)

Atom	x	y	z
Cr	3.206842	-0.194694	-2.060321
C	2.704264	-1.872770	-2.776283
O	2.363272	-2.892292	-3.183724
C	4.788111	-0.149871	-3.051281
O	5.765997	-0.120829	-3.663165
C	4.072955	-1.083265	-0.631640
O	4.574413	-1.624879	0.249720
C	3.581316	1.456127	-1.253823
O	3.774393	2.475673	-0.748467
C	2.287746	0.666253	-3.453483
O	1.724713	1.206130	-4.303236
C	1.474925	-0.321903	-0.928469
C	-0.558822	0.926030	-0.184557
C	-1.135524	-0.058156	0.573859
N	1.126394	-1.385606	-0.235015
P	-0.212384	-1.568494	0.670716
C	-1.167266	-2.975842	0.059534
H	-0.525907	-3.861717	0.058381
H	-1.485621	-2.769269	-0.965068
H	-2.041174	-3.145506	0.692295
C	0.262857	-1.960149	2.370241
H	0.913110	-2.839538	2.357169
H	-0.623739	-2.154704	2.977602
H	0.818062	-1.116126	2.786345
C	-1.197220	2.291775	-0.361884
C	-2.454371	0.143374	1.187641
O	-2.776004	-0.902740	1.979147
O	-1.131297	2.992190	0.759791
O	-3.190151	1.088187	1.012891
O	-1.605543	2.673961	-1.427629
C	-1.791185	4.263725	0.720220
H	-1.620254	4.708924	1.698685
H	-2.858038	4.111180	0.544557
H	-1.369880	4.888896	-0.069529
C	-4.059780	-0.825858	2.604066
H	-4.845433	-0.740665	1.850404
H	-4.106380	0.038313	3.270318
H	-4.166263	-1.750949	3.169261
N	0.603623	0.797593	-0.863986
H	0.879243	1.587491	-1.431287

Table S31. Thermodynamic data (298.15 K) [Cr(CNPMe$_2$CRCRNH)(CO)$_5$] (R = CO$_2$Me) (ωB97X-D/6-31G/LANL2Dζ)

Zero Point Energy :	670.25	kJ/mol
Temperature Correction :	68.01	kJ/mol
Enthalpy Correction :	738.27	kJ/mol
Enthalpy :	-2712.923843	au
Entropy :	680.97	J/mol•K
Gibbs Energy :	-2713.001174	au
Cv :	458.30	J/mol•K

Lowest frequency vibrational mode (Uncorrected) 9 cm^{-1}.

6.17 [Cr(CNHPMe$_2$CRCRN)(CO)$_5$] (R = CO$_2$Me)

For completeness, the alternative isomer which varies in the site of N-protonation *viz.* [Cr(CNHPMe$_2$CRCRN)(CO)$_5$] (R = CO$_2$Me) was also considered and found to lie some 11.6 kcalmol^{-1} higher in energy.

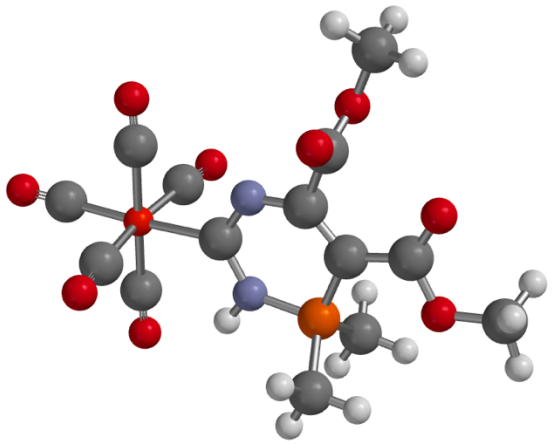

Figure S36. Optimised geometry for [Cr(CNHPMe$_2$CRCRN)(CO)$_5$] (R = CO$_2$Me) at the ωB97X-D/6-31G/LANL2Dζ level of DFT. Selected distances (Å) and angles (°): Cr-C 2.058, C–NH 1.402, C-N 1.342, N–P 1.673, N-C-C 118.1.

Table S32. Cartesian Coordinates [Cr(CNHPMe$_2$CRCRN)(CO)$_5$] (R = CO$_2$Me)

Atom	x	y	z
Cr	-3.217439	0.029200	-1.910271
C	-3.670641	1.745284	-1.379988
O	-3.896357	2.826403	-1.022636
C	-4.836529	-0.129856	-2.839956

Atom	x	y	z
O	-5.835054	-0.217249	-3.409249
C	-3.922081	-0.646618	-0.297174
O	-4.308810	-1.032120	0.716380
C	-2.755245	-1.755998	-2.457067
O	-2.531682	-2.822053	-2.808896
C	-2.291847	0.736129	-3.392558
O	-1.685663	1.196184	-4.256340
C	-1.410686	0.087908	-0.926693
C	0.561404	-0.998678	-0.220537
C	1.175488	-0.003105	0.537275
P	0.395644	1.549280	0.599544
C	1.312447	2.906562	-0.171691
H	0.706843	3.818352	-0.175852
H	1.551557	2.623984	-1.199779
H	2.236247	3.082589	0.384187
C	-0.085048	2.115124	2.251028
H	-0.695892	3.020232	2.174414
H	0.809442	2.328321	2.840287
H	-0.665218	1.326516	2.736123
C	1.288350	-2.318403	-0.412892
C	2.433324	-0.218448	1.248822
O	2.834121	0.934240	1.854849
O	0.904258	-3.207414	0.494676
O	3.058804	-1.248262	1.329819
O	2.051776	-2.509102	-1.322661
C	1.550363	-4.479702	0.400968
H	1.122116	-5.082787	1.200154
H	2.626894	-4.358713	0.541604
H	1.356159	-4.934693	-0.572585
C	4.045478	0.838131	2.607609
H	4.875187	0.549458	1.959191
H	3.940087	0.098859	3.404855
H	4.212113	1.830218	3.026453
N	-0.597449	-0.978850	-0.877731
N	-0.994842	1.264052	-0.286429
H	-1.647621	2.035021	-0.367252

Table S33. Thermodynamic data (298.15 K) [Cr(CNHPMe$_2$CRCRN)(CO)$_5$] (R = CO_2Me) (ωB97X-D/6-31G/LANL2Dζ)

Zero Point Energy :	667.75	kJ/mol
Temperature Correction :	68.23	kJ/mol
Enthalpy Correction :	735.97	kJ/mol
Enthalpy :	-2712.905183	au
Entropy :	682.85	J/mol•K
Gibbs Energy :	-2712.982726	au
Cv :	459.29	J/mol•K

Lowest frequency vibrational mode (Uncorrected) 8 cm^{-1}.

6.18 [Mn(CNHPMe$_2$CHCHCH)(CO)$_2$(η^5-C$_5$H$_5$)]

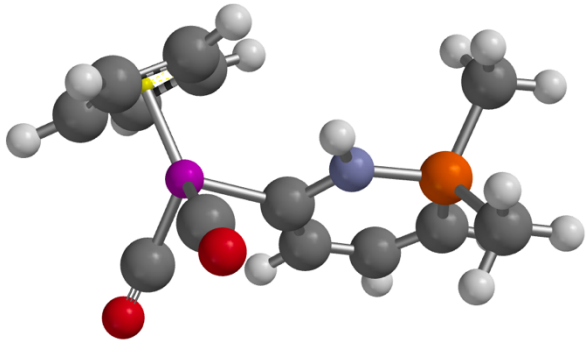

Figure S37. Optimised geometry for [Mn(CNHPMe$_2$CHCHCH)(CO)$_2$(η^5-C$_5$H$_5$)] at the ωB97X-D/6-31G/LANL2Dζ level of DFT. Selected distances (Å) and angles (°): Mn-C 1.957, C–N 1.410, N–P 1.664, C–C= 1.394, N-C-C 115.3.

Table S34. Cartesian Coordinates [Mn(CNHPMe$_2$CHCHCH)(CO)$_2$(η^5-C$_5$H$_5$)]

Atom	x	y	z
C	-1.628031	-1.061336	0.788316
H	-2.247944	-0.791870	1.634398
C	-2.066582	-2.114597	-0.027385
H	-3.021964	-2.568947	0.233083
C	-1.430413	-2.646287	-1.135308
H	-1.851989	-3.465919	-1.705992
C	-0.464516	-0.321295	0.583013
Mn	0.181085	1.254565	1.547404
H	2.110798	3.386528	1.664268
C	1.129794	3.137482	1.282915
C	-0.095753	3.327688	1.958729
H	1.575188	2.367636	-0.779608
H	-0.217738	3.743311	2.949418
C	-1.148704	2.878987	1.100715
H	-2.206036	2.893851	1.325068
C	-0.557544	2.423523	-0.099974
H	-1.092732	2.003892	-0.941793
C	0.850355	2.572939	-0.002569
C	-0.624275	0.729364	3.030634
O	-1.187032	0.419726	3.997835
C	1.690921	0.436453	1.937442
O	2.715438	-0.079729	2.137854
P	0.104852	-1.998069	-1.566266
C	0.237447	-1.406562	-3.281957
H	1.223557	-0.967511	-3.465197
H	-0.534557	-0.653491	-3.455223
H	0.091880	-2.238783	-3.978336
C	1.503710	-3.151759	-1.395755
H	1.540083	-3.500469	-0.360908
H	2.449114	-2.658393	-1.643860
H	1.365534	-4.009672	-2.061998
N	0.310127	-0.713318	-0.528525
H	1.154452	-0.162691	-0.634658

Table S35. Thermodynamic data (298.15 K) [Mn(CNHPMe$_2$CHCHCH)(CO)$_2$(η^5-C$_5$H$_5$)] (ωB97X-D/6-31G/LANL2Dζ)

Zero Point Energy :	632.86	kJ/mol
Temperature Correction :	45.32	kJ/mol
Enthalpy Correction :	678.18	kJ/mol
Enthalpy :	-2201.346004	au
Entropy :	521.86	J/mol•K
Gibbs Energy :	-2201.405266	au
Cv :	312.03	J/mol•K

Lowest frequency vibrational mode (Uncorrected) 8 cm^{-1}.

ν_{CO} = 1936, 1885 cm^{-1} (λ = 0.9297). k_{CK}(CO) = 14.74 Ncm^{-1}.

6.19 [Mn(CNHPMe$_2$CHCHN)(CO)$_2$(η^5-C$_5$H$_5$)]

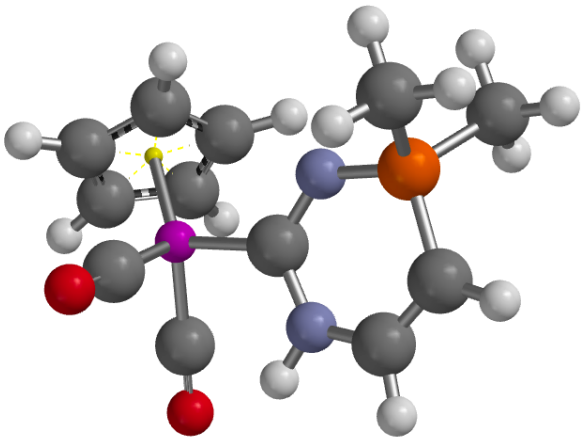

Figure S38. Optimised geometry for [Mn(CNHPMe$_2$CHCHN)(CO)$_2$(η^5-C$_5$H$_5$)] at the ωB97X-D/6-31G/LANL2Dζ level of DFT. Selected distances (Å) and angles (°): Mn-C 1.933, C–N 1.336, C–NH 1.413, N–P 1.613, C–C= 1.356, N-C-N 116.0.

Table S36. Cartesian Coordinates [Mn(CNHPMe$_2$CHCHCH)(CO)$_2$(η^5-C$_5$H$_5$)]

Atom	x	y	z
N	-1.187891	-1.352746	0.942551
H	-1.640459	-1.157932	1.822648
C	-1.452407	-2.561375	0.373641
H	-2.119200	-3.188077	0.960586
C	-0.969259	-3.003825	-0.813621
H	-1.229967	-3.987989	-1.183864
N	0.204936	-0.528919	-0.735375
C	-0.366009	-0.312889	0.452685
Mn	-0.056845	1.274823	1.511667
H	2.266362	2.836255	2.213609
C	1.415523	2.827629	1.545183
C	0.147054	3.391492	1.813646
H	2.188024	1.706618	-0.238945
H	-0.141896	3.915190	2.714300
C	-0.681277	3.154797	0.673598
H	-1.710798	3.467542	0.564605
C	0.084832	2.449185	-0.281630
H	-0.265339	2.079989	-1.234944
C	1.383206	2.236560	0.249316
C	-1.500206	1.089322	2.496252
O	-2.456304	0.983310	3.154983
C	0.925582	0.277834	2.580418
O	1.606871	-0.372153	3.261101
P	0.081737	-1.860137	-1.638065
C	-0.556081	-1.454453	-3.287294
H	0.094051	-0.707079	-3.751274
H	-1.561785	-1.039349	-3.186117
H	-0.592990	-2.346586	-3.920278
C	1.720266	-2.576419	-1.942772
H	2.167074	-2.855680	-0.985749
H	2.356496	-1.830565	-2.428006
H	1.645783	-3.461150	-2.582965

Table S39. Thermodynamic data (298.15 K) [Mn(CNHPMe$_2$CHCHCH)(CO)$_2$(η^5-C$_5$H$_5$)] (ωB97X-D/6-31G/LANL2Dζ)

Zero Point Energy :	606.94	kJ/mol
Temperature Correction :	44.59	kJ/mol
Enthalpy Correction :	651.53	kJ/mol
Enthalpy :	-2217.422087	au
Entropy :	518.42	J/mol•K
Gibbs Energy :	-2217.480959	au
Cv :	305.40	J/mol•K

Lowest frequency vibrational mode (Uncorrected) 16 cm^{-1}.

ν_{CO} = 1932, 1874 cm^{-1} (λ = 0.9297). k_{CK}(CO) = 14.63 Ncm^{-1}.

6.20 [AuCl(CNHPMe$_2$CRCRCH)] (R = CO$_2$Me)

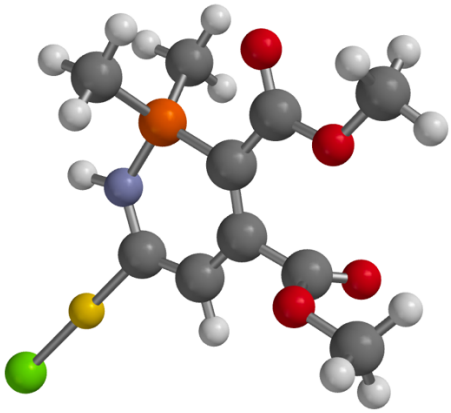

Figure S39. Optimised geometry for [AuCl(CNHPMe$_2$CRCRCH)] (R = CO$_2$Me) at the ωB97X-D/6-31G/LANL2Dζ level of DFT. Selected distances (Å) and angles (°): Au-C 2.004, Au–Cl 2.335, C–N 1.384, N–P 1.684, C–C= 1.393, N-C-C 118.3.

Table S40. Cartesian Coordinates [AuCl(CNHPMe$_2$CRCRCH)] (R = CO$_2$Me)

Atom	x	y	z
C	0.423650	2.388959	-1.449365
C	-0.678679	1.538265	-1.429402
H	-1.546665	1.841567	-2.000679
C	-0.746177	0.342172	-0.708026
C	0.276707	-0.199417	0.067346

Atom	x	y	z
N	1.552157	2.018242	-0.738160
H	2.316072	2.681732	-0.787670
P	1.824935	0.610091	0.143461
C	3.198144	-0.291870	-0.618168
H	4.105065	0.321014	-0.608507
H	2.931583	-0.530434	-1.650648
H	3.370066	-1.213649	-0.057874
C	2.373510	1.095839	1.798819
H	3.272487	1.716269	1.725765
H	2.592164	0.198558	2.381003
H	1.577017	1.666835	2.281476
C	-2.049251	-0.413058	-0.844083
C	0.272491	-1.435373	0.838061
O	-0.883719	-2.094762	0.847099
O	-2.910476	-0.046160	0.102100
O	1.273744	-1.821076	1.430423
O	-2.272790	-1.188114	-1.737119
C	-4.180133	-0.703034	0.051718
H	-4.757271	-0.285450	0.875145
H	-4.049350	-1.780469	0.177682
H	-4.673686	-0.509149	-0.903015
C	-0.897299	-3.327770	1.569709
H	-0.690635	-3.150956	2.627436
H	-0.151884	-4.015131	1.164495
H	-1.900447	-3.729586	1.435723
Au	0.482028	4.137175	-2.426576
Cl	0.546639	6.178741	-3.558167

Table S41. Thermodynamic data (298.15 K) [AuCl(CNHPMe$_2$CRCRCH)] (R = CO_2Me) (ωB97X-D/6-31G/LANL2Dζ)

Zero Point Energy :	631.74	kJ/mol
Temperature Correction :	48.42	kJ/mol
Enthalpy Correction :	680.16	kJ/mol
Enthalpy :	-1681.681447	au
Entropy :	565.99	J/mol•K
Gibbs Energy :	-1681.745721	au
Cv :	310.53	J/mol•K

Lowest frequency vibrational mode (Uncorrected) 16 cm^{-1}.

6.21 [Au(C_6F_5)(CNHPMe$_2$CRCRCH)] (R = CO_2Me)

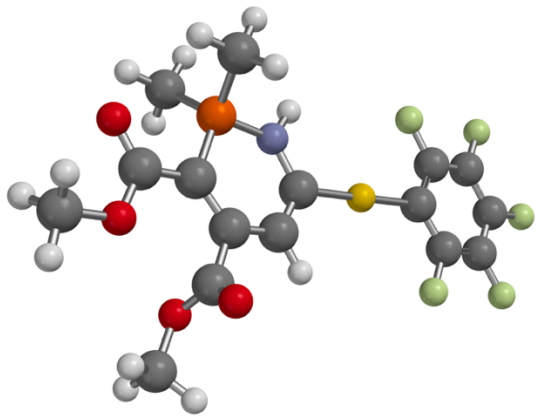

Figure S40. Optimised geometry for [Au(C_6F_5)(CNHPMe$_2$CRCRCH)] (R = CO_2Me) at the ωB97X-D/6-31G/LANL2Dζ level of DFT. Selected distances (Å) and angles (°): Au=C 2.047, Au–C 2.055, C–N 1.383, N–P 1.683, C–C= 1.392, N-C-C 118.1.

Table S42. Cartesian Coordinates [Au(C_6F_5)(CNHPMe$_2$CRCRCH)] (R = CO_2Me)

Atom	x	y	z
C	0.256982	0.586911	-0.430070
C	-0.836389	-0.275188	-0.410971
H	-1.703393	0.016296	-0.990753
C	-0.899268	-1.468591	0.315057
C	0.124740	-1.998192	1.098191
N	1.382837	0.228889	0.289761
H	2.141849	0.898723	0.240867
P	1.660349	-1.166047	1.190325
C	3.057573	-2.056996	0.458537
H	3.954382	-1.429414	0.472158
H	2.808409	-2.312062	-0.574344
H	3.236857	-2.968891	1.032309
C	2.178833	-0.661180	2.850003
H	3.071747	-0.031088	2.785465
H	2.398609	-1.551163	3.442940
H	1.368764	-0.095478	3.316003
C	-2.199704	-2.228533	0.183932
C	0.130606	-3.235470	1.866465
O	-1.008258	-3.924809	1.842266
O	-3.042063	-1.897737	1.160721
O	1.125177	-3.597914	2.484343
O	-2.440128	-2.974758	-0.729129
C	-4.306824	-2.563684	1.119263
H	-4.864836	-2.183867	1.973672
H	-4.164323	-3.644034	1.199327
H	-4.828396	-2.337264	0.186782
C	-1.011008	-5.156442	2.566752
H	-0.829914	-4.974529	3.628293
H	-0.243229	-5.828729	2.178254
H	-2.002522	-5.579501	2.412740
Au	0.321127	2.367407	-1.437184
C	0.403510	4.162438	-2.433261
C	0.513152	6.638332	-3.798065
C	-0.666551	4.650282	-3.170257
C	1.530468	4.971883	-2.411795
C	1.609627	6.191512	-3.072730
C	-0.637248	5.862402	-3.849226
F	2.625529	4.589733	-1.723314
F	2.718513	6.937403	-3.021477
F	0.564725	7.806372	-4.440814
F	-1.693217	6.292187	-4.547022
F	-1.807090	3.940790	-3.254013

Table S43. Thermodynamic data (298.15 K) [Au(C_6F_5)(CNHPMe$_2$CRCRCH)] (R = CO_2Me) (ωB97X-D/6-31G/LANL2Dζ)

Zero Point Energy :	759.73	kJ/mol
Temperature Correction :	65.70	kJ/mol
Enthalpy Correction :	825.43	kJ/mol
Enthalpy :	-1948.989221	au
Entropy :	677.31	J/mol•K
Gibbs Energy :	-1949.066136	au (
Cv :	438.94	J/mol•K

Lowest frequency vibrational mode (Uncorrected) 11 cm^{-1}.

6.22 [Mo(CNHPMe$_2$CRCRCH)(CO)$_5$] (R = CO$_2$Me)

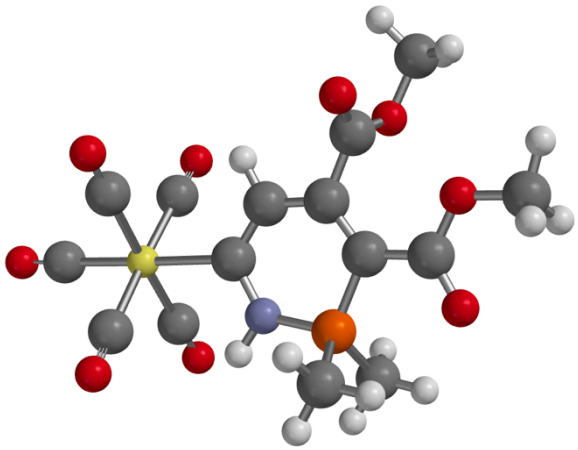

Figure S41. Optimised geometry for [Mo(CNHPMe$_2$CRCRCH)(CO)$_5$] (R = CO$_2$Me) at the ωB97X-D/6-31G/LANL2Dζ level of DFT. Selected distances (Å) and angles (°): Mo=C 2.238, C–N 1.386, N–P 1.683, C–C= 1.404, N-C-C 116.4.

Table S44. Cartesian Coordinates [Mo(CNHPMe$_2$CRCRCH)(CO)$_5$] (R = CO$_2$Me)

Atom	x	y	z
Mo	0.562437	3.352044	-1.933325
C	0.369099	1.389034	-0.875281
C	-0.826999	0.676181	-0.695244
H	-1.724678	1.110085	-1.118813
C	-0.961185	-0.524474	-0.003764
C	0.077661	-1.248587	0.593437
N	1.511922	0.820042	-0.334996
H	2.354484	1.364910	-0.476519
P	1.708064	-0.641522	0.476118
C	-2.371090	-1.062669	0.070556
C	0.016513	-2.521381	1.289170
O	-2.937811	-0.744990	1.235137
O	1.022438	-3.054044	1.747370
O	-2.914198	-1.641072	-0.834820
O	-1.198422	-3.066250	1.377371
C	2.846428	-1.678131	-0.479529
H	3.817511	-1.182748	-0.578433
H	2.420232	-1.841327	-1.472303
H	2.970090	-2.635020	0.032381
C	2.530351	-0.293821	2.052278
H	3.496130	0.189773	1.873779
H	2.681023	-1.232852	2.588656
H	1.894736	0.371635	2.641054
C	-1.106501	3.983981	-0.893603
O	-2.037064	4.311463	-0.305326
C	-0.653888	2.590821	-3.421893
O	-1.331653	2.156122	-4.240097
C	2.207787	2.634361	-2.917392
O	3.141003	2.203191	-3.439694
C	0.699099	5.142477	-2.908023
O	0.778747	6.152574	-3.457512
C	1.757284	4.039173	-0.420846
O	2.441191	4.391803	0.438258
C	-1.268787	-4.332579	2.032506
H	-0.942691	-4.244000	3.071356
H	-0.641243	-5.064021	1.519117
H	-2.316448	-4.626521	1.983182
C	-4.272283	-1.225123	1.406048
H	-4.585546	-0.875461	2.388798
H	-4.286306	-2.317067	1.362334
H	-4.927438	-0.826009	0.628509

Table S45. Thermodynamic data (298.15 K) [Mo(CNHPMe$_2$CRCRCH)(CO)$_5$] (R = CO$_2$Me) (ωB97X-D/6-31G/LANL2Dζ)

Zero Point Energy :	736.97	kJ/mol
Temperature Correction :	67.34	kJ/mol
Enthalpy Correction :	804.31	kJ/mol
Enthalpy :	-1720.008920	au
Entropy :	679.62	J/mol•K
Gibbs Energy :	-1720.086098	au
Cv :	452.55	J/mol•K

Lowest frequency vibrational mode (Uncorrected) 11 cm^{-1}.

6.23 [W(CNHPMe$_2$CRCRCH)(CO)$_5$] (R = CO$_2$Me)

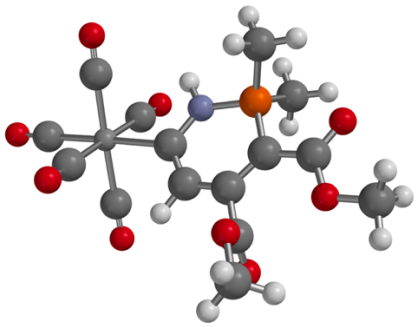

Figure S42. Optimised geometry for [W(CNHPMe$_2$CRCRCH)(CO)$_5$] (R = CO$_2$Me) at the ωB97X-D/6-31G/LANL2Dζ level of DFT. Selected distances (Å) and angles (°): W=C 2.222, C–N 1.388, N–P 1.682, C–C= 1.404, N-C-C 116.3.

Table S46. Cartesian Coordinates [W(CNHPMe$_2$CRCRCH)(CO)$_5$] (R = CO$_2$Me)

Atom	x	y	z
W	0.559928	-1.926118	-3.341458
C	0.369098	-0.869543	-1.395644
C	-0.826624	-0.691823	-0.680744
H	-1.724213	-1.115680	-1.114185
C	-0.960536	-0.001903	0.520643
C	0.077460	0.594388	1.246488
N	1.512435	-0.327342	-0.824782
H	2.355260	-0.465562	-1.370136
P	1.707839	0.477380	0.639167
C	-2.370801	0.069875	1.058375
C	0.016958	1.287029	2.521273
O	-2.938531	1.234120	0.742338
O	1.025156	1.742353	3.052246
O	-2.912990	-0.837160	1.634907
O	-1.197275	1.374347	3.067231
C	2.844275	-0.484087	1.672435
H	3.815495	-0.582851	1.177271

Atom	x	y	z
H	2.416301	-1.476777	1.831657
H	2.968550	0.023865	2.631389
C	2.532398	2.053286	0.296815
H	3.497915	1.874889	-0.187316
H	2.683863	2.585626	1.238007
H	1.897726	2.645557	-0.366396
C	-1.100639	-0.903466	-3.987185
O	-2.033729	-0.322231	-4.325449
C	-0.653834	-3.402123	-2.582535
O	-1.335943	-4.220689	-2.151084
C	2.201575	-2.898802	-2.624522
O	3.140170	-3.419416	-2.198223
C	0.695870	-2.909114	-5.116961
O	0.773581	-3.463644	-6.126671
C	1.752621	-0.428011	-4.038497
O	2.441551	0.425450	-4.400680
C	-1.265026	2.028291	4.334285
H	-0.935205	3.065976	4.247154
H	-0.639740	1.511713	5.065625
H	-2.312860	1.981911	4.627684
C	-4.273833	1.402715	1.221385
H	-4.587193	2.386357	0.874458
H	-4.289374	1.355184	2.313113
H	-4.927679	0.626031	0.818524

Table S47. Thermodynamic data (298.15 K) [W(CNHPMe$_2$CRCRCH)(CO)$_5$] (R = CO_2Me) (ωB97X-D/6-31G/LANL2Dζ)

Zero Point Energy :	738.64	kJ/mol
Temperature Correction :	66.76	kJ/mol
Enthalpy Correction :	805.39	kJ/mol (
Enthalpy :	-1720.313035	au
Entropy :	678.75	J/mol•K
Gibbs Energy :	-1720.390113	au
Cv :	450.20	J/mol•K

Lowest frequency vibrational mode (Uncorrected) 9 cm^{-1}.

7 Mechanistic Conjecture

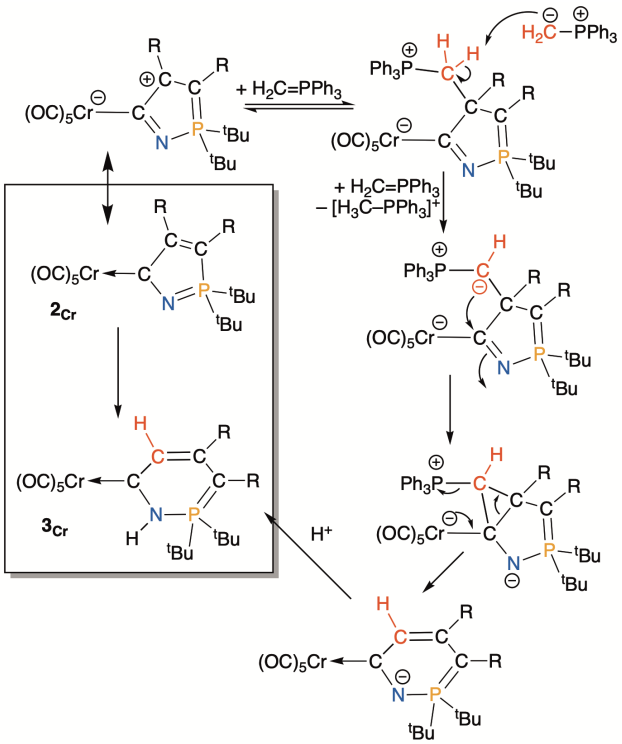

Scheme S3: Mechanistic conjecture to account for the formation of **3$_{Cr}$** from **2$_{Cr}$** (R = CO_2Me) and H_2C=PPh_3

8 Failed Reactions

The following observations regarding attempted but unsuccessful reactions are provided for information only. It should not be taken as definitively establishing that a reaction which failed in our hands under the employed conditions might not proceed successfully under other circumstances.

Table S48. Unsuccessful Investigations

Carbene complex	Reagent	Solvent, conditions, time	Observations
Ring transfer attempts			
2$_{Mo}$	Ceric ammonium nitrate	MeCN, RT, 24 h	Black suspension, TLC immobile materials
2$_{Mo}$	CO, CO_2, CS_2	DCM, RT, 24 h	No reaction by NMR
2$_{Mo}$	Trimethylamine *N*-oxide	MeCN, RT, 5 days	Very slowly formed brown suspension, TLC immobile materials
2$_{Mo}$	$BH_3.SMe_2$	C_6D_6, RT, 24 h, NMR tube	Went yellow with brown solids overnight, filtration and evaporation gave poorly soluble (DCM, C_6D_6) yellow residue, new ^{31}P signal at 98 ppm but no apparent ^{11}B signal, ^{1}H messy
2$_{Mo}$	$B(C_6F_5)_3$	DCM, RT, 48 h, NMR tube	No reaction, no change to NMR
2$_{Mo}$	Excess S or Se, few drops *N*-methylimidazole	DCM, reflux or THF, reflux	No reaction, only starting material on TLC plate, recovered SM via column in low yield, some decomp.
2$_{Mo}$	$(PPh)_5$	C_6D_6, ~45 C°, 24 h, NMR tube	No reaction by NMR
2$_{Cr}$	PhLi then MeI	Et_2O, -78 C° to RT	Went black upon addition of **2$_{Cr}$** to PhLi at low temp, then black/green when MeI added, immobile on TLC except for starting material
2$_{Mo}$	½[$PdCl_2(NCMe)_2$], ½[$Pd(OAc)_2$], ½[$PtCl_2(NCMe)_2$]	THF, RT or reflux, 2—24 h	All went black/brown, immobile on TLC, NMR spectra messy
2$_{Mo}$	½[$Cp^*RhCl_2]_2$, ½[$Cp^*IrCl_2]_2$, [$RhCl(PPh_3)_3$], ½[(cymene)$RuCl_2]_2$, ½[$Rh(cod)Cl]_2$, ½[$Rh(nbd)Cl]_2$	DCM, RT, NMR tube, 24—72 h	No reaction by NMR
2$_{Mo}$	AgCl, [AgCl(THT)], [$AgCl(PPh_3)$]	DCM, RT, 24 h	No reaction, AgCl precipitated
2$_{Mo}$	$[Ni(CO)_4]$	Toluene, RT, 24 h, CO atm	No reaction by TLC, nickel mirror

Ring expansion attempts			
$\mathbf{2}_{Cr}$ $\mathbf{2}_{Mo}$ $\mathbf{2}_{W}$	$Ph_3P=CHMe$, $Ph_3P=CMe_2$, $Ph_3P=CHPh$, $Ph_3P=CPh_2$, $Ph_3P=CHBr$, $Me_2S=CH_2$,	Et_2O, RT, 2—24 h NaHMDS as base.	No reaction, only starting material observed on TLC plate with immobile decomp. Usually recovered SM via column in variable yield
$\mathbf{2}_{Mo}$	Benzophenone, acetophenone	Toluene, reflux, 24 h	Went black presumably decomp, no SM on TLC plate
$\mathbf{2}_{Mo}$	$TMSCH=N_2$	DCM, reflux, 24 h	No reaction
$\mathbf{2}_{Mo}$	Ethyl diazoacetate	DCM, reflux, 24 h	No reaction

9 References

[3] R. D. Kirk and A. F. Hill, *Angew. Chem., Int. Ed.*, **2025**, *64*, e202504620.

[9] J. A. Steed, H. R. Sharpe, H. J. Futcher, A. J. Wooles, S. T. Liddle, *Angew. Chem., Int. Ed.* **2020,** *59*, 15870-15874.

[10] E. J. Corey, J. Kang, K. Kyler, *Tetrahedron Lett*. **1985**, *26*, 555-558.

[18] H. C. Ong, J. T. S. Coimbra, M. J. Ramos, B. Xing, R. A. Fernandes, F. Garcia. Chem. Sci., 2023,14, 4126-4133

[19] CrysAlisPRO®, Oxford Diffraction/Agilent Technologies UK Ltd., Yarton, England, 2010.

[20] O. V. Dolomanov, L. J. Bourhis, R. J. Gildea, J. A. K. Howard and H. Puschmann, *J. Appl. Crystallogr.*, 2009, 42, 339-341.

[21] G. M. Sheldrick, *Acta Crystallogr. Sect. C: Cryst. Struct. Commun.,* 2015, 71, 3-8.

[22] C. F. Macrae, I. J. Bruno, J. A. Chisholm, P. R. Edgington, P. McCabe, E. Pidcock, L. Rodriguez-Monge, R. Taylor, J. van de Streek and P. A. Wood, J. *Appl. Crystallogr.,* 2008, 41, 466-470.

[23] *Spartan 24*® (2024) Wavefunction, Inc., 18401 Von Karman Ave., Suite 370 Irvine, CA 92612 U.S.A.

[24] a) J. D. Chai and M. Head-Gordon, *Phys. Chem. Chem. Phys.*, **2008**, *10*, 6615-6620. b) W. R. Wadt and P. J. Hay, *J. Chem. Phys.*, **1985**, *82*, 284-298. c) W. J. Hehre, R. Ditchfeld and J. A. Pople, *J. Chem. Phys.*, **1972**, *56*, 2257–2261.

[25] a) Löwden, P.-O., *J. Mol. Spec.*, 1963, **10**, 12-33; b) Löwden, P.-O., *J. Mol. Spec.*, 1964, **13**, 320-337; c) Löwden, P.-O., *J. Math. Phys.*, 1962, **3**, 969–982; d) Löwden, P.-O., *J. Mol. Spec.*, 1964, **14**, 112-118.

[26] a) R. G. Parr, W. Yang, *J. Am. Chem. Soc.,* **1984**, *106*, 4049-4050. b) W. Yang, W. J. Mortier, *J. Am. Chem. Soc.,* **1986**, *108*, 5708-5711.

10 Selected Spectra

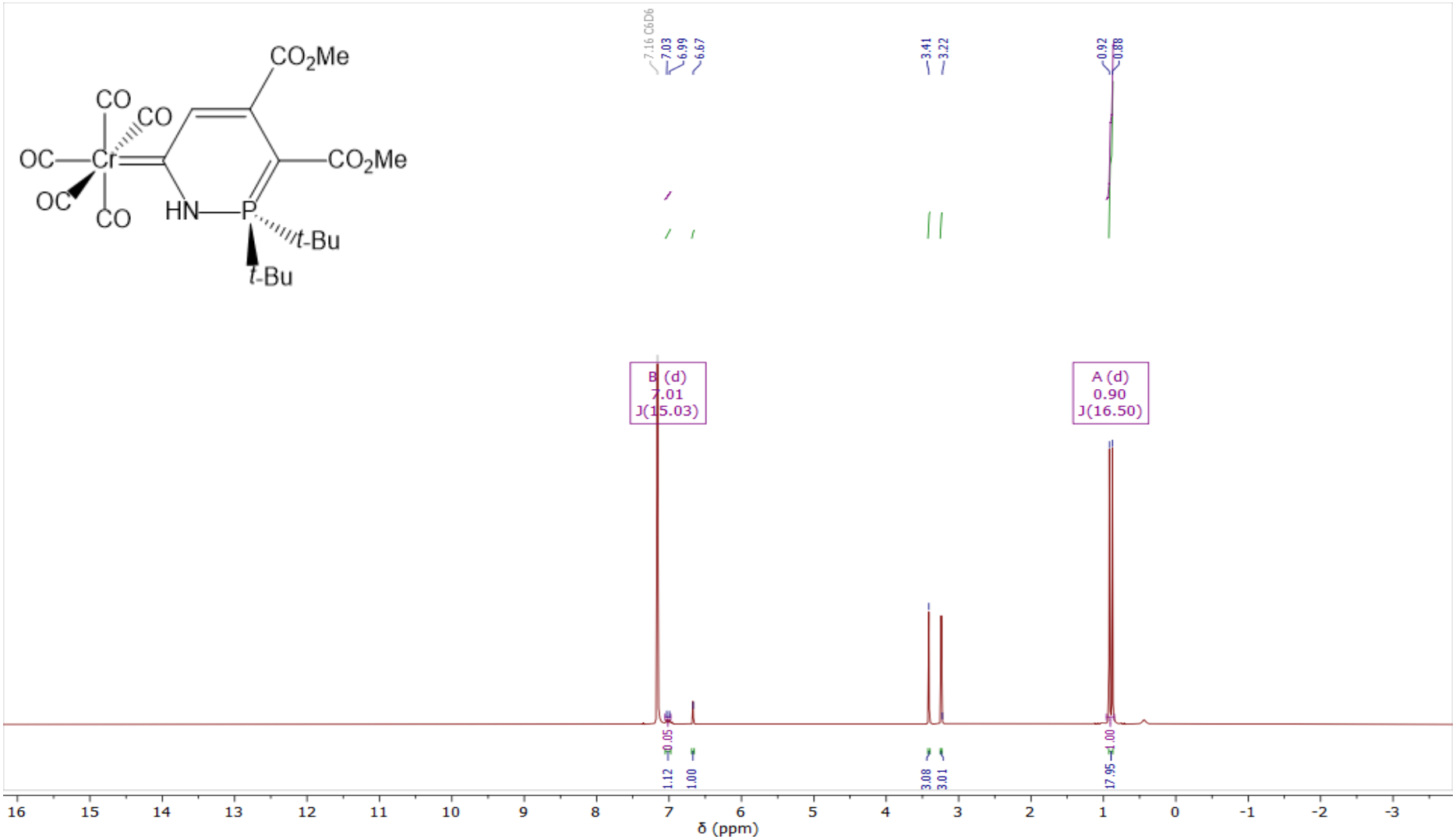

Figure S43: The ^{1}H NMR spectrum of [Cr{CN(H)P^{t}Bu$_2$C(CO$_2$Me)C(CO$_2$Me)CH}(CO)$_5$] (C_6D_6, 400 MHz, 25 °C).

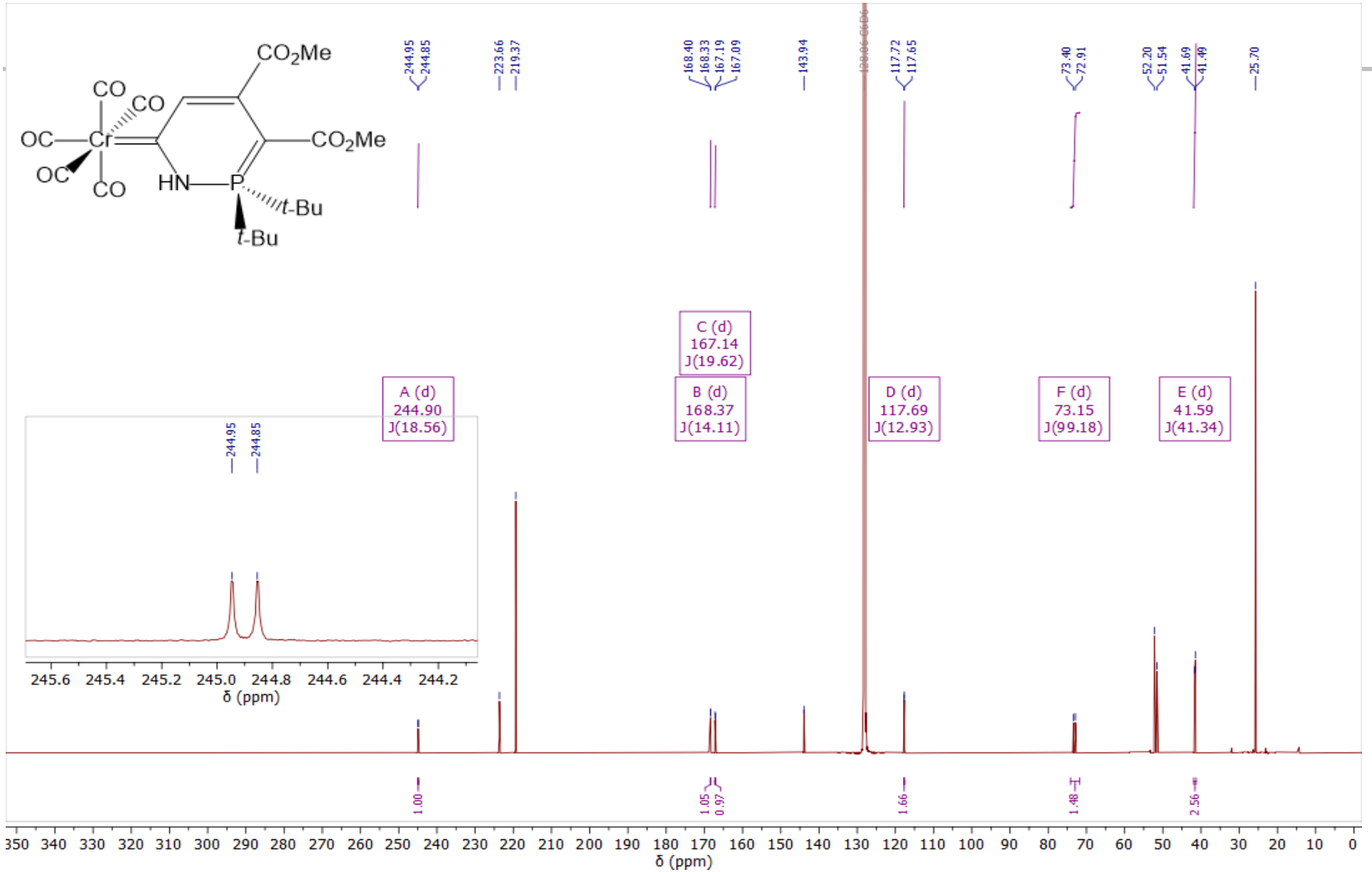

Figure S44: The $^{13}C\{^{1}H\}$ NMR spectrum of $[Cr\{CN(H)P^{t}Bu_2C(CO_2Me)C(CO_2Me)CH\}(CO)_5]$ (C_6D_6, 201 MHz, 25 °C).

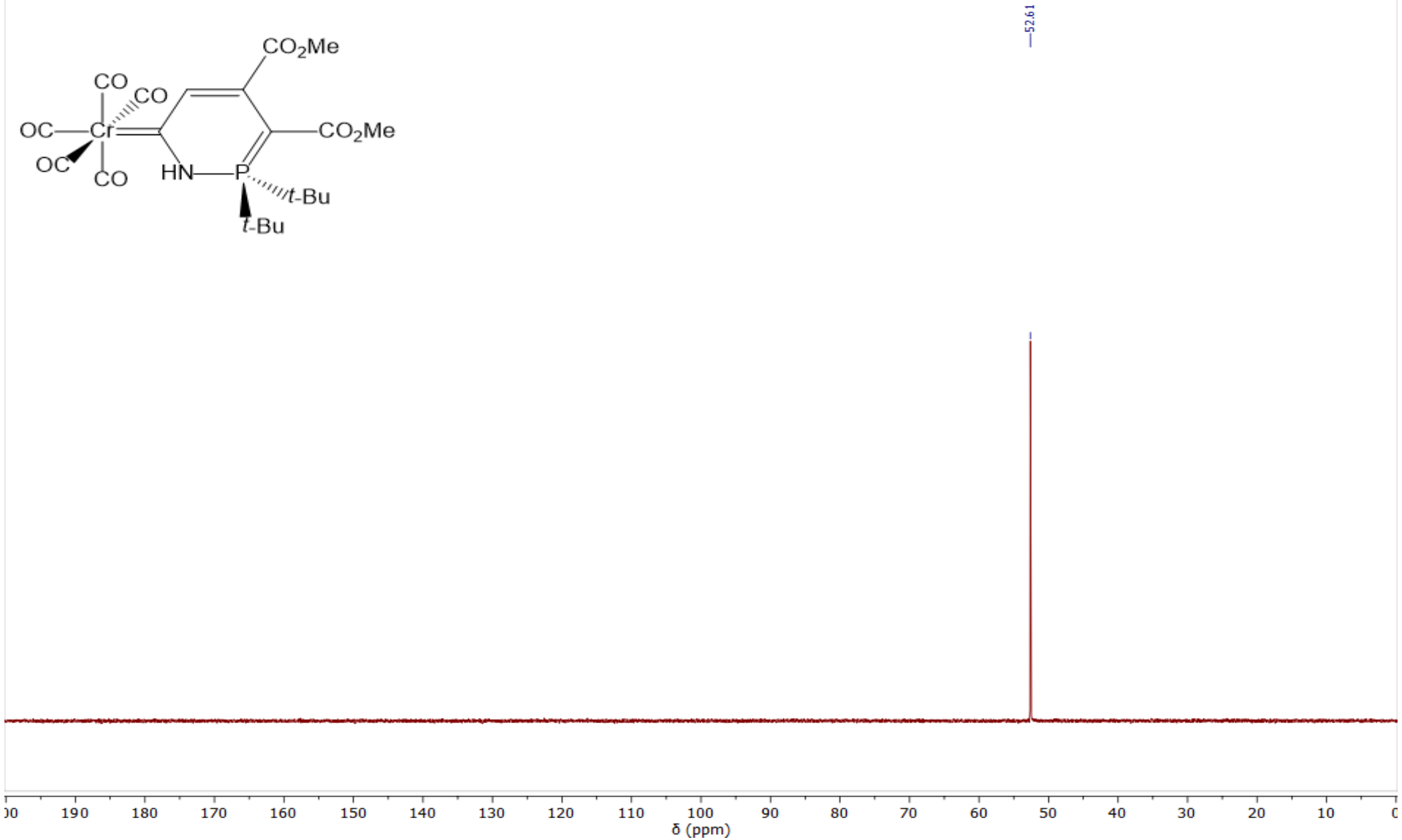

Figure S45: The $^{31}P\{^{1}H\}$ NMR spectrum of [Cr{CN(H)P^{t}Bu$_2$C(CO$_2$Me)C(CO$_2$Me)CH}(CO)$_5$] (C_6D_6, 162 MHz, 25 °C).

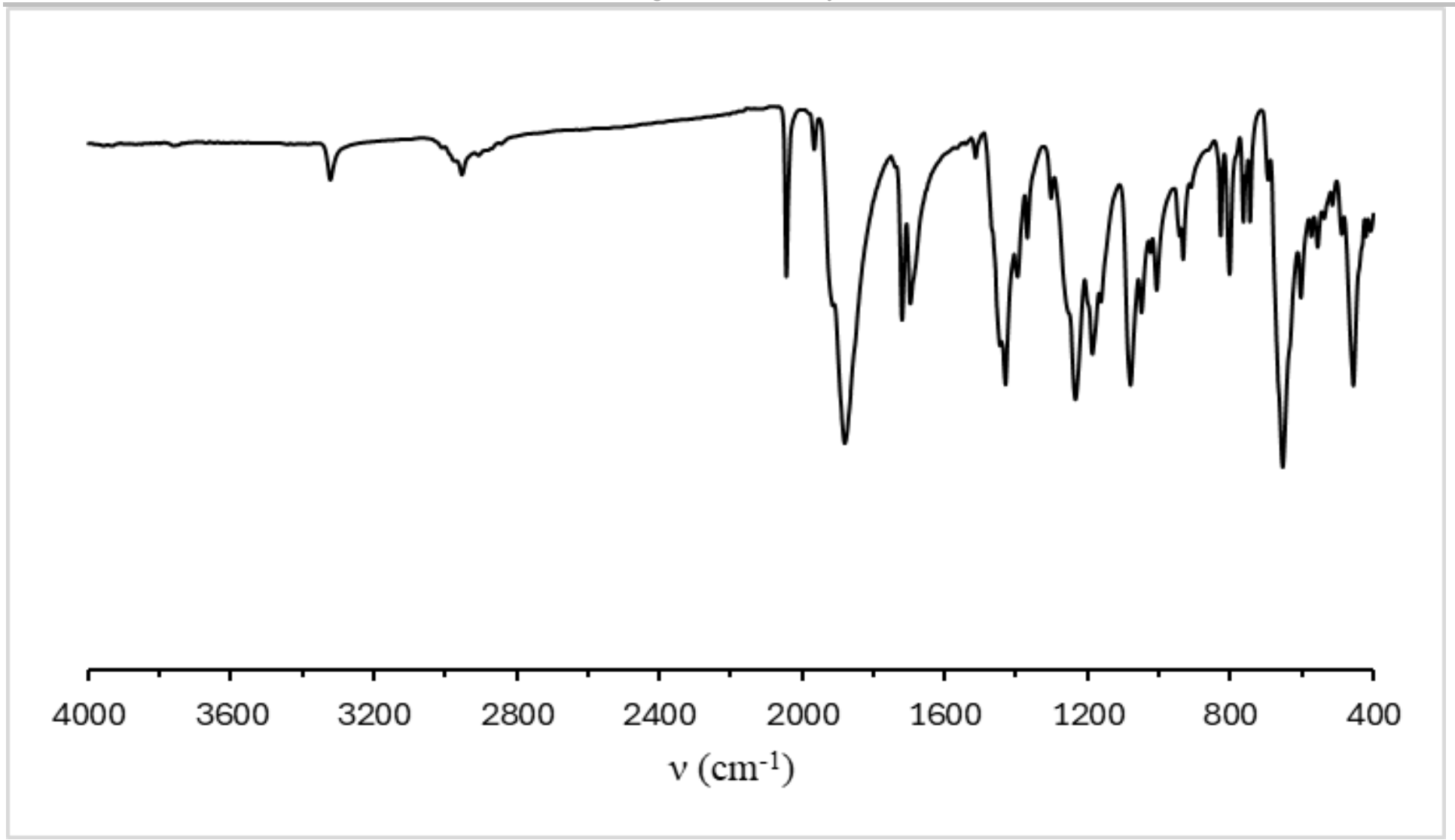

Figure S46: IR spectrum (ATR) of [Cr{CN(H)P^{t}Bu$_2$C(CO$_2$Me)C(CO$_2$Me)CH}(CO)$_5$].

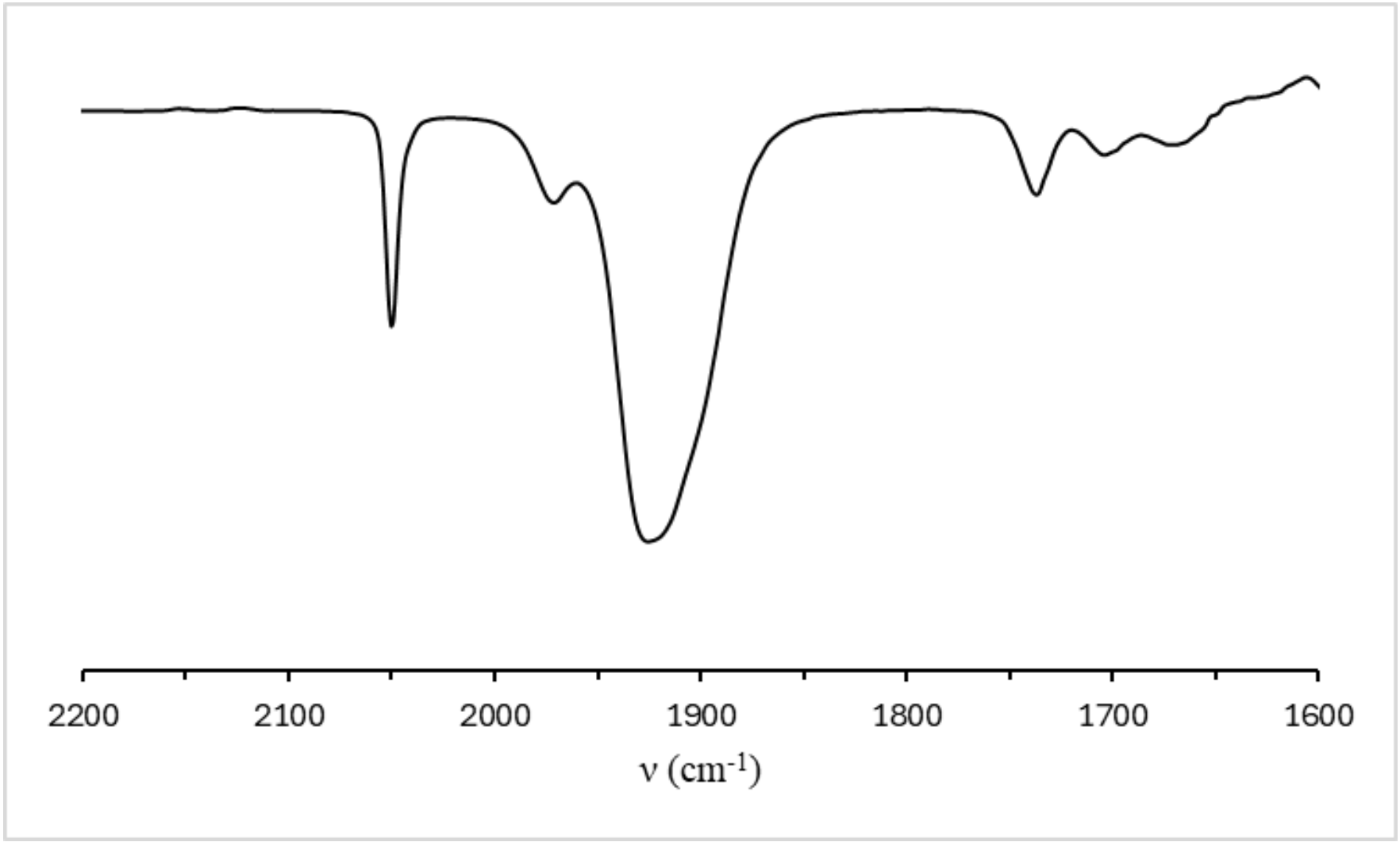

Figure S47: IR spectrum of [Cr{CN(H)P^{t}Bu$_2$C(CO$_2$Me)C(CO$_2$Me)CH}(CO)$_5$] (CH$_2$Cl$_2$).

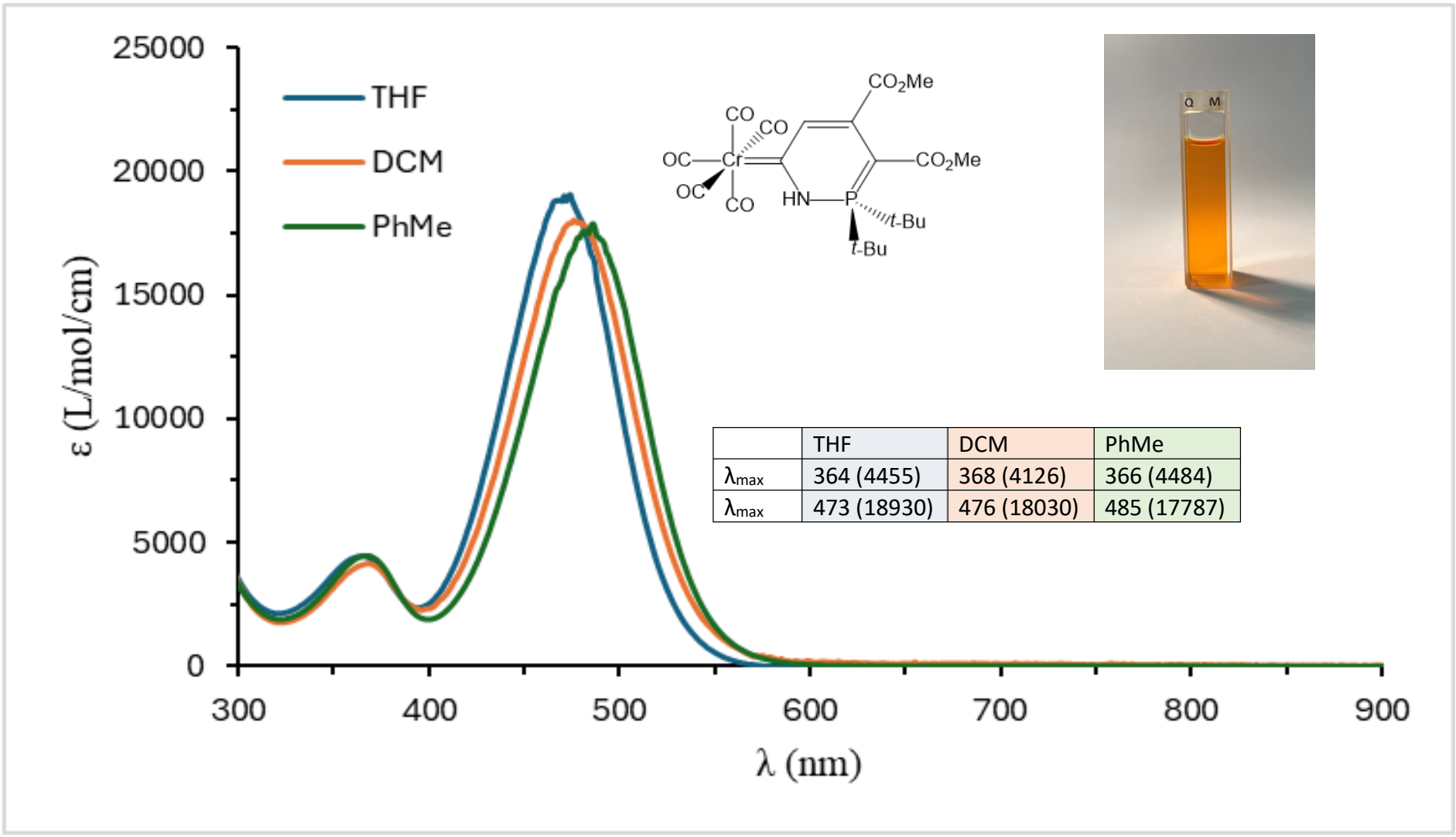

	THF	DCM	PhMe
λ_{max}	364 (4455)	368 (4126)	366 (4484)
λ_{max}	473 (18930)	476 (18030)	485 (17787)

Figure S46: Electronic spectra of [Cr{CN(H)P^{t}Bu$_2$C(CO$_2$Me)C(CO$_2$Me)CH}(CO)$_5$] measured in tetrahydrofuran, dichloromethane and toluene solutions (*conc.* = 7.7 x 10^{-5} mol/L, 25 °C). Values for λ_{max} are tabulated for convenience and corresponding extinction constants are given in parentheses. Inset: photograph of [Cr{CN(H)P^{t}Bu$_2$C(CO$_2$Me)C(CO$_2$Me)CH}(CO)$_5$] in CH_2Cl_2 solution.

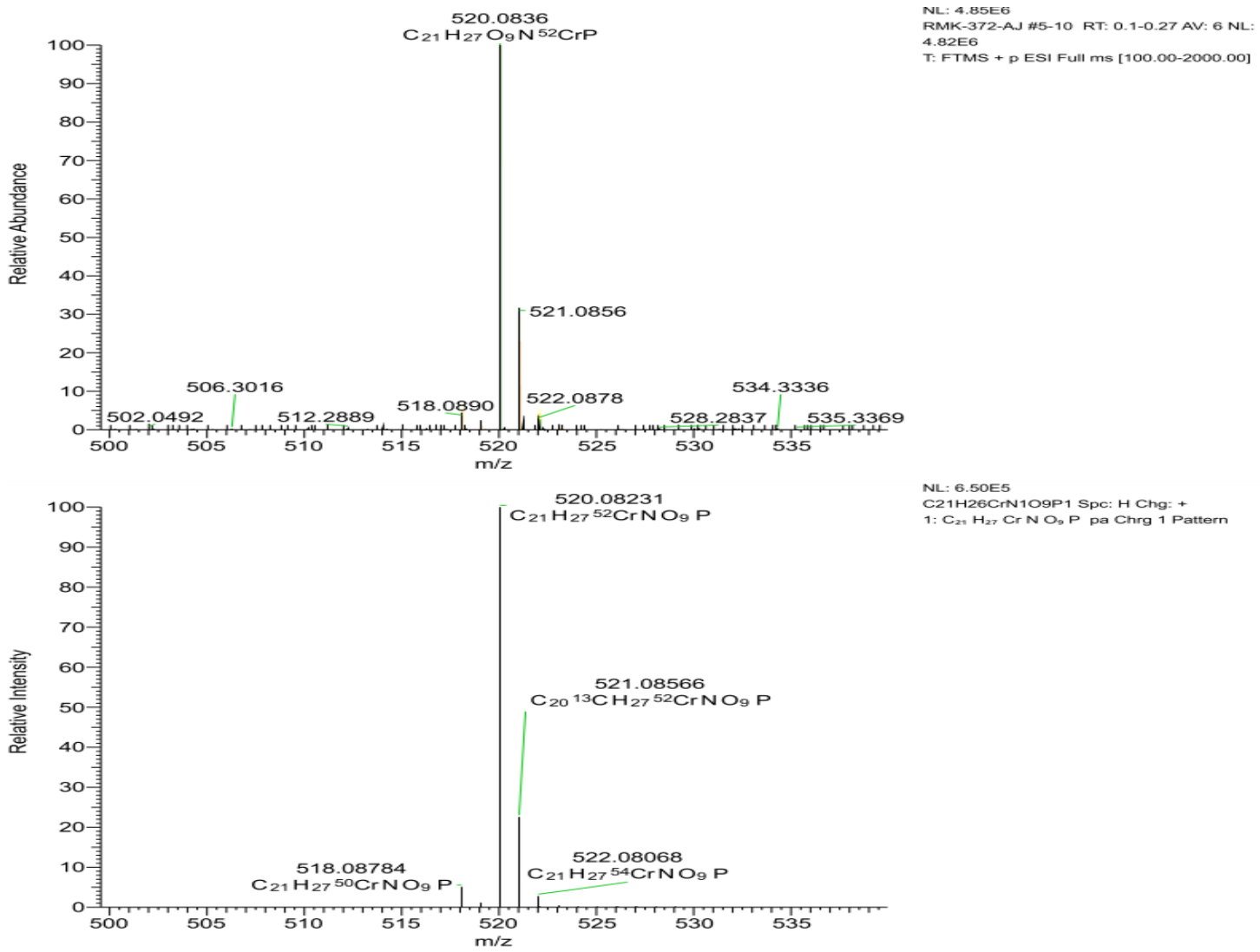

Figure S47. The HR-MS of [Cr{CN(H)P^{t}Bu$_2$C(CO$_2$Me)C(CO$_2$Me)CH}(CO)$_5$] (ESI, MeCN, [*M* + H]$^+$ ion).

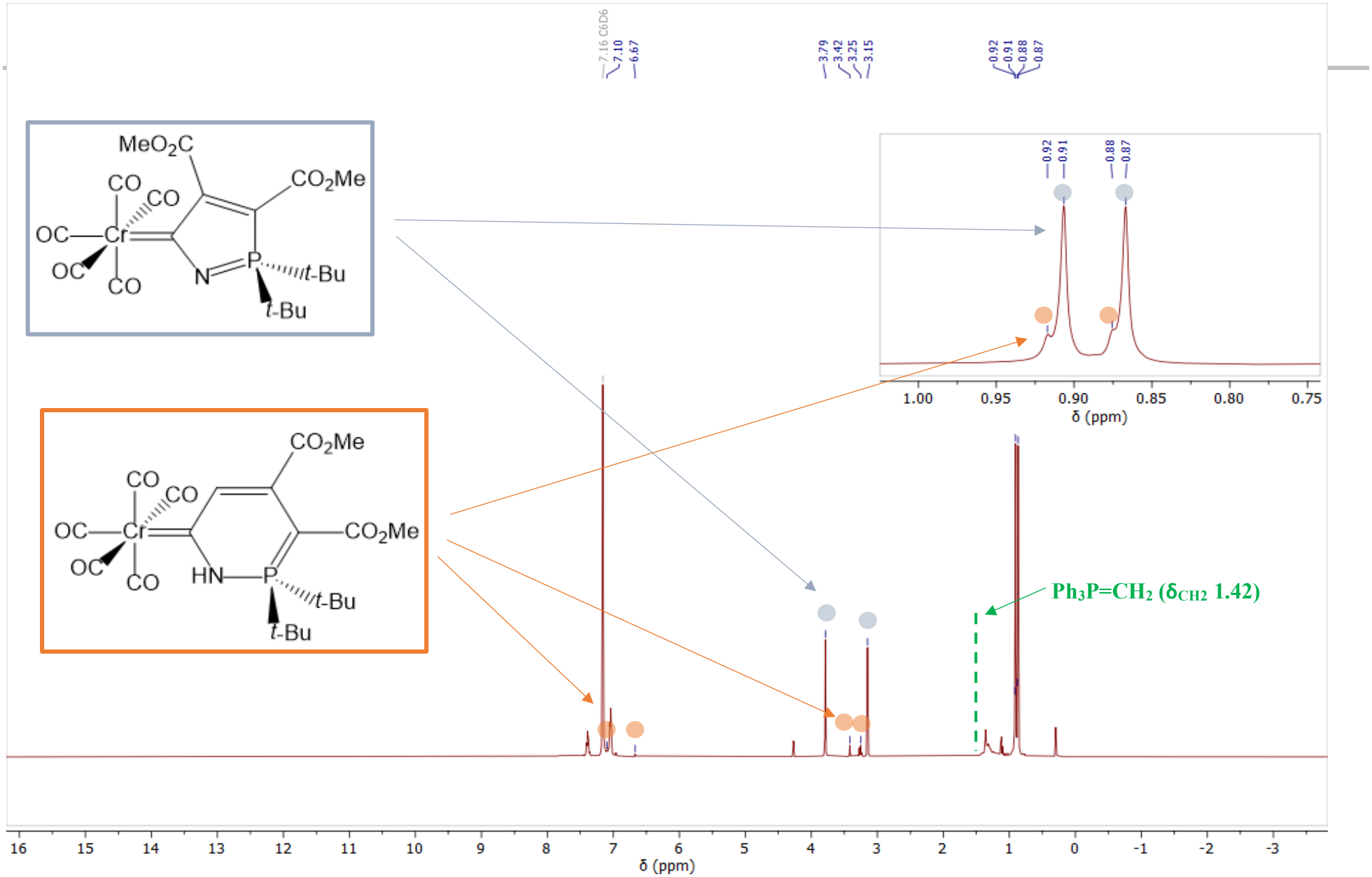

Figure S48: The 1H NMR spectrum of an equimolar mixture of $\mathbf{2_{Cr}}$ and $Ph_3P{=}CH_2$ after standing for ~16 h (C_6D_6, 400 MHz, 25 °C). The ^1H chemical shift of an authentic sample of $Ph_3P{=}CH_2$ (methylene resonances only) measured in C6D6 is indicated in green for convenience.

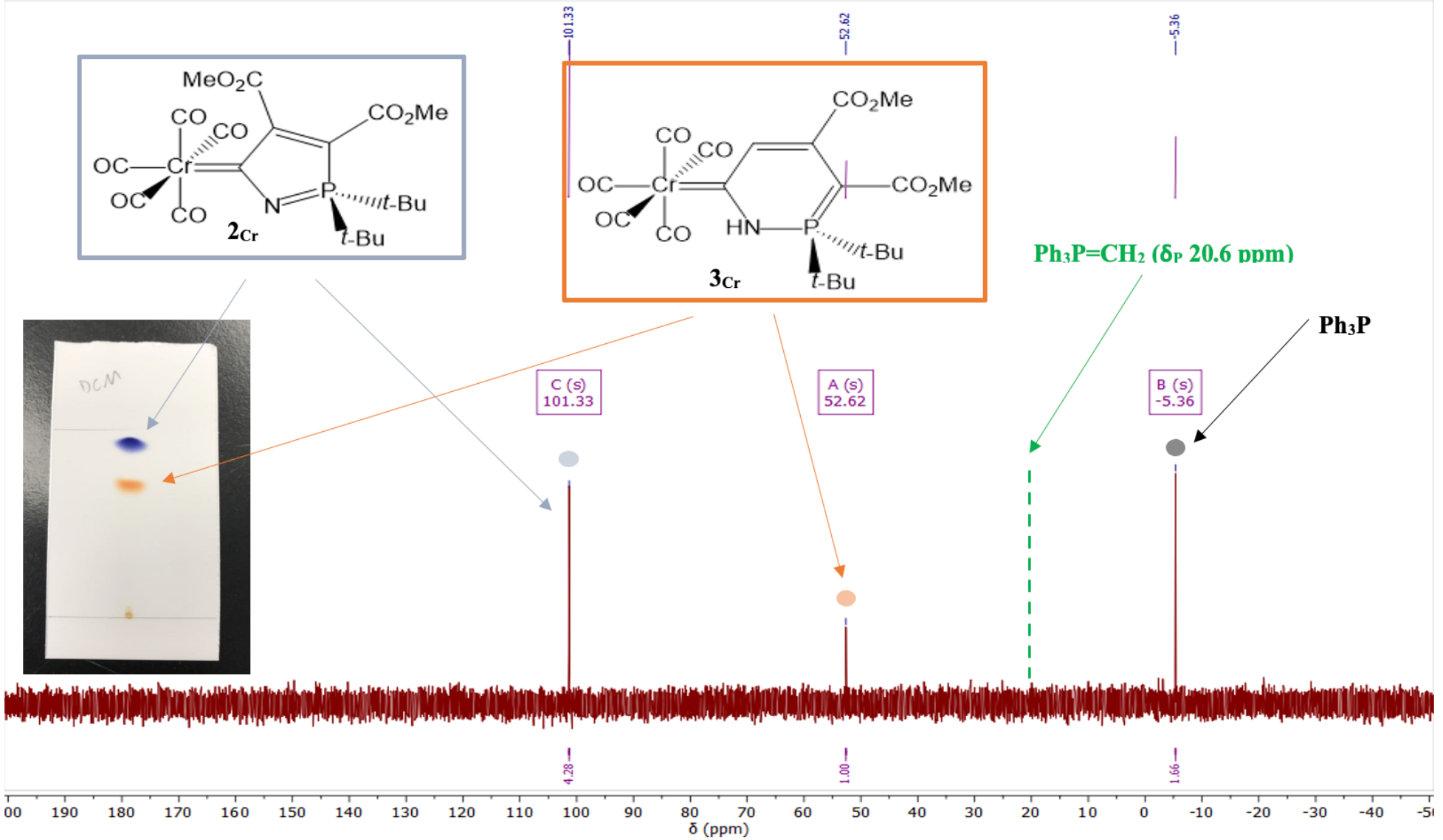

Figure 49: The $^{31}P\{^{1}H\}$ NMR spectrum of an equimolar mixture of $\mathbf{2_{Cr}}$ and $Ph_3P{=}CH_2$ after standing for ~16 h (C_6D_6, 162 MHz, 25 °C). The $^{31}P\{^{1}H\}$ chemical shift of an authentic sample of $Ph_3P{=}CH_2$ measured in C_6D_6 is indicated in green for convenience. Inset: photograph of a silica gel TLC plate developed from the same NMR-scale reaction.

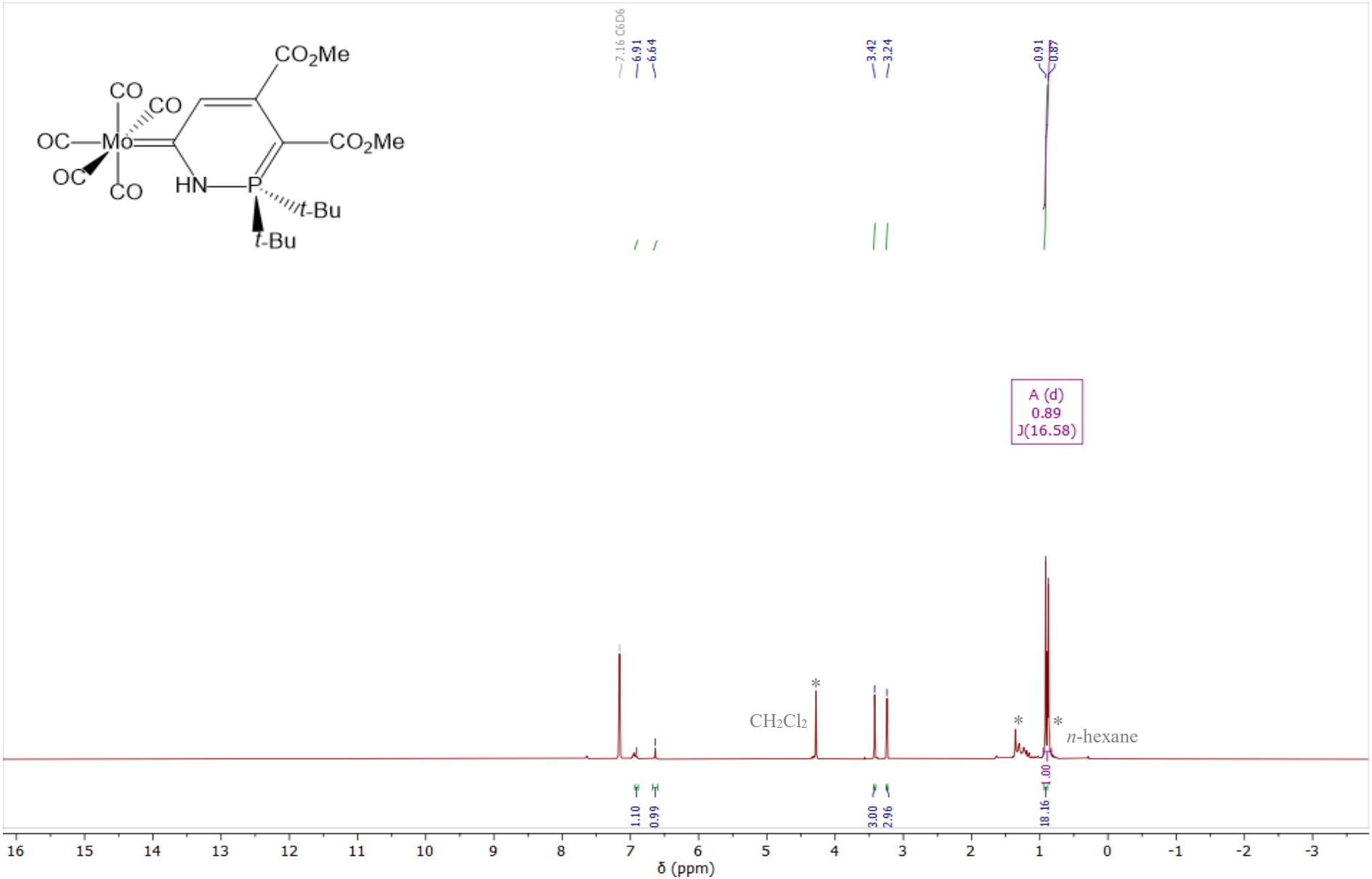

Figure S50: The ^{1}H NMR spectrum of [Mo{CN(H)P^{t}Bu$_2$C(CO$_2$Me)C(CO$_2$Me)CH}(CO)$_5$] (C_6D_6, 400 MHz, 25 °C).

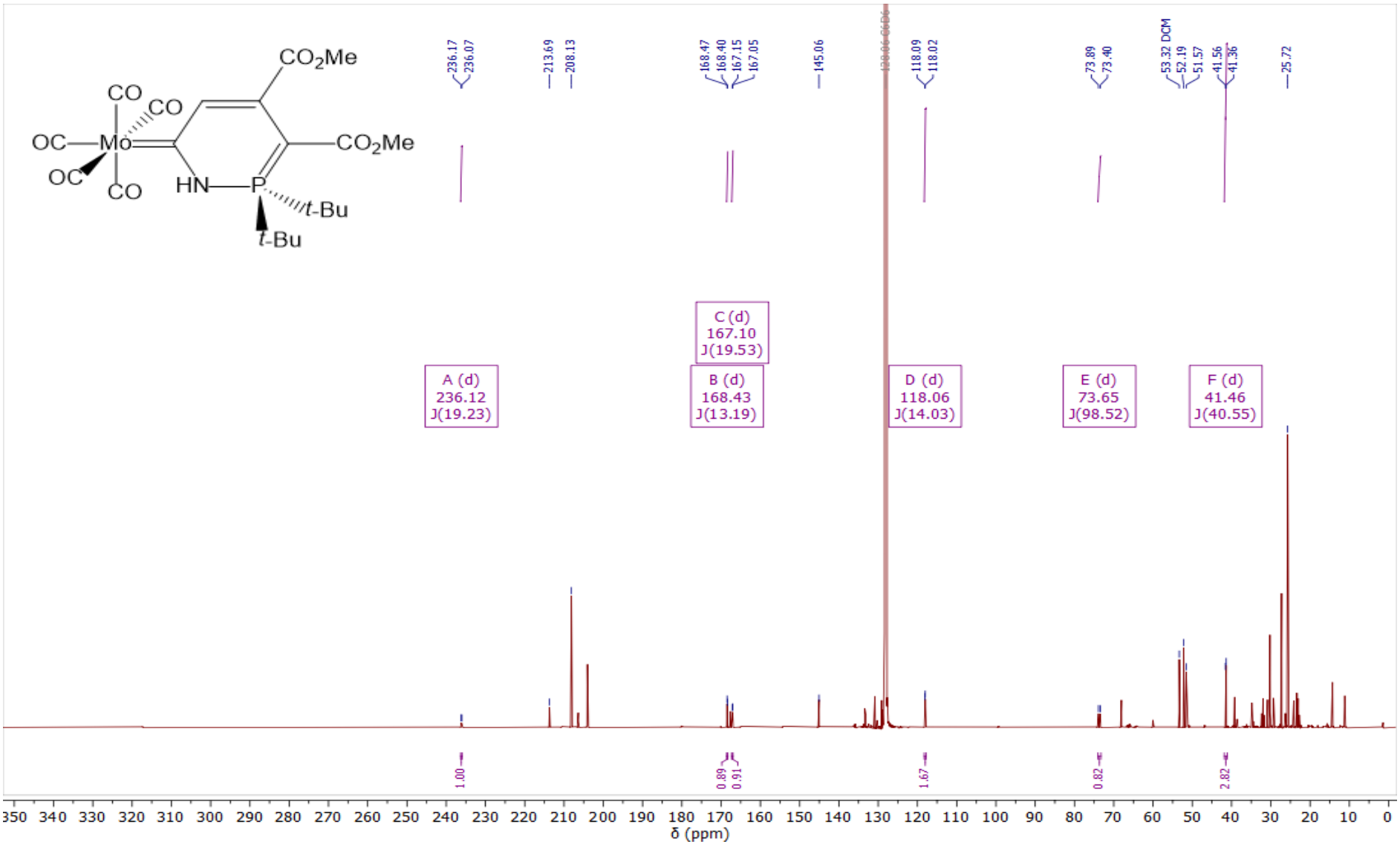

Figure S51: The $^{13}C\{^{1}H\}$ NMR spectrum of [Mo{CN(H)P^{t}Bu$_2$C(CO$_2$Me)C(CO$_2$Me)CH}(CO)$_5$] (C_6D_6, 201 MHz, 25 °C). Partial decomposition was observed during acquisition of the spectrum (~14 hours) and only those signals which correspond to the product are labelled.

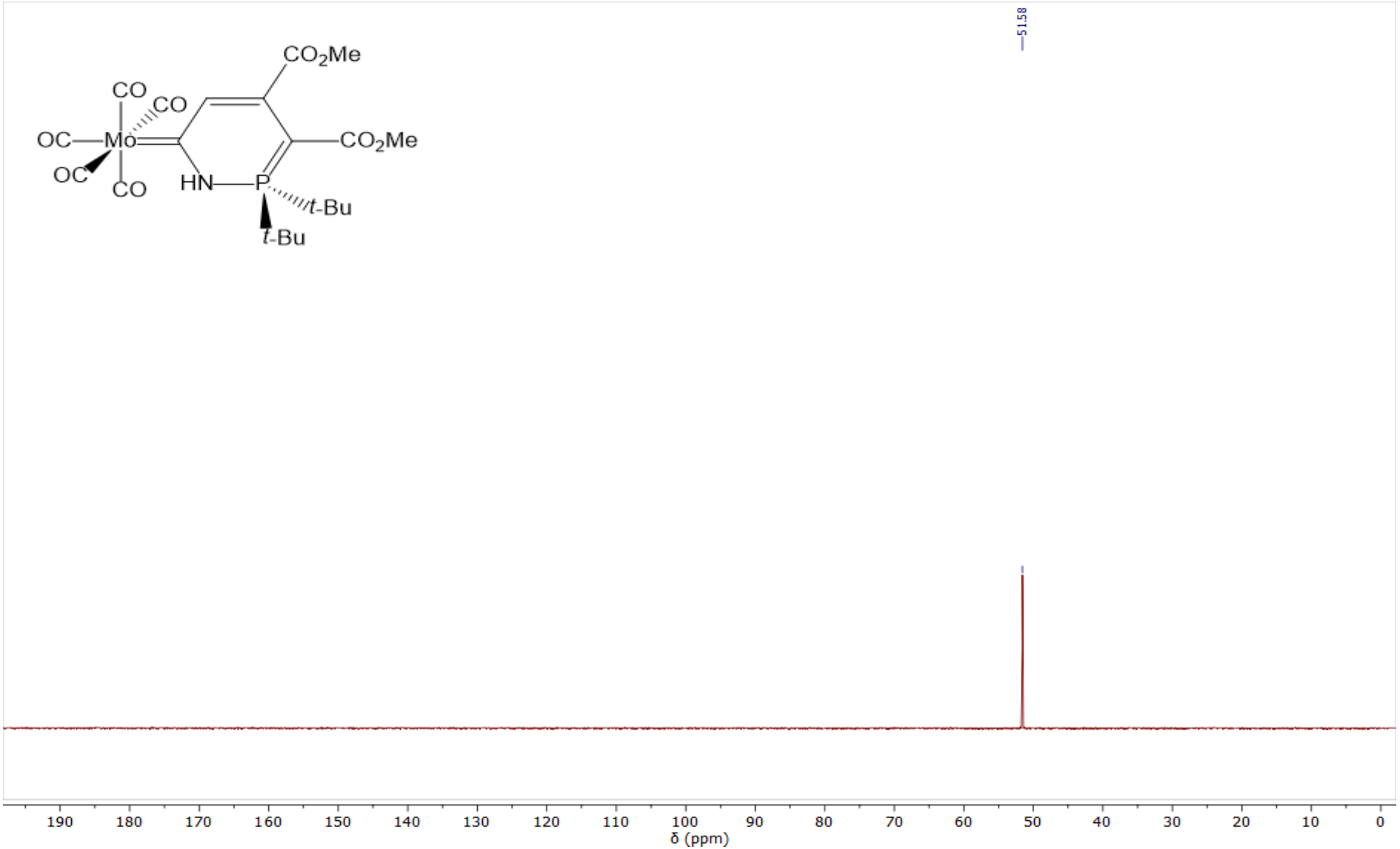

Figure S52: The $^{31}P\{^{1}H\}$ NMR spectrum of [Mo{CN(H)P^{t}Bu$_2$C(CO$_2$Me)C(CO$_2$Me)CH}(CO)$_5$] (C_6D_6, 162 MHz, 25 °C).

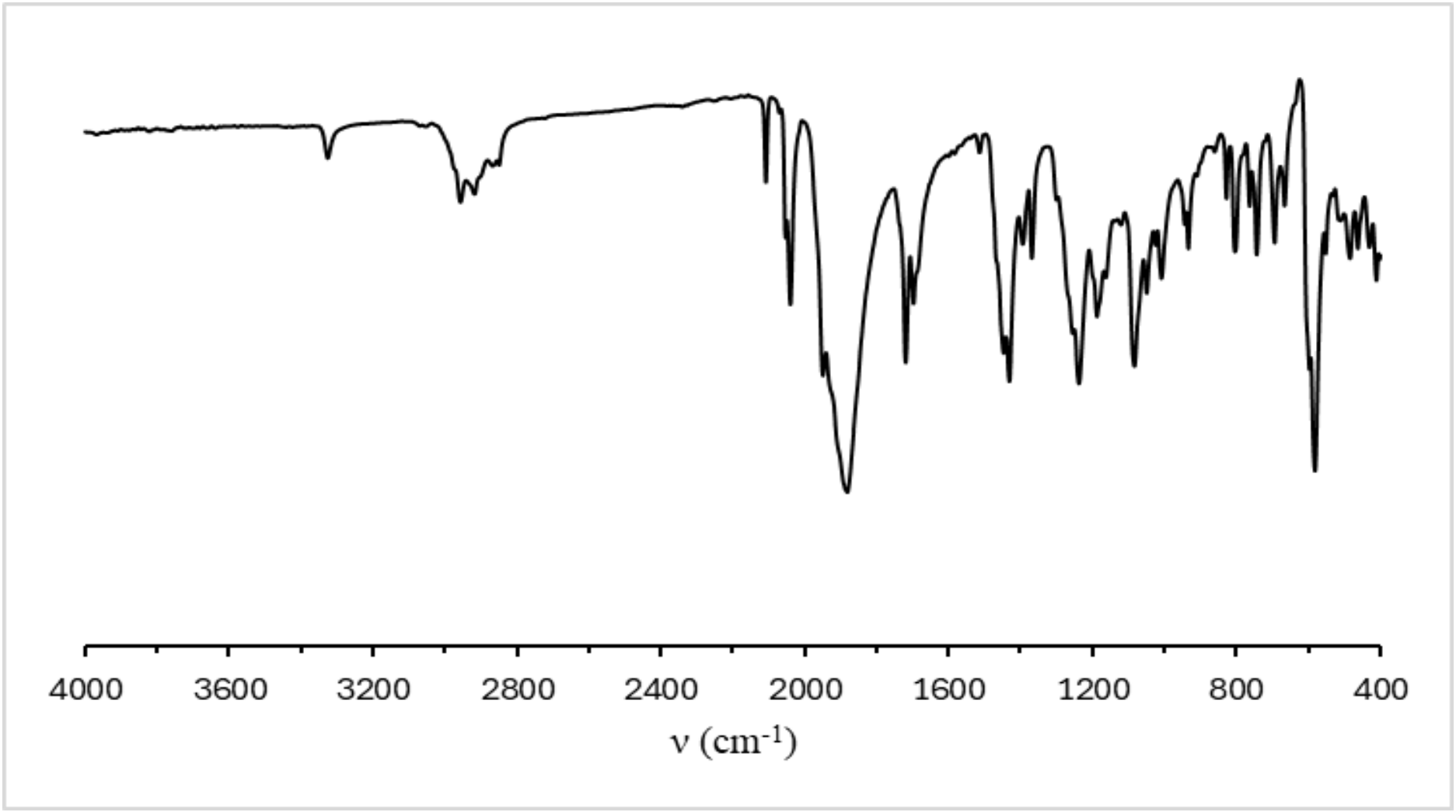

Figure S53: IR spectrum (ATR) of [Mo{CN(H)P^{t}Bu$_2$C(CO$_2$Me)C(CO$_2$Me)CH}(CO)$_5$].

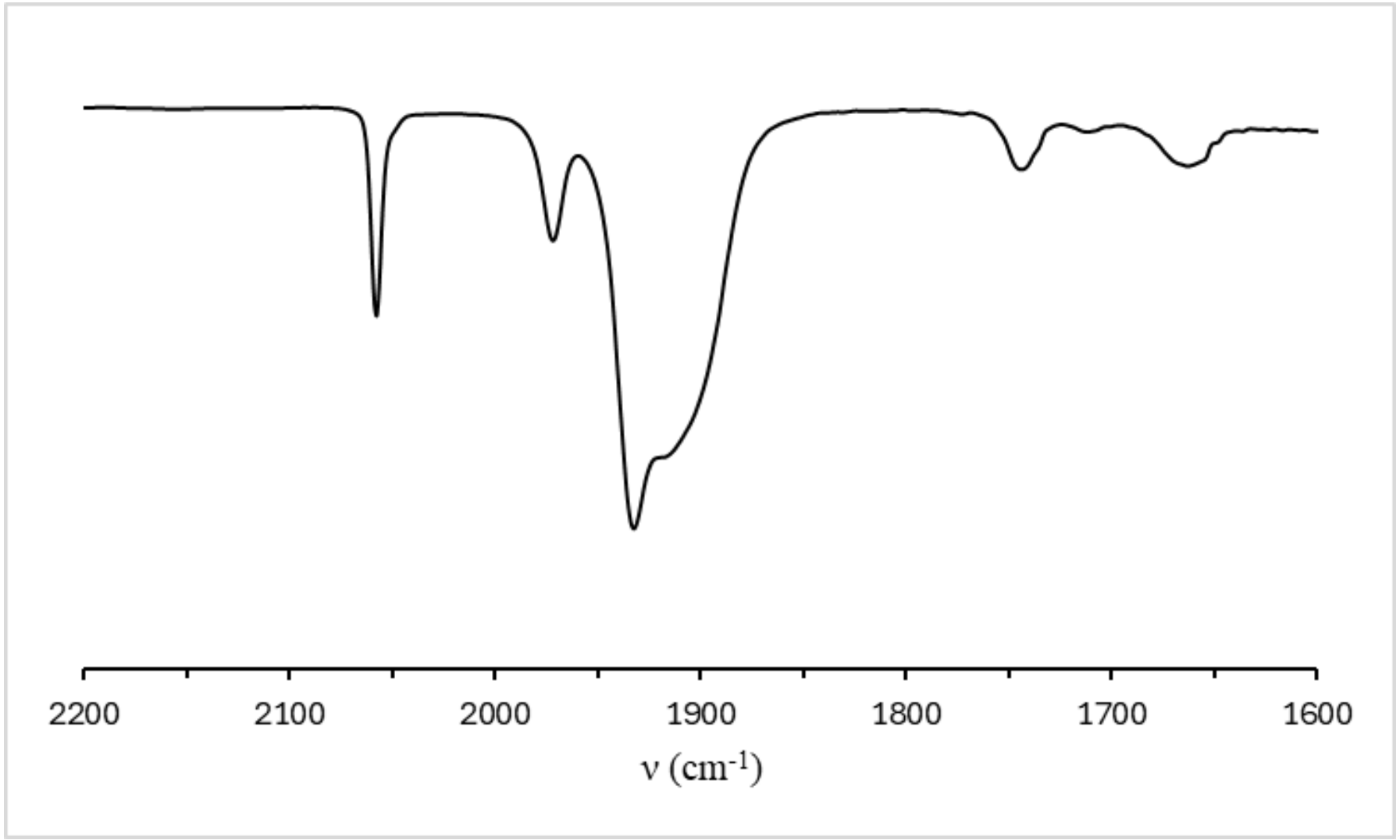

Figure S54: IR spectrum (CH_2Cl_2) of [Mo{CN(H)P^{t}Bu$_2$C(CO_2Me)C(CO_2Me)CH}$(CO)_5$].

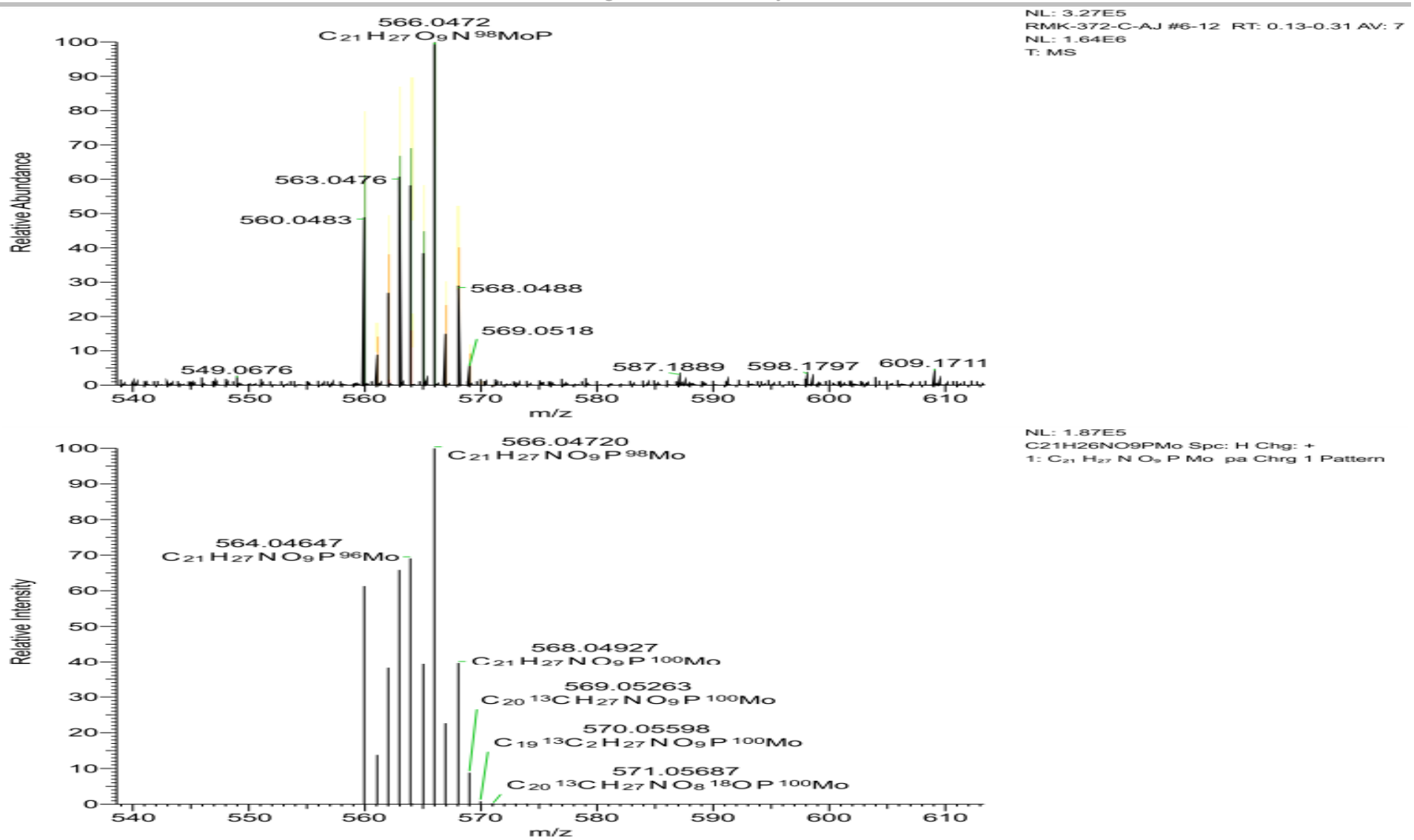

Figure S55: The HR-MS of [Mo{CN(H)P^{t}Bu$_2$C(CO$_2$Me)C(CO$_2$Me)CH}(CO)$_5$] (ESI, MeCN, [*M* + H]$^+$ ion).

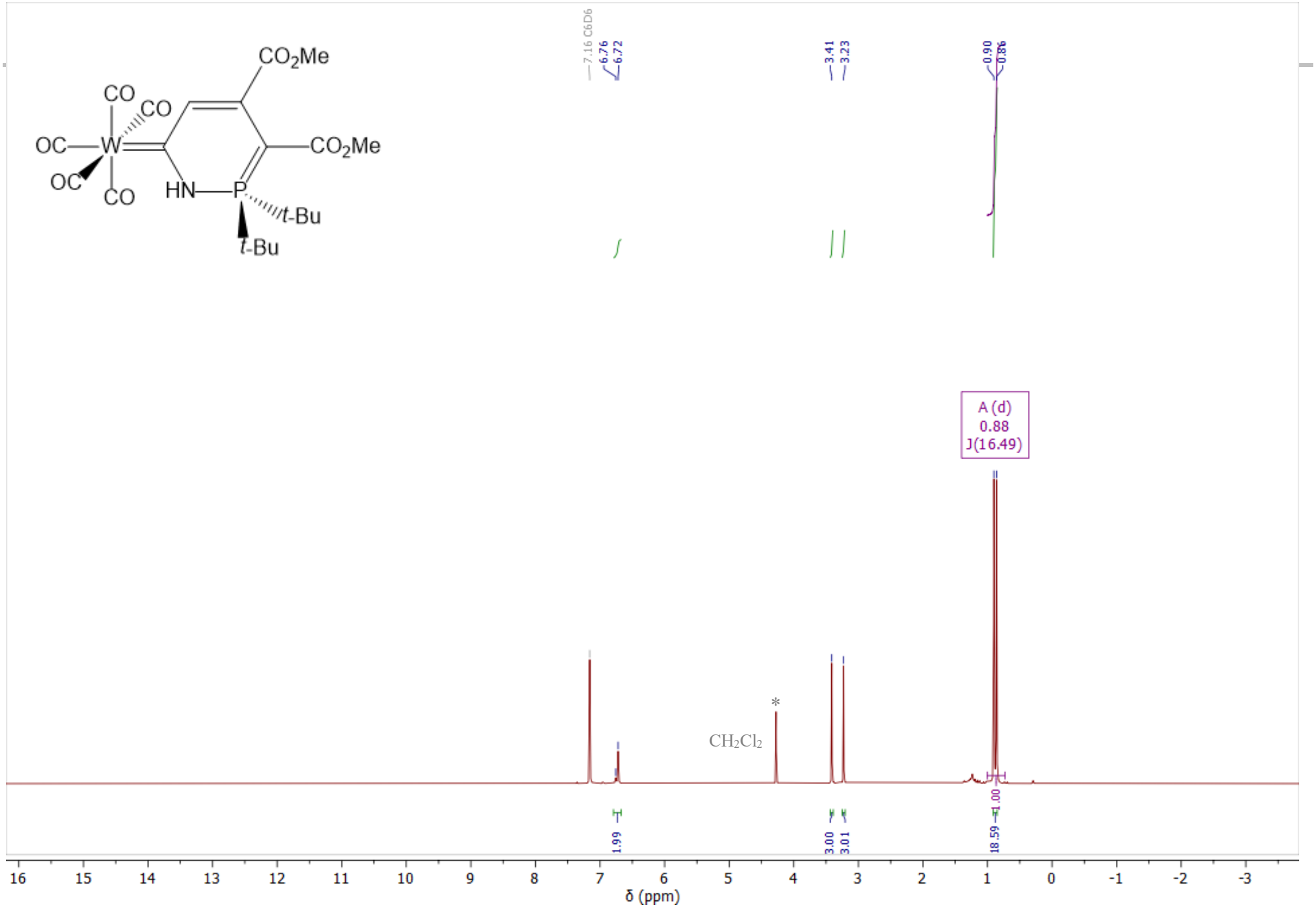

Figure S56: The ^{1}H NMR spectrum of [W{CN(H)P^{t}Bu$_2$C(CO$_2$Me)C(CO$_2$Me)CH}(CO)$_5$] (C_6D_6, 400 MHz, 25 °C).

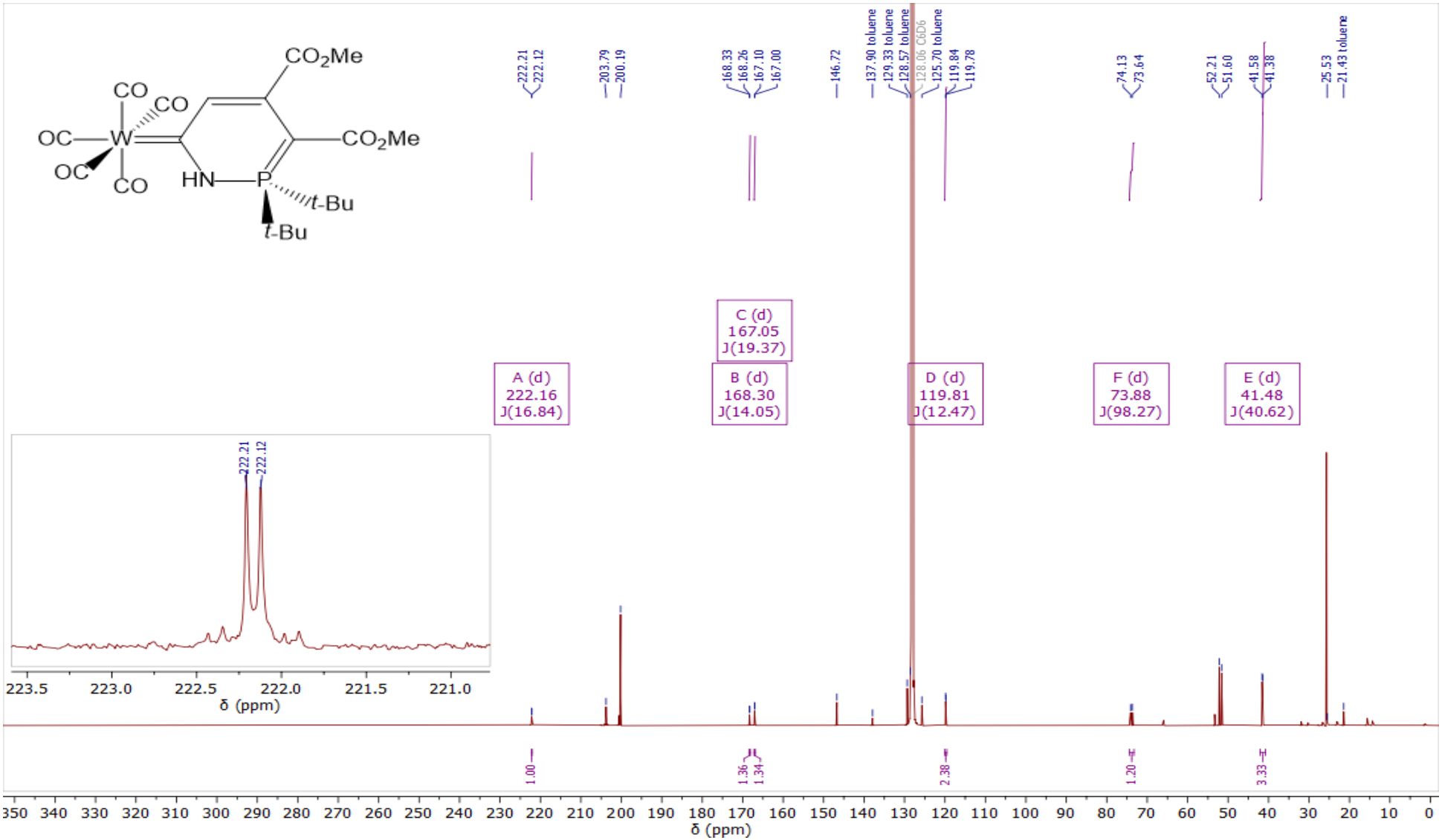

Figure S57: The $^{13}C\{^{1}H\}$ NMR spectrum of [W{CN(H)P^{t}Bu$_2$C(CO$_2$Me)C(CO$_2$Me)CH}(CO)$_5$] (C_6D_6, 201 MHz, 25 °C).

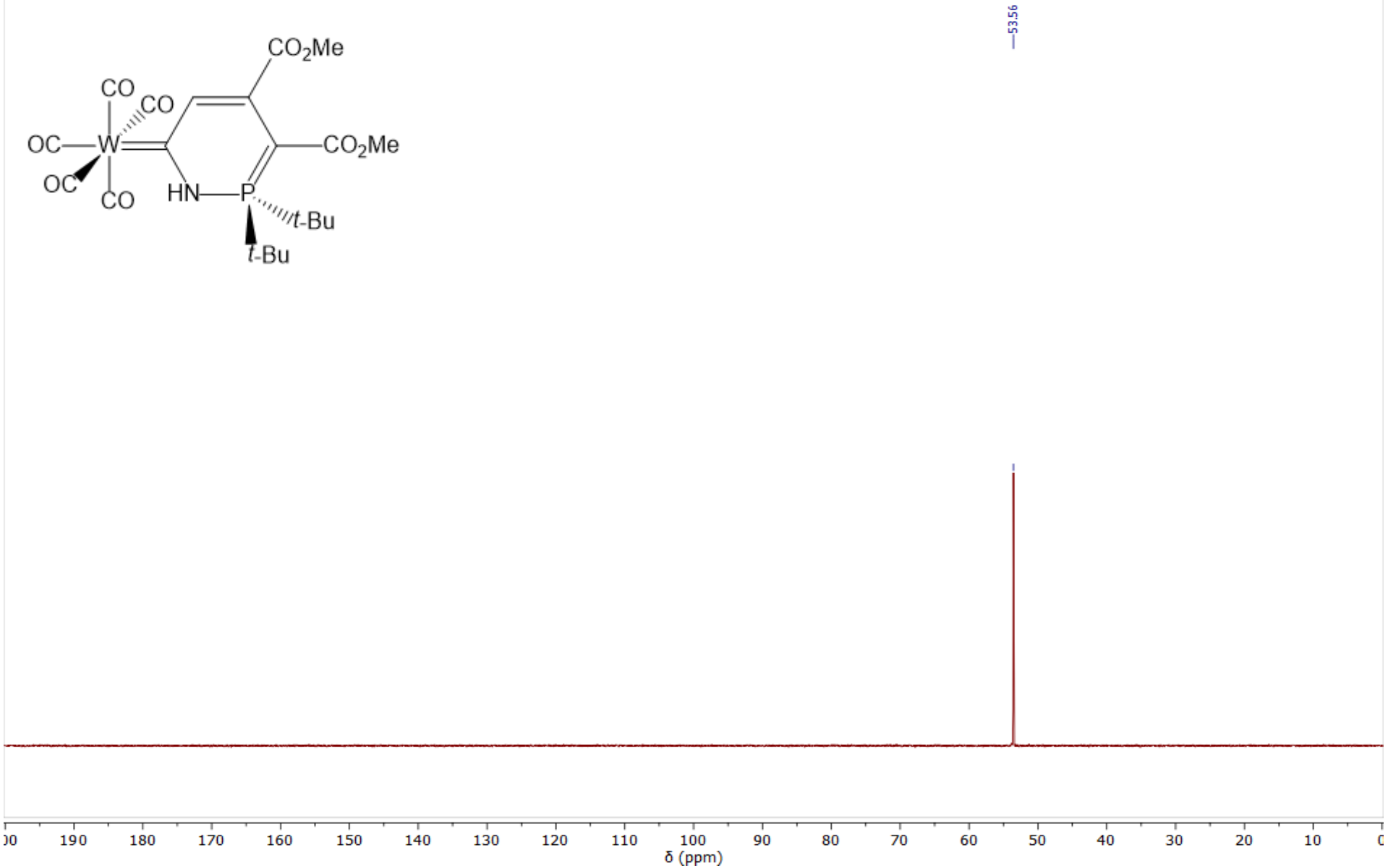

Figure S58: The $^{31}P\{^{1}H\}$ NMR spectrum of [W{CN(H)P^{t}Bu$_2$C(CO$_2$Me)C(CO$_2$Me)CH}(CO)$_5$] (C_6D_6, 162 MHz, 25 °C).

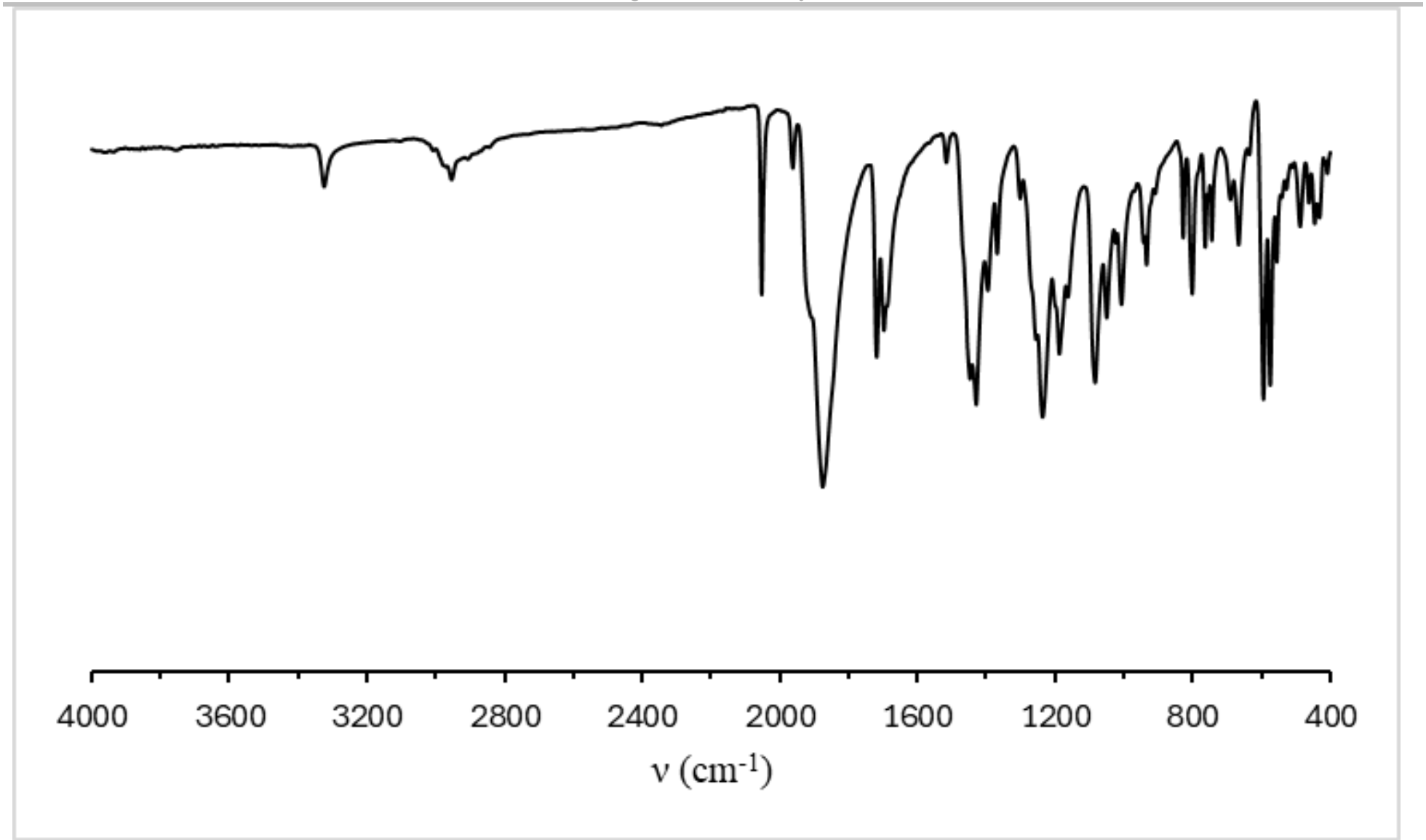

Figure S59: IR spectrum (ATR) of [W{CN(H)P^{t}Bu$_2$C(CO$_2$Me)C(CO$_2$Me)CH}(CO)$_5$].

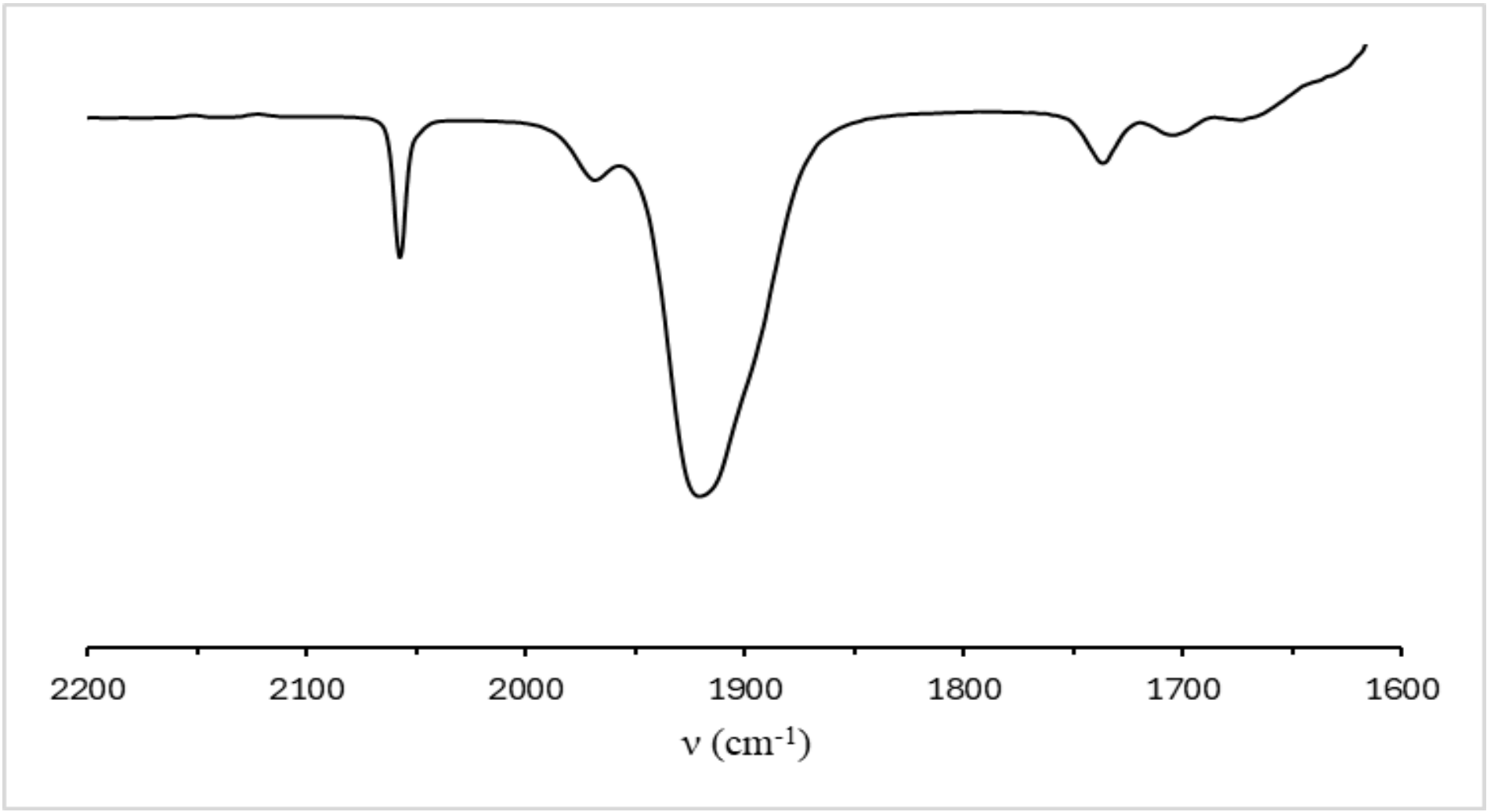

Figure S60: IR spectrum (CH_2Cl_2) of [W{CN(H)P^{t}Bu$_2$C(CO_2Me)C(CO_2Me)CH}(CO)$_5$].

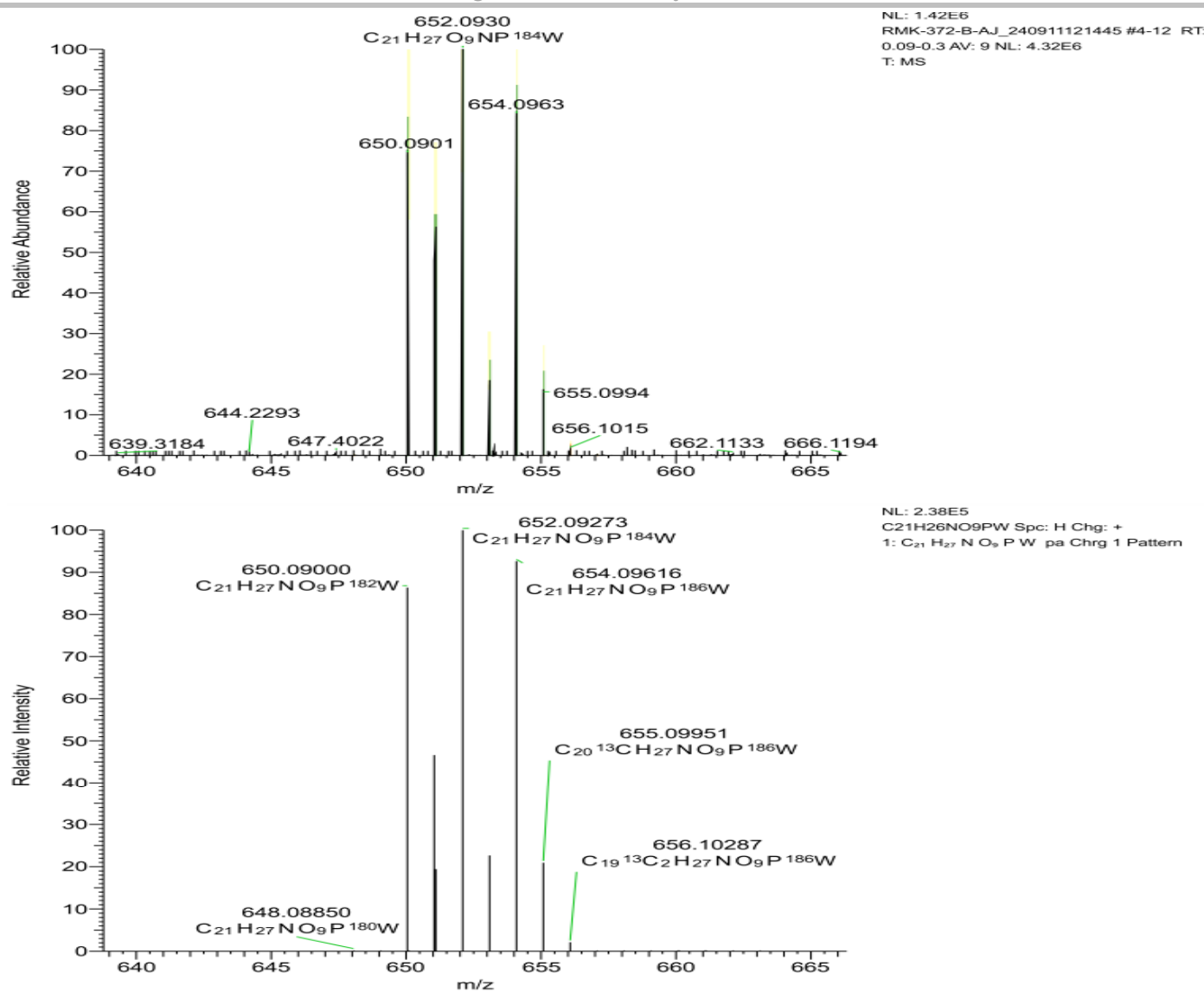

Figure S61: The HR-MS of [W{CN(H)P^{t}Bu$_2$C(CO$_2$Me)C(CO$_2$Me)CH}(CO)$_5$] (ESI, MeCN, [*M* + H]$^+$ ion).

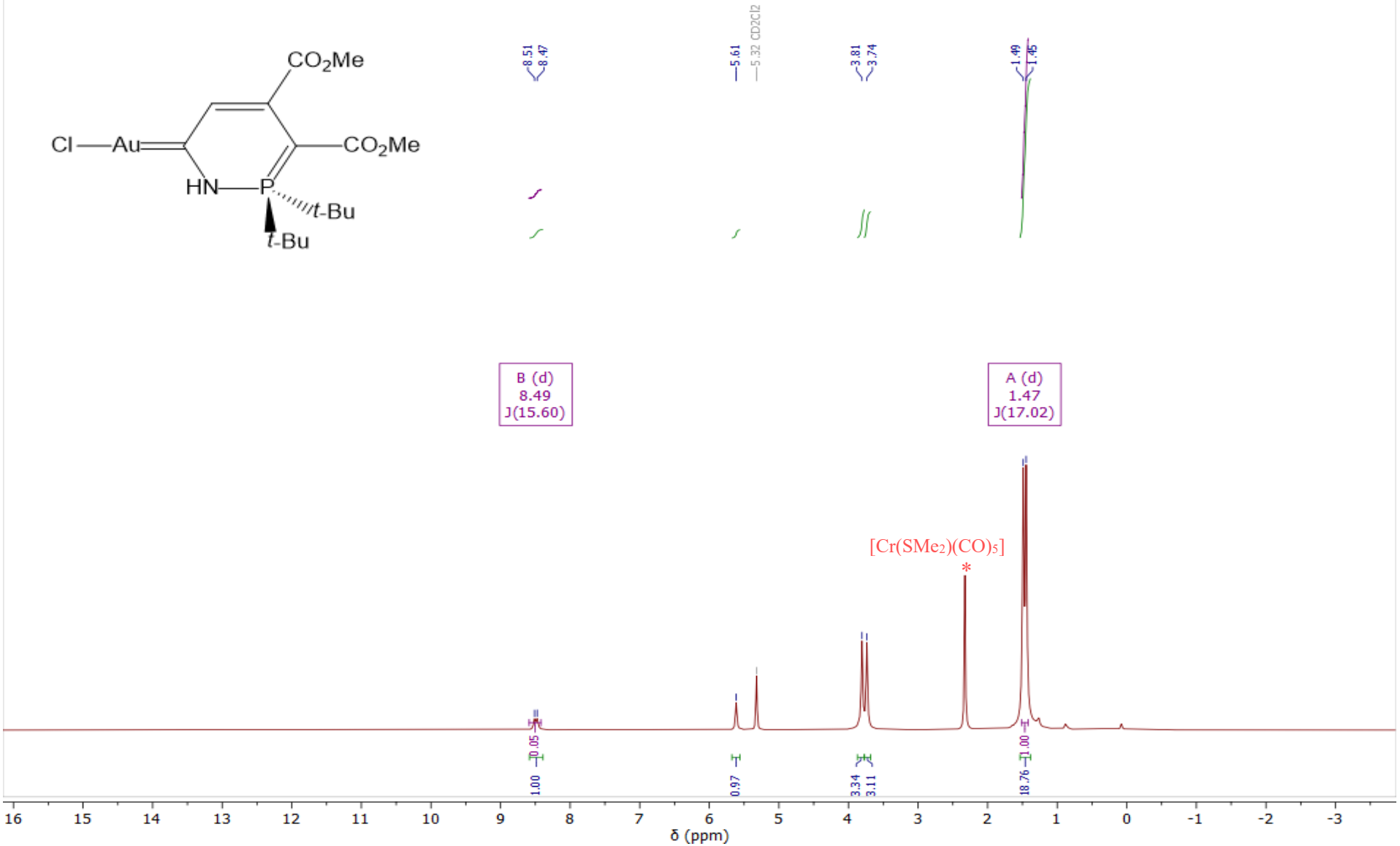

Figure S62: The ^{1}H NMR spectrum of crude [AuCl{CNHP^{i}Bu$_2$C(CO$_2$Me)C(CO$_2$Me)CH}] (CD2Cl2, 400 MHz, 25 °C).

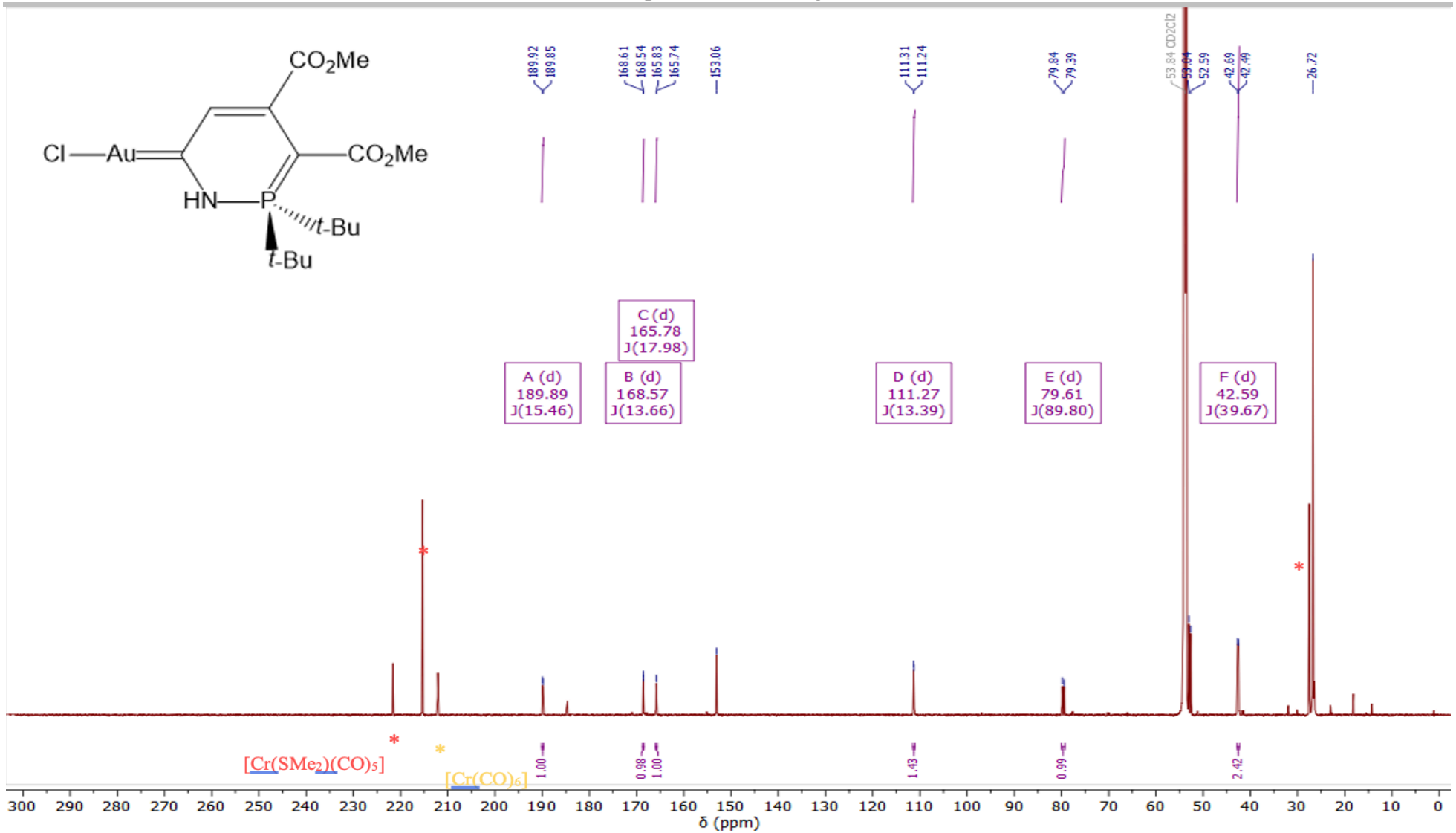

Figure S63: The $^{13}C\{^{1}H\}$ NMR spectrum of crude [AuCl{CN(H)P^{t}Bu$_2$C(CO$_2$Me)C(CO$_2$Me)CH}] (CD_2Cl_2, 201 MHz, 25 °C).

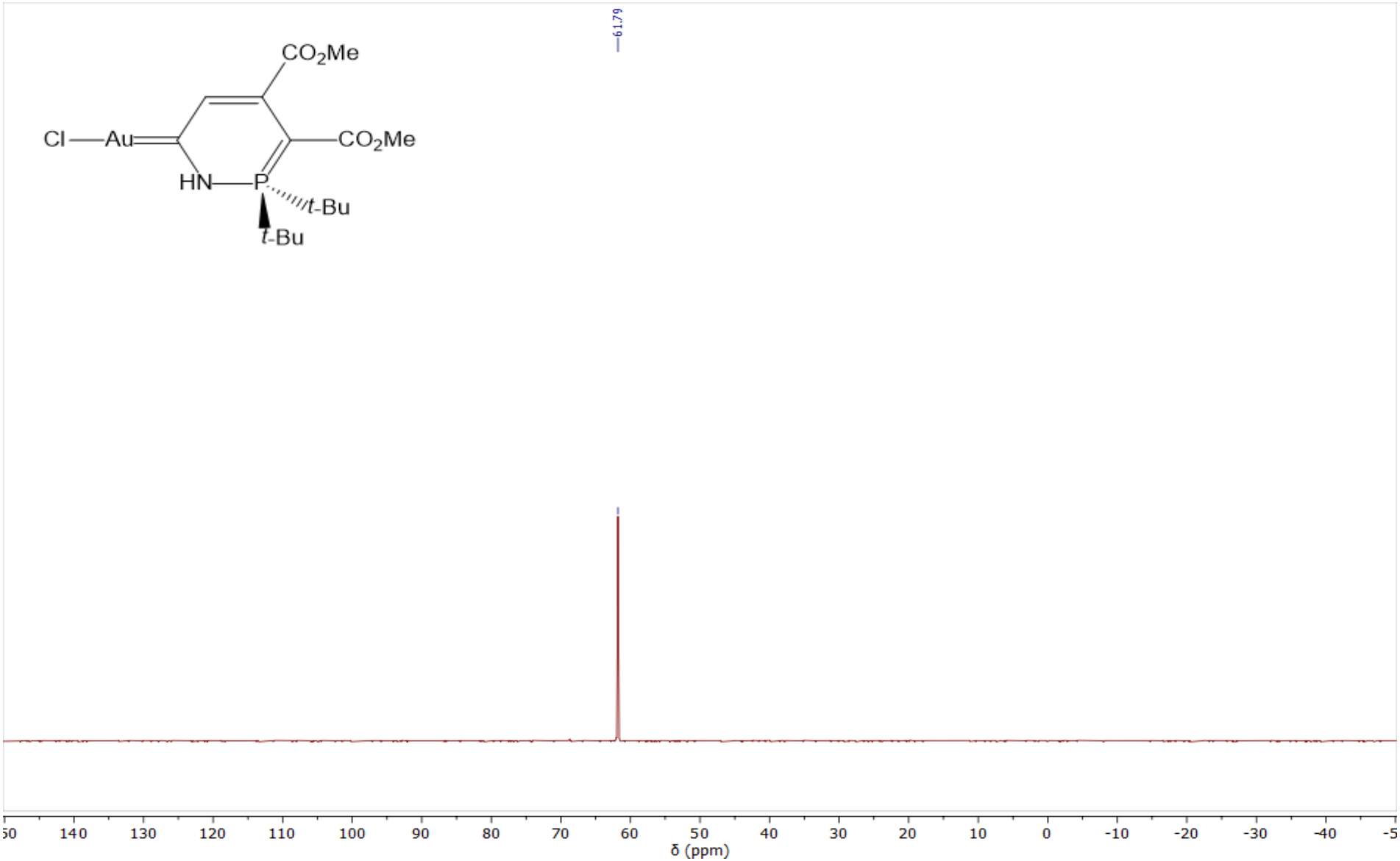

Figure S64: The $^{31}P\{^{1}H\}$ NMR spectrum of crude [AuCl{CN(H)P^{t}Bu$_2$C(CO$_2$Me)C(CO$_2$Me)CH}] (CD_2Cl_2, 162 MHz, 25 °C).

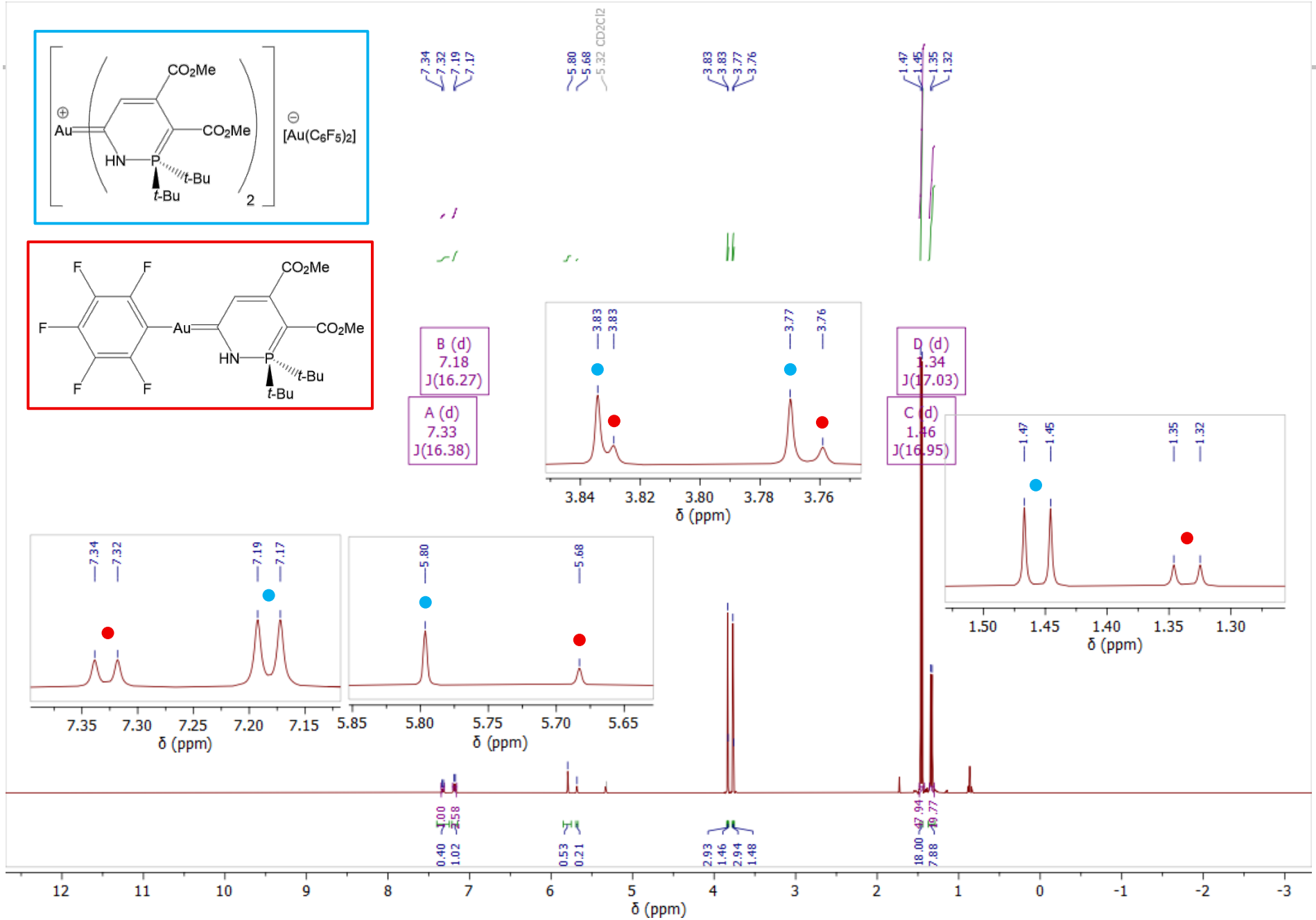

Figure S65: The ^{1}H NMR spectrum of $[Au\{CN(H)P^{t}Bu_2C(CO_2Me)C(CO_2Me)CH\}_2][Au(C_6F_5)_2]$ and $[Au(C_6F_5)\{CN(H)P^{t}Bu_2C(CO_2Me)C(CO_2Me)CH\}]$ (CD_2Cl_2, 800 MHz, 25 °C).

Figure S66: The $^{13}C\{^{1}H\}$ NMR spectrum of $[Au\{CN(H)P^tBu_2C(CO_2Me)C(CO_2Me)CH\}_2][Au(C_6F_5)_2]$ and $[Au(C_6F_5)\{CN(H)P^tBu_2C(CO_2Me)C(CO_2Me)CH\}]$ (CD_2Cl_2, 201 MHz, 25 °C).

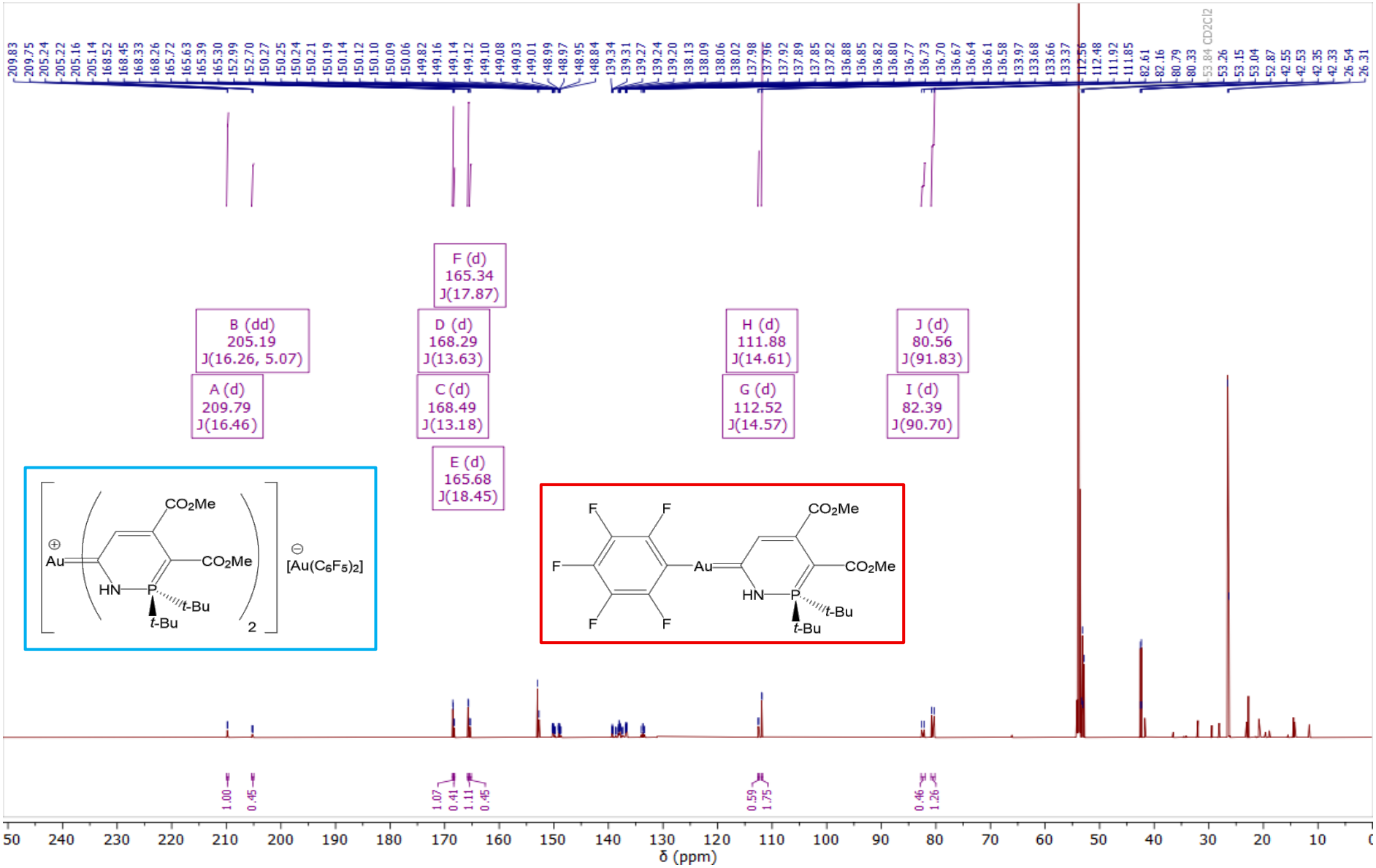

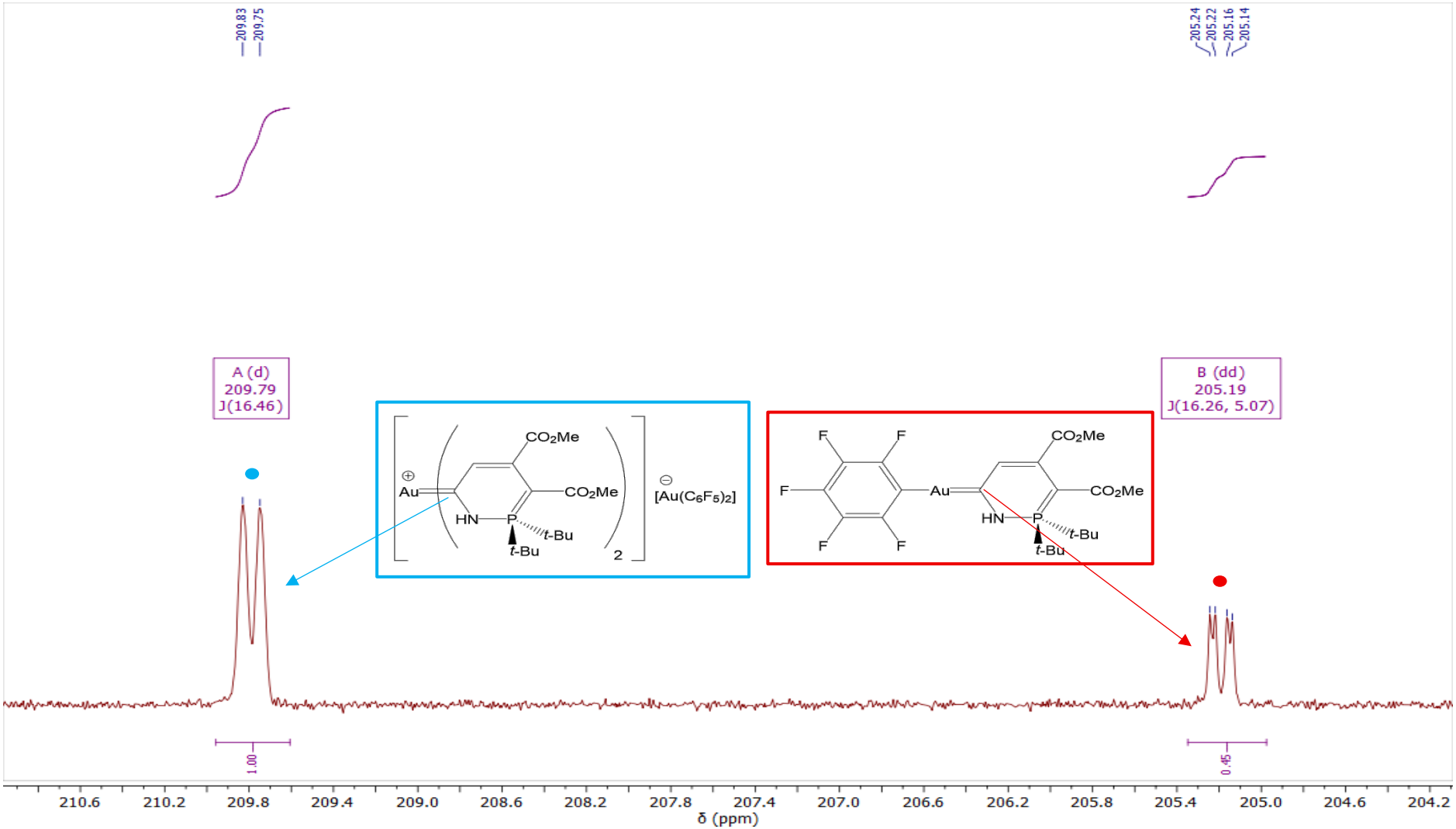

Figure S67: Expansion of the $^{13}C\{^{1}H\}$ NMR spectrum shown from previous spectrum (S66) highlighting carbene signals (CD_2Cl_2, 201 MHz, 25 °C).

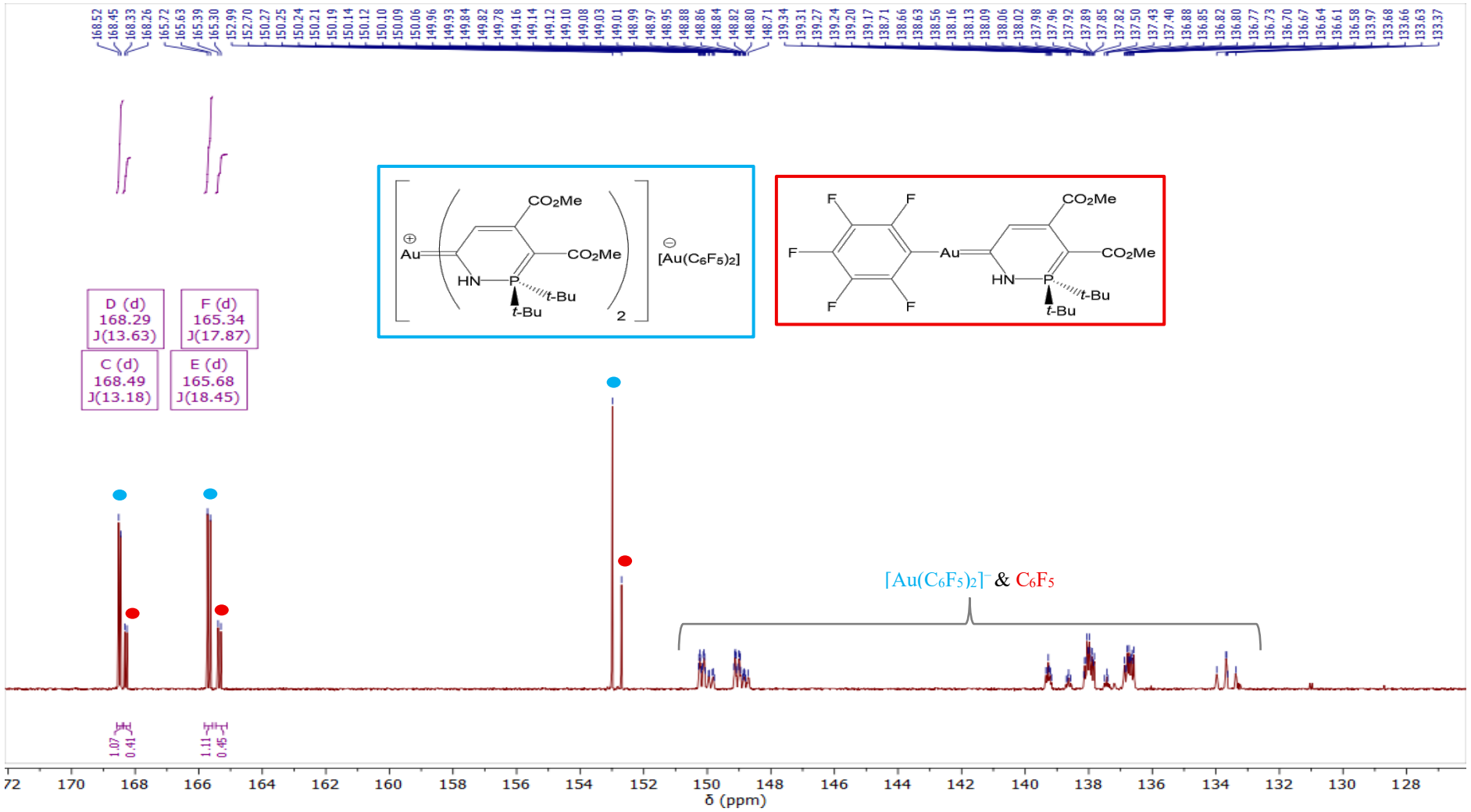

Figure S68: Expansion of the $^{13}C\{^{1}H\}$ NMR spectrum shown in Figure 66 highlighting methyl ester, allylic, and C_6F_5 signals (CD_2Cl_2, 201 MHz, 25 °C).

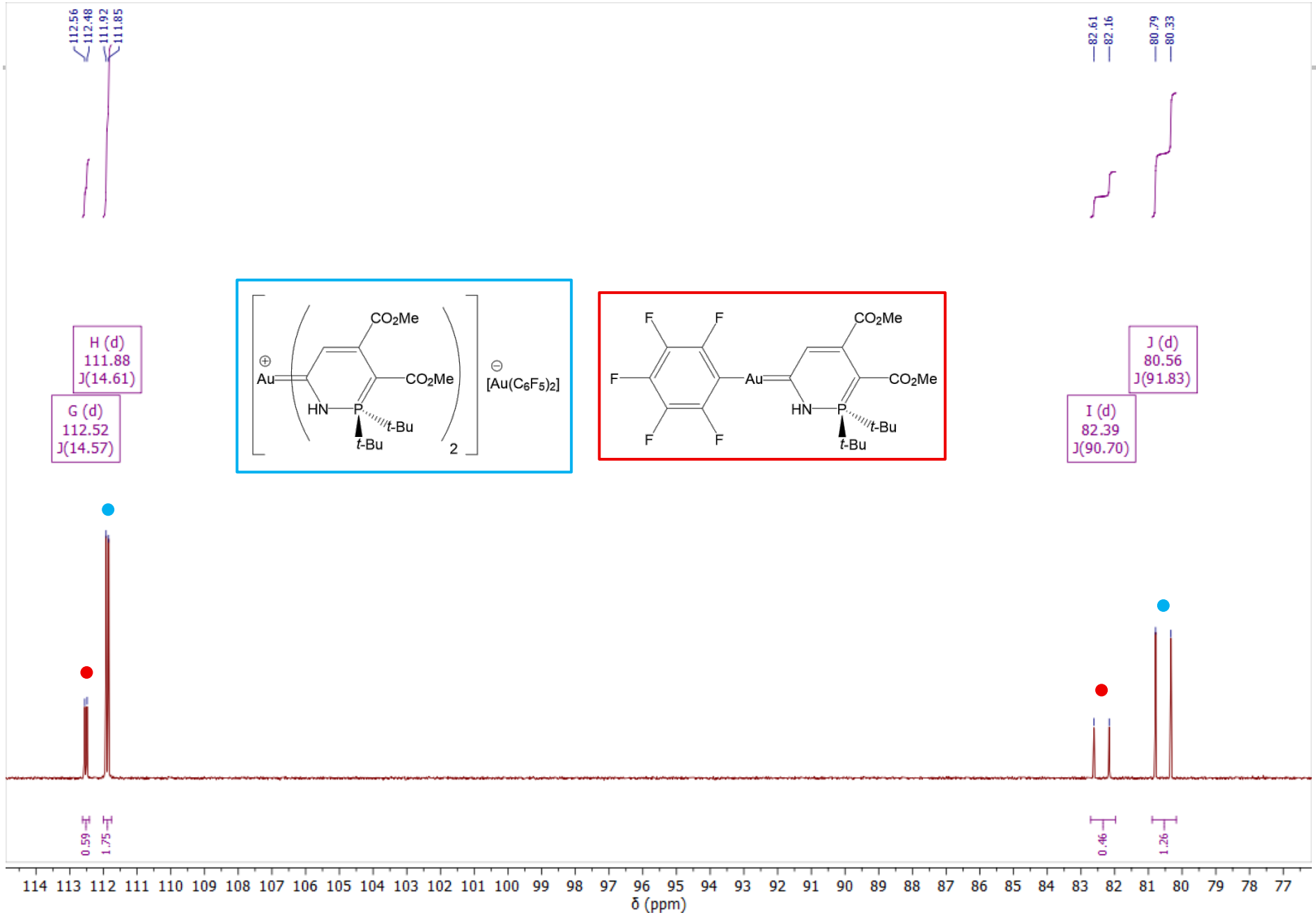

Figure S69: Expansion of the $^{13}C\{^{1}H\}$ NMR spectrum shown in Figure 66 highlighting allylic signals.

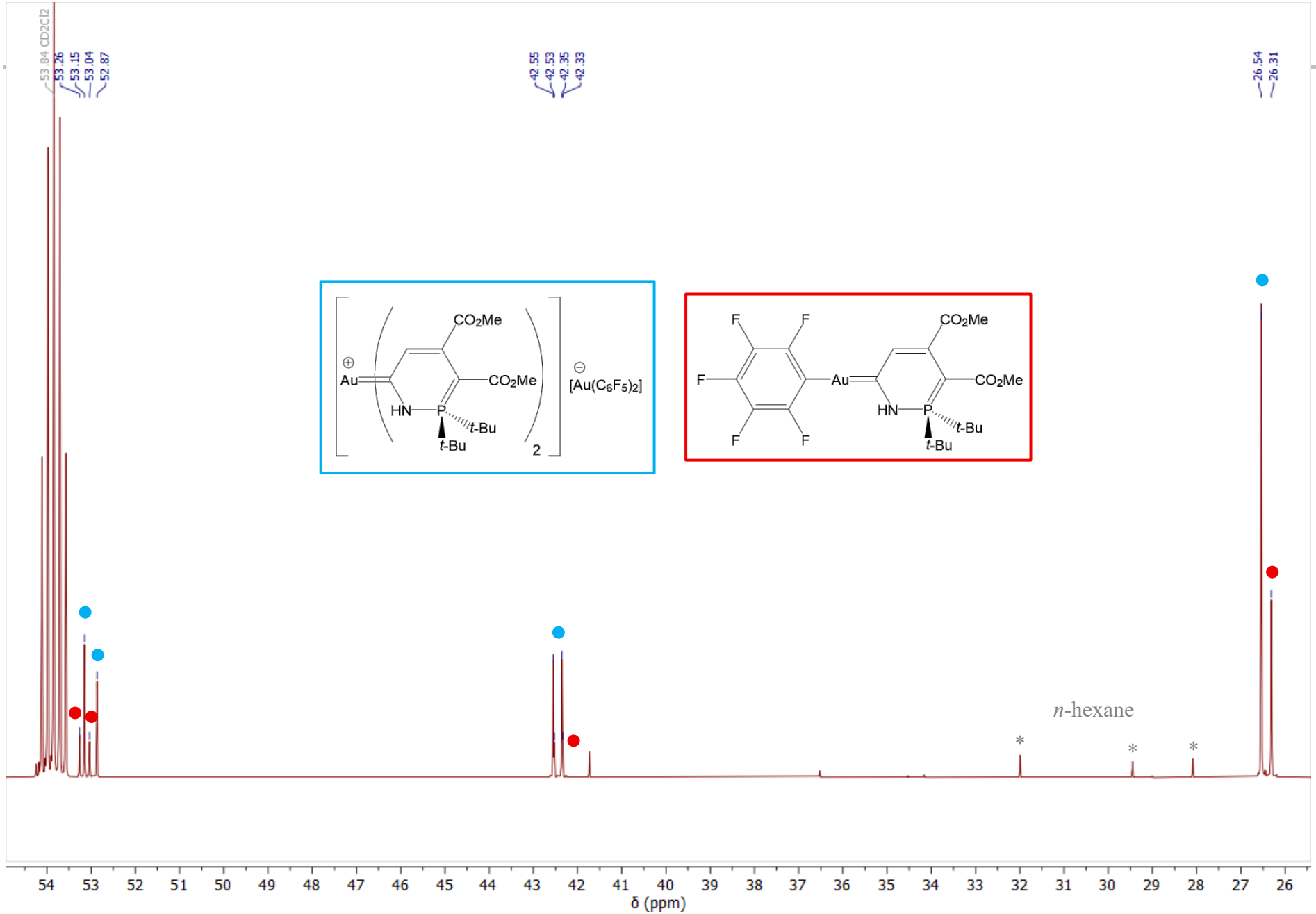

Figure S70: Expansion of the $^{13}C\{^{1}H\}$ NMR spectrum shown in Figure 66 highlighting alkyl signals.

Figure S71: The $^{19}F\{^{1}H\}$ NMR spectrum of $[Au\{CN(H)P^tBu_2C(CO_2Me)C(CO_2Me)CH\}_2][Au(C_6F_5)_2]$ and $[Au(C_6F_5)\{CN(H)P^tBu_2C(CO_2Me)C(CO_2Me)CH\}]$ (CD_2Cl_2, 376 MHz, 25 °C).

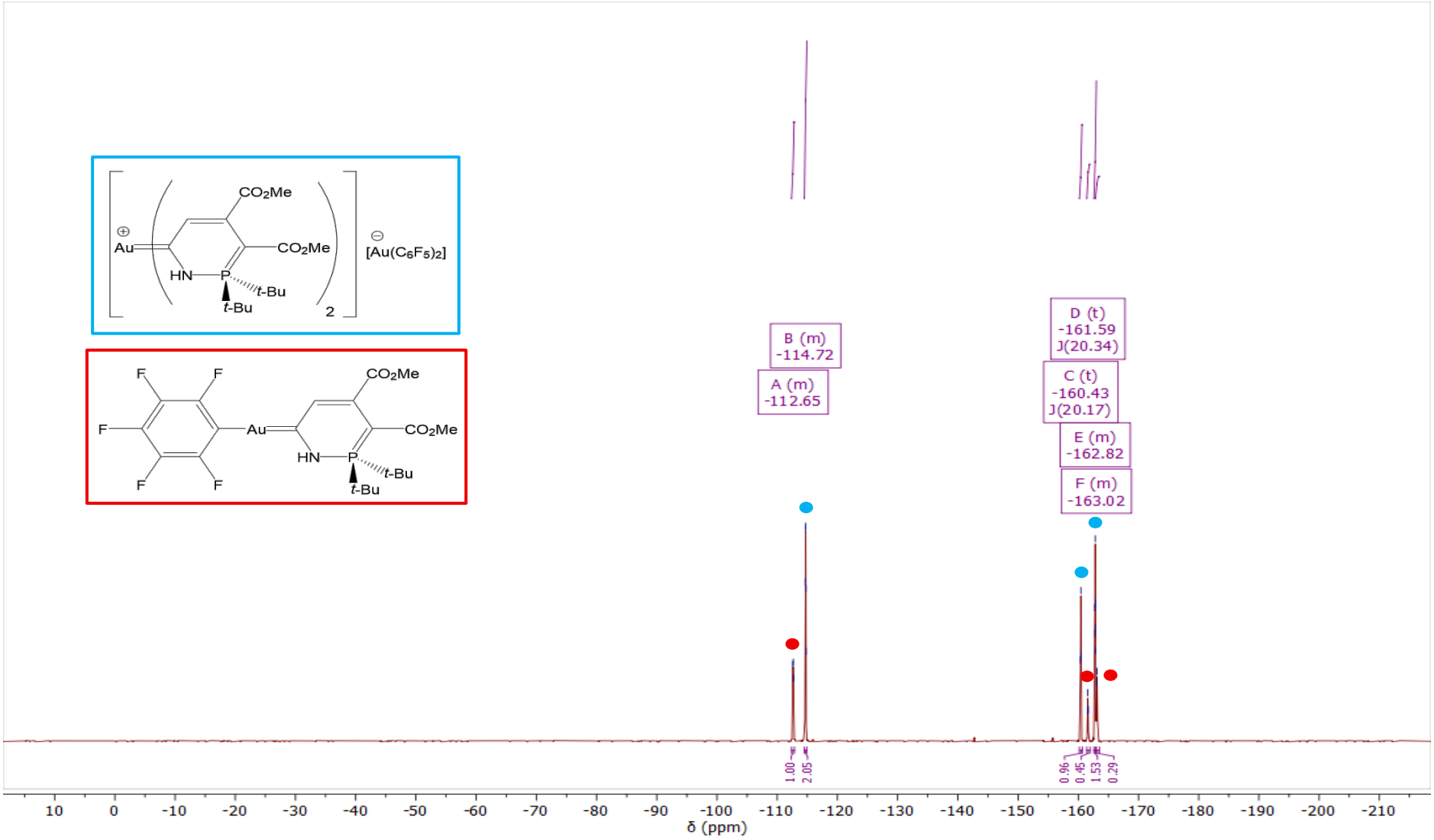

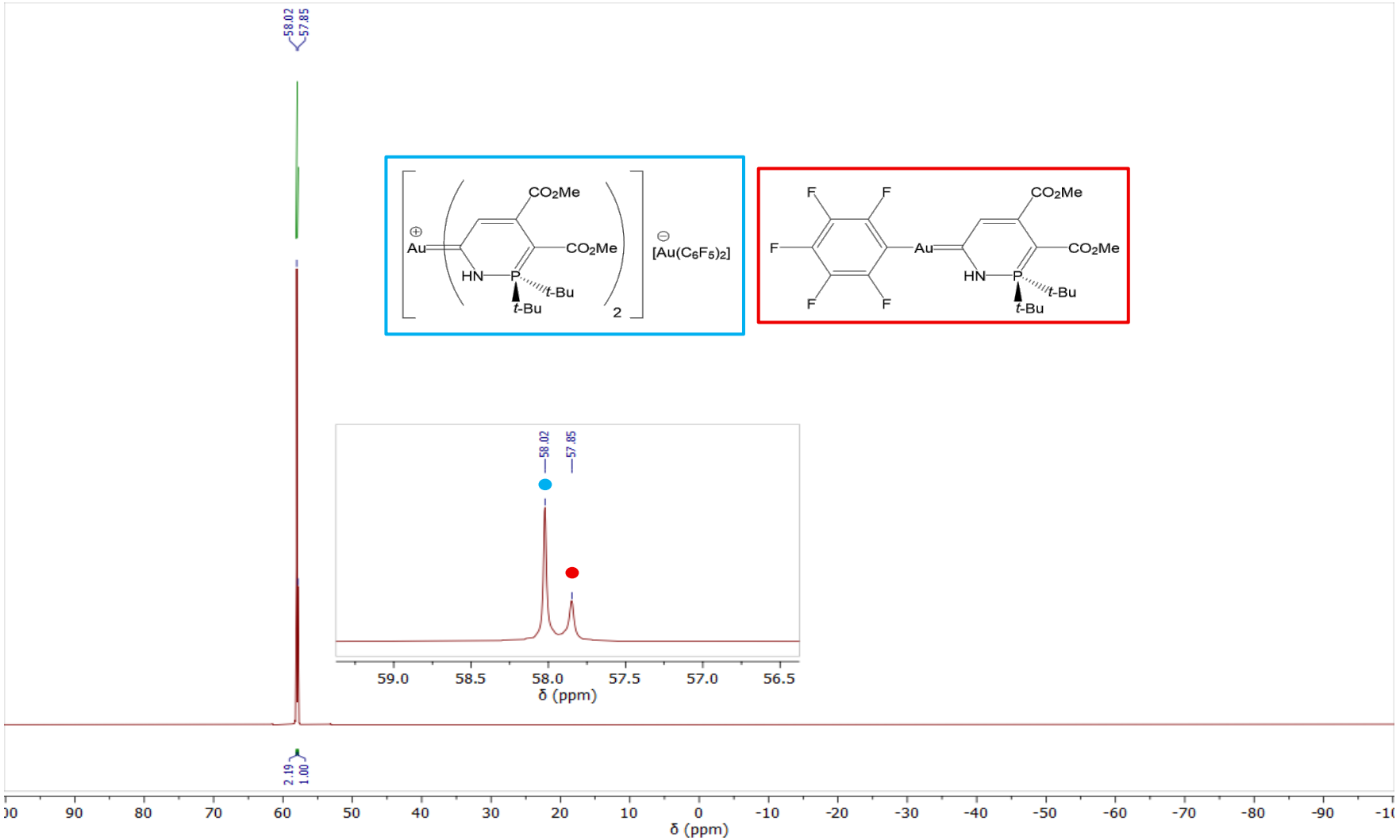

Figure S72: The $^{31}P\{^{1}H\}$ NMR spectrum of [Au{CN(H)P^{t}Bu$_2$C(CO$_2$Me)C(CO$_2$Me)CH}$_2$][Au(C$_6$F$_5$)$_2$] and [Au(C$_6$F$_5$){CN(H)P^{t}Bu$_2$C(CO$_2$Me)C(CO$_2$Me)CH}] (CD_2Cl_2, 162 MHz, 25 °C).

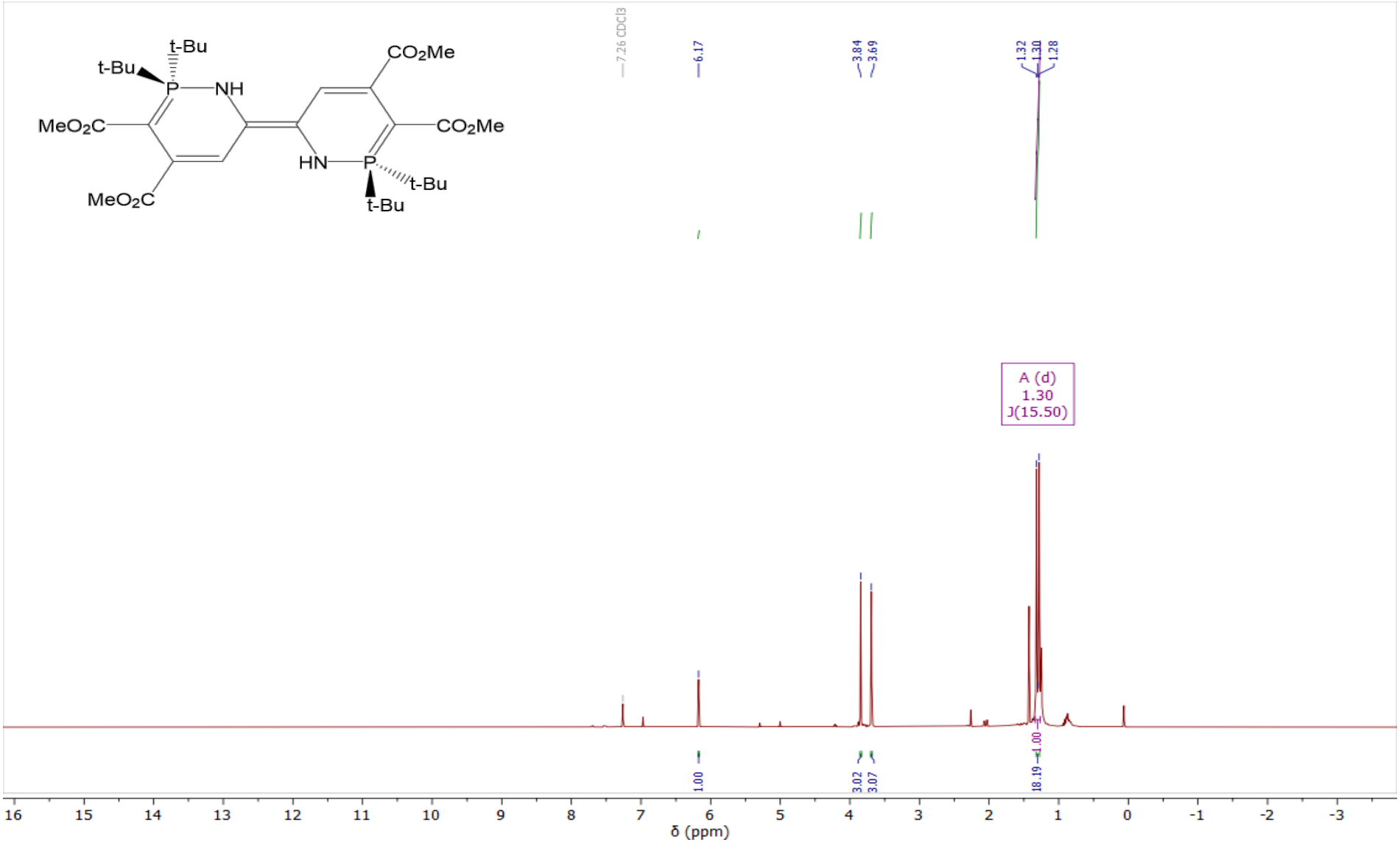

Figure S73: The ^{1}H NMR spectrum of crude *E*-{CN(H)P^{t}Bu$_2$C(CO$_2$Me)C(CO$_2$Me)CH}$_2$ (CDCl$_3$, 400 MHz, 25 °C).

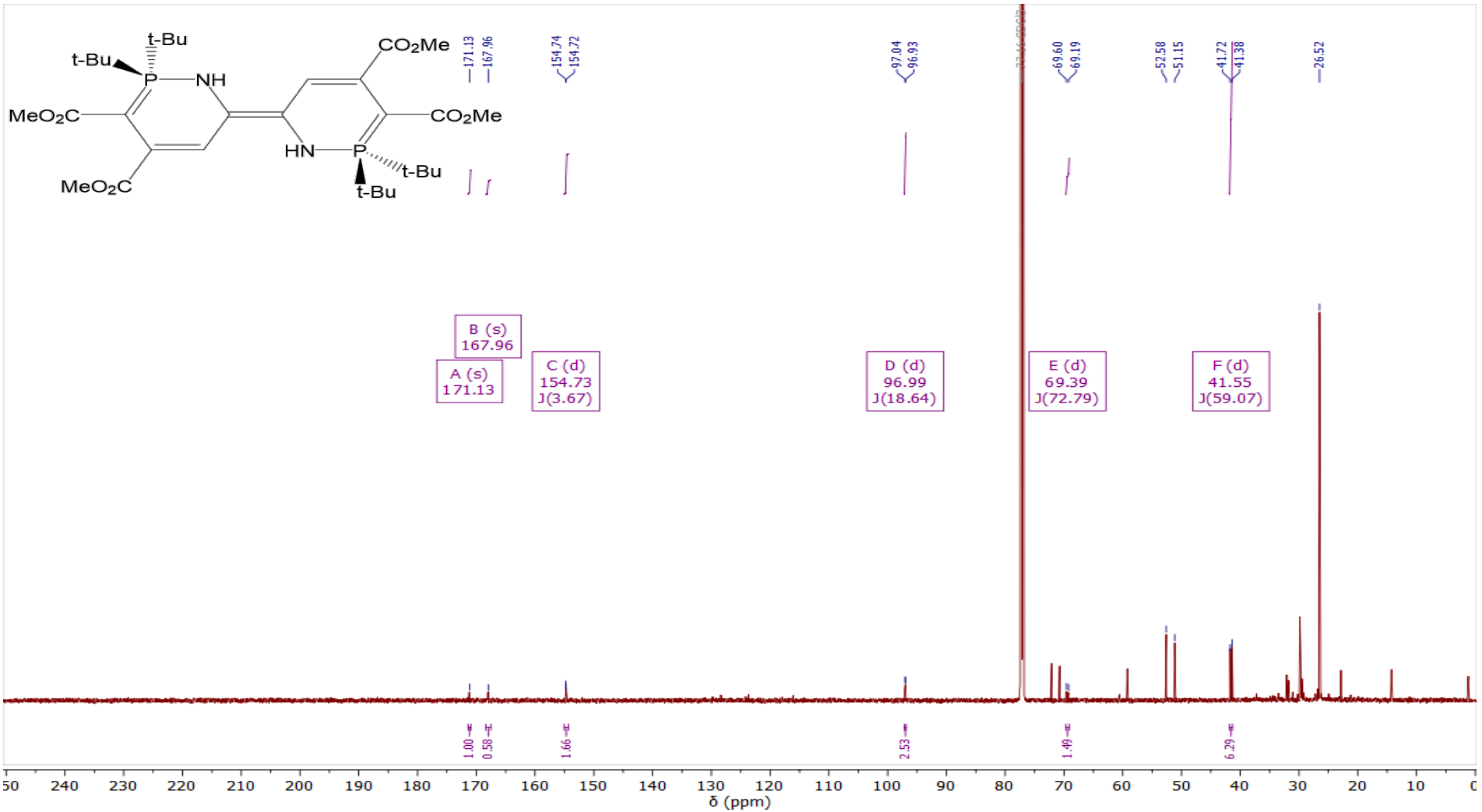

Figure S74: The $^{13}C\{^{1}H\}$ NMR spectrum of crude *E*-{CN(H)P^{t}Bu$_2$C(CO$_2$Me)C(CO$_2$Me)CH}$_2$ (CDCl$_3$, 176 MHz, 25 °C).

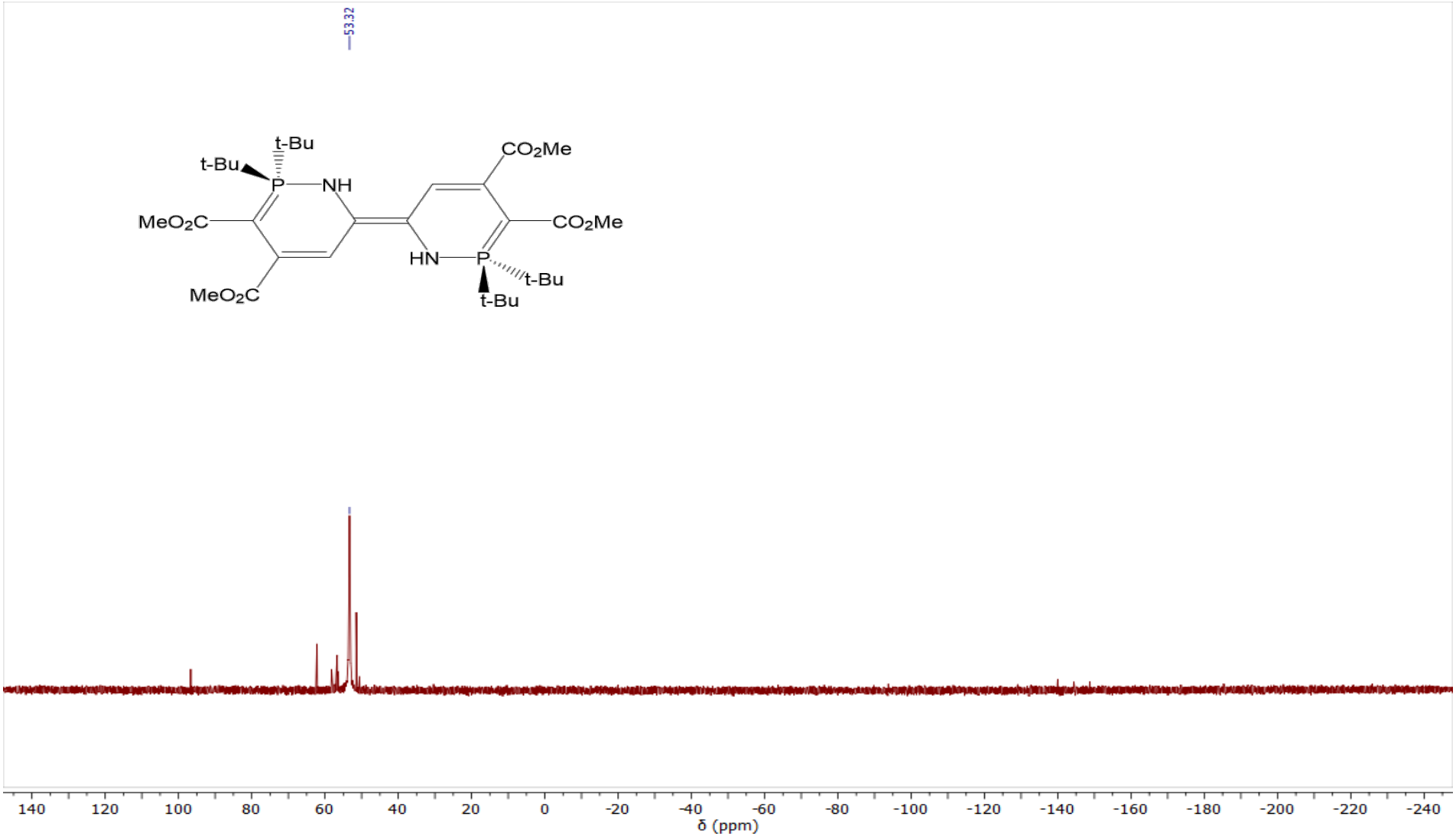

Figure S75: The $^{31}P\{^{1}H\}$ NMR spectrum of crude *E*-{CN(H)P^{t}Bu$_2$C(CO$_2$Me)C(CO$_2$Me)CH}$_2$ (CDCl$_3$, 162 MHz, 25 °C).

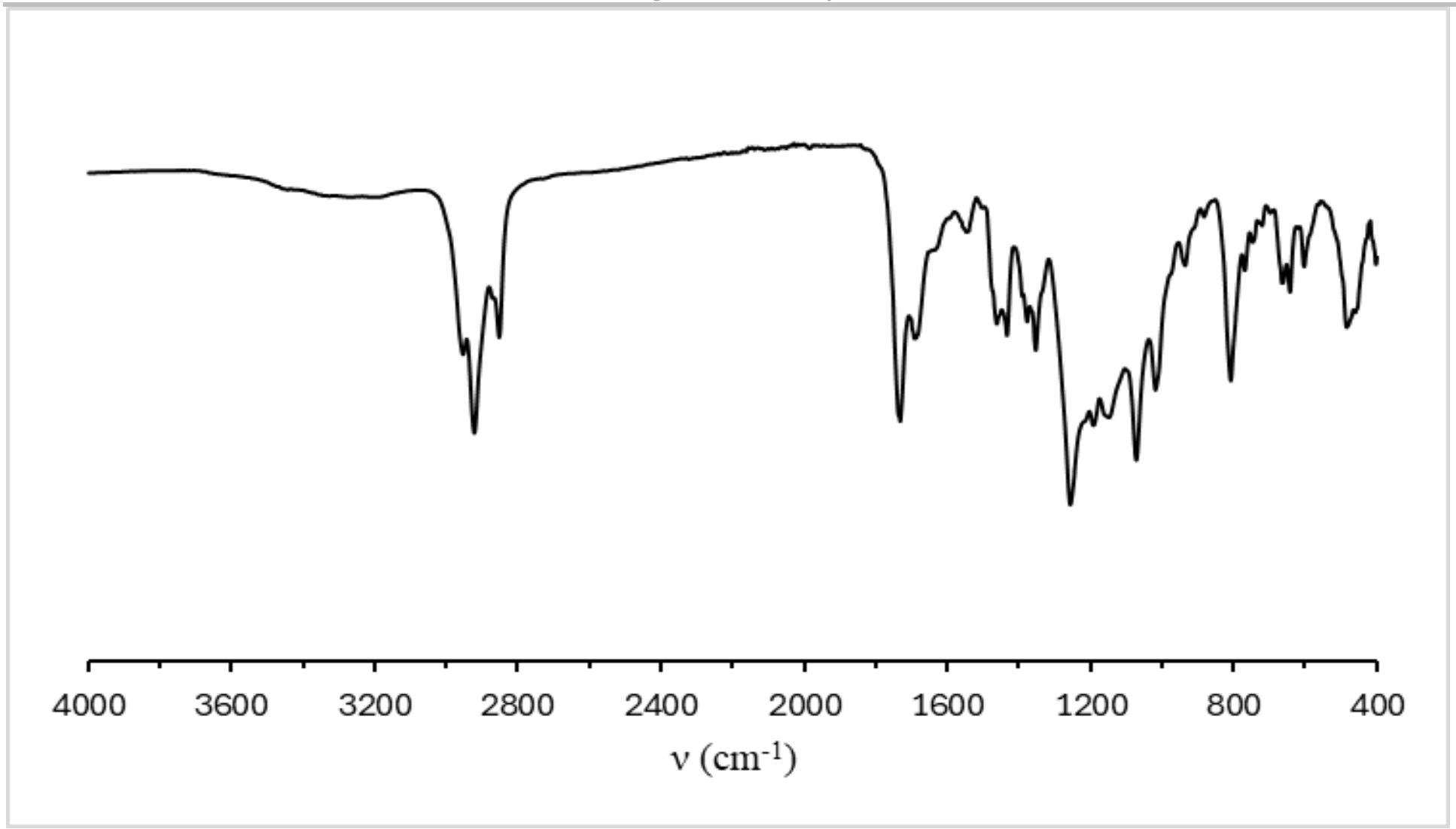

Figure S76: The ATR IR spectrum of crude *E*-{CN(H)P^{t}Bu$_2$C(CO$_2$Me)C(CO$_2$Me)CH}$_2$.

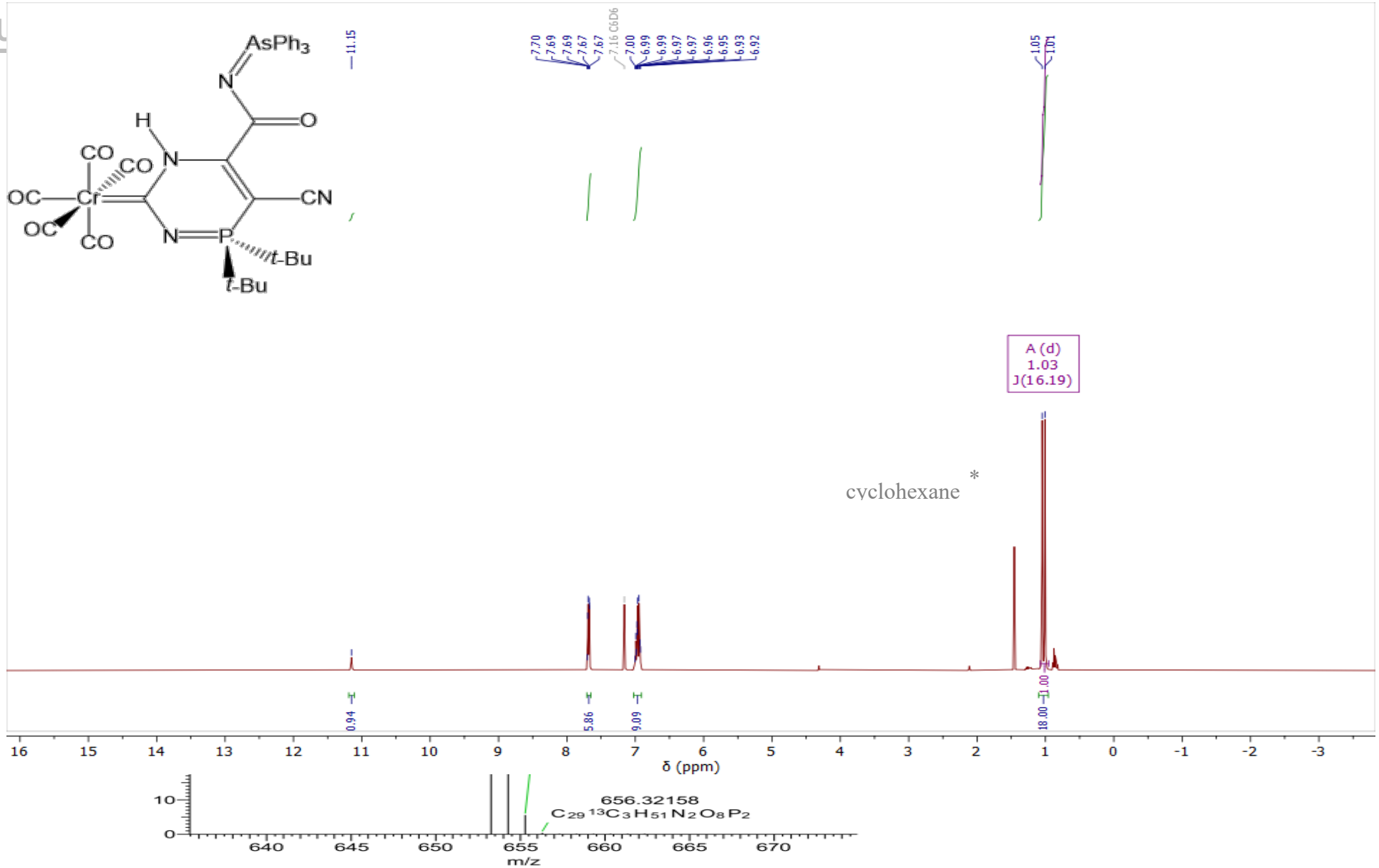

Figure S77: The HR-MS of *E*-{CN(H)P^{t}Bu$_2$C(CO$_2$Me)C(CO$_2$Me)CH}$_2$ (ESI, MeCN, [*M* + H]$^+$ ion).

Figure S78: The ^{1}H NMR spectrum of [Cr{CNP^{i}Bu$_2$C(CN)C(C(O)NAsPh$_3$)NH}(CO)$_5$] (C$_6$D$_6$, 400 MHz, 25 °C).

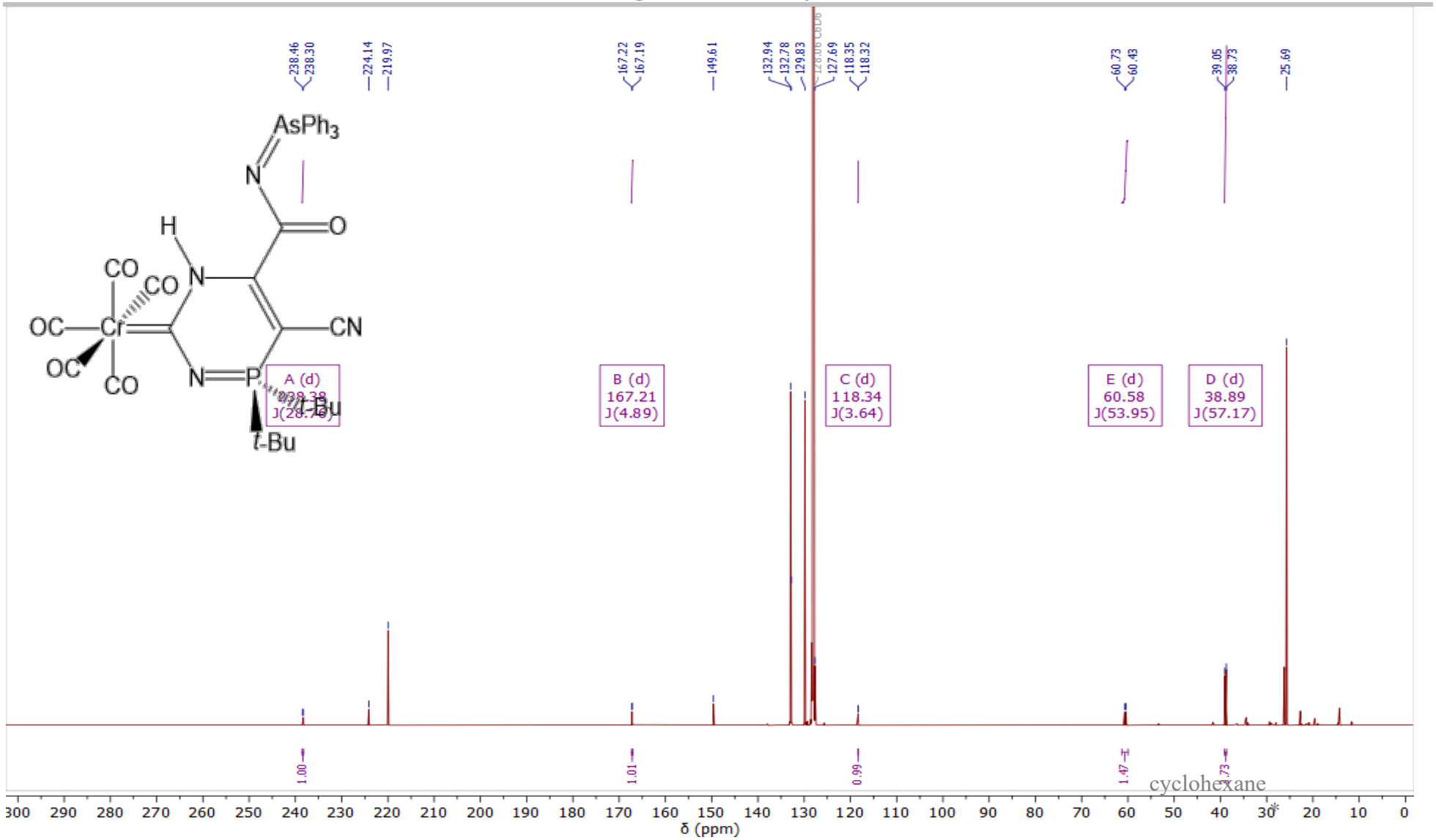

Figure S79: The $^{13}C\{^{1}H\}$ NMR spectrum of [Cr{CNP^{t}Bu$_2$C(CN)C(C(O)NAsPh$_3$)NH}(CO)$_5$] (C_6D_6, 162 MHz, 25 °C).

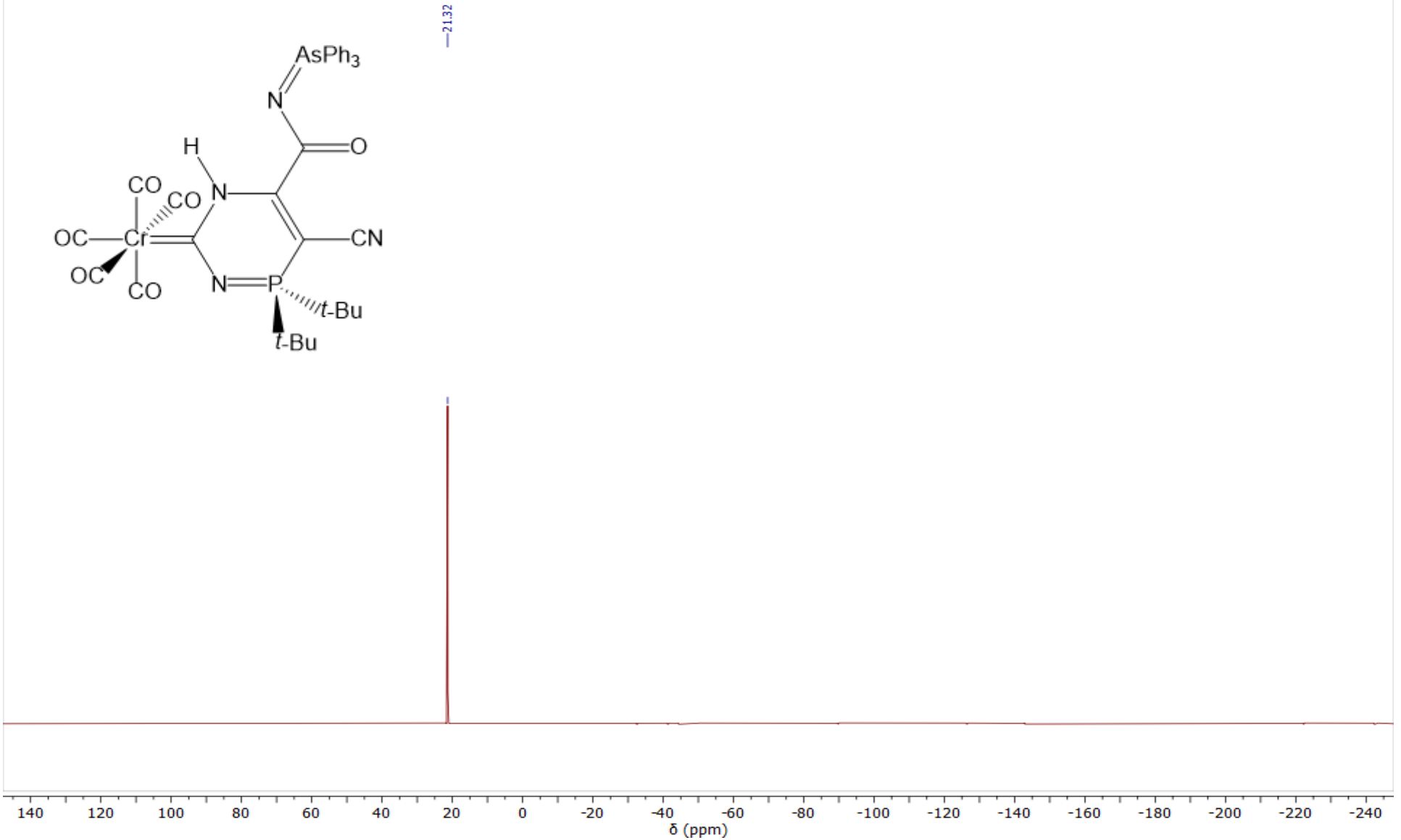

Figure S80: The $^{31}P\{^{1}H\}$ NMR spectrum of [Cr{CNP^{t}Bu$_2$C(CN)C(C(O)NAsPh$_3$)NH}(CO)$_5$] (C_6D_6, 162 MHz, 25 °C).

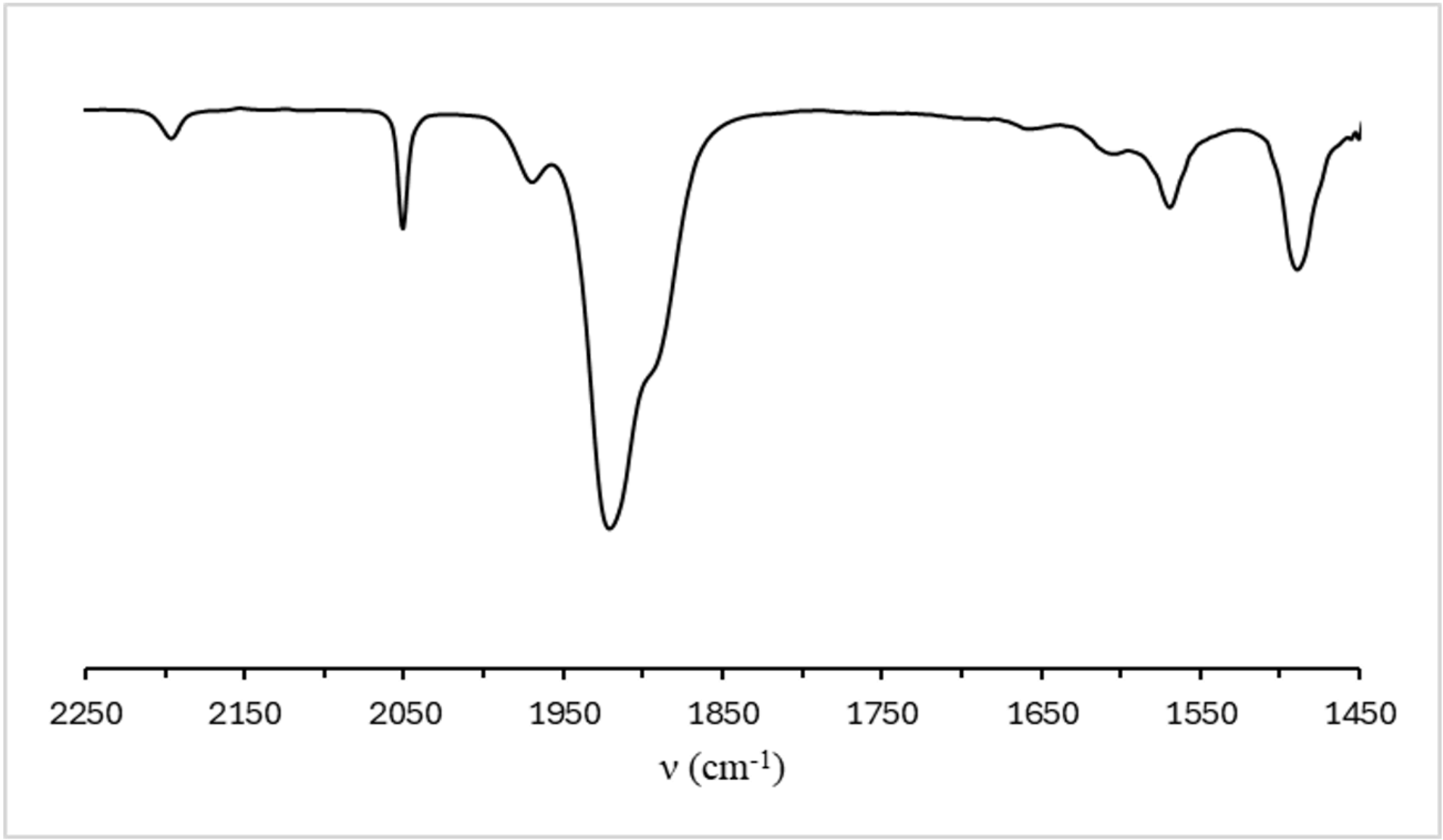

Figure S81: IR spectrum (CH_2Cl_2) of [Cr{CNP^{t}Bu$_2$C(CN)C(C(O)NAsPh$_3$)NH}(CO)$_5$].

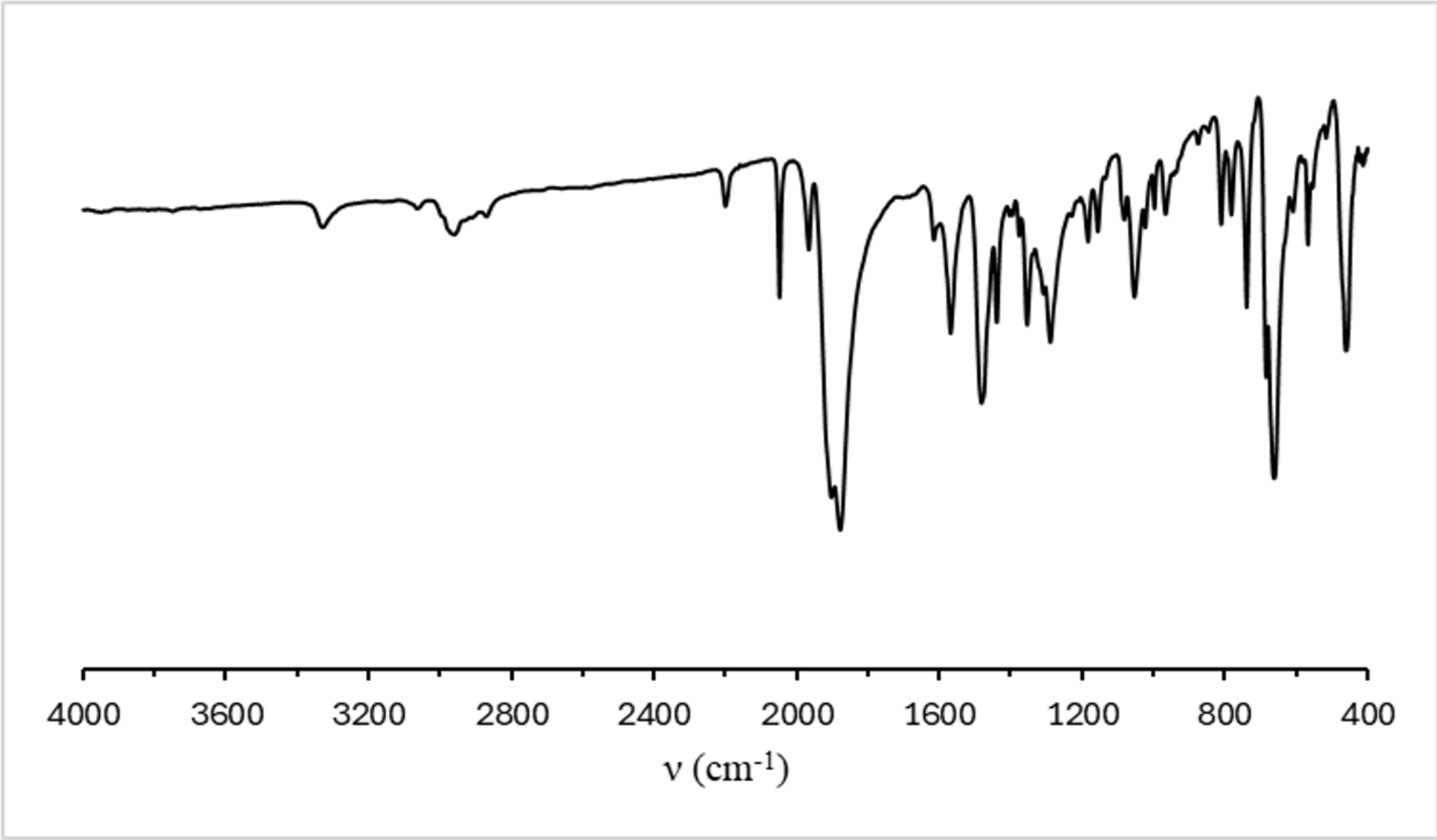

Figure S82: IR spectrum (ATR) of [Cr{CNP^{t}Bu$_2$C(CN)C(C(O)NAsPh$_3$)NH}(CO)$_5$].

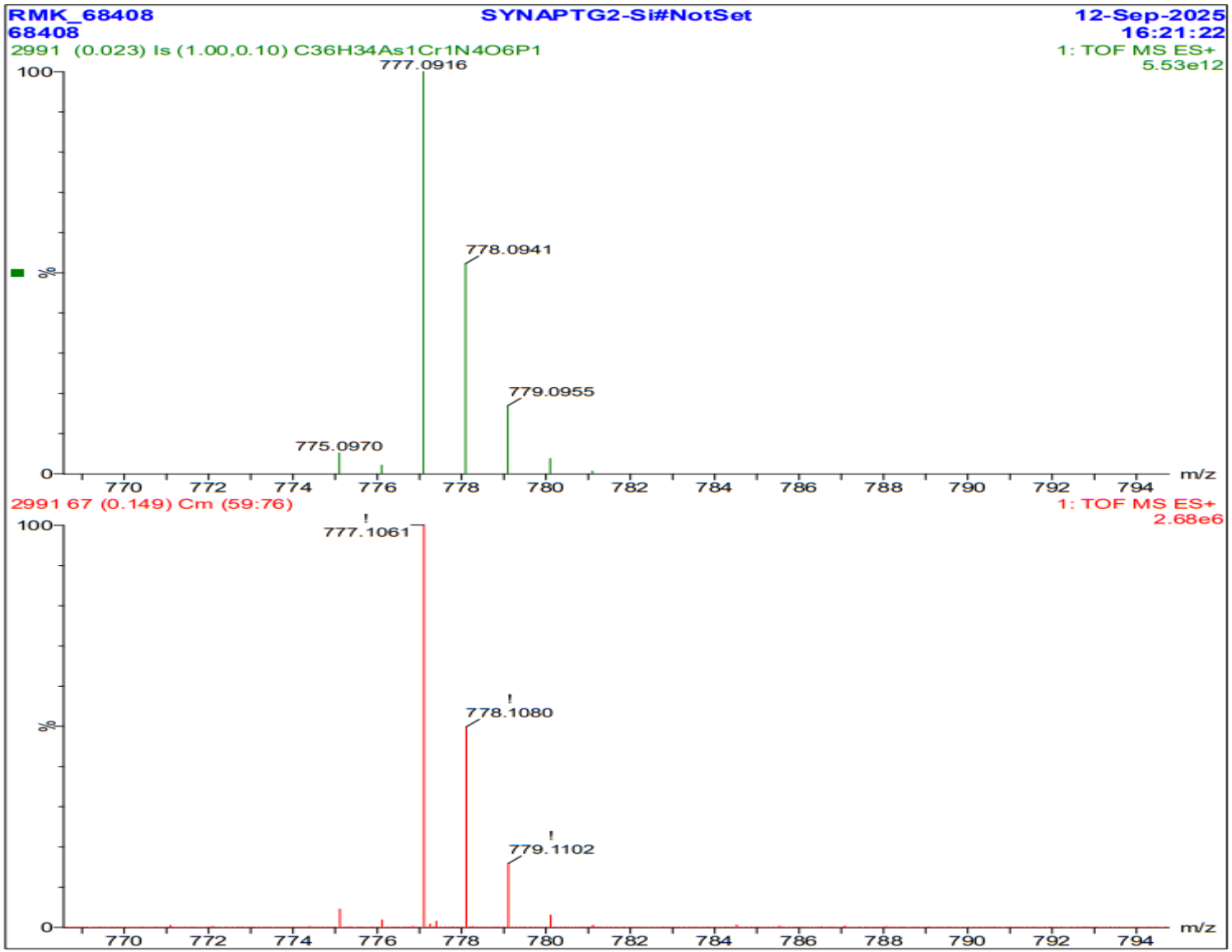

Figure S83: The HR-MS of [Cr{CNP^{t}Bu$_2$C(CN)C(C(O)NAsPh$_3$)NH}(CO)$_5$] (ESI, MeCN, [*M* + H]$^+$ ion).

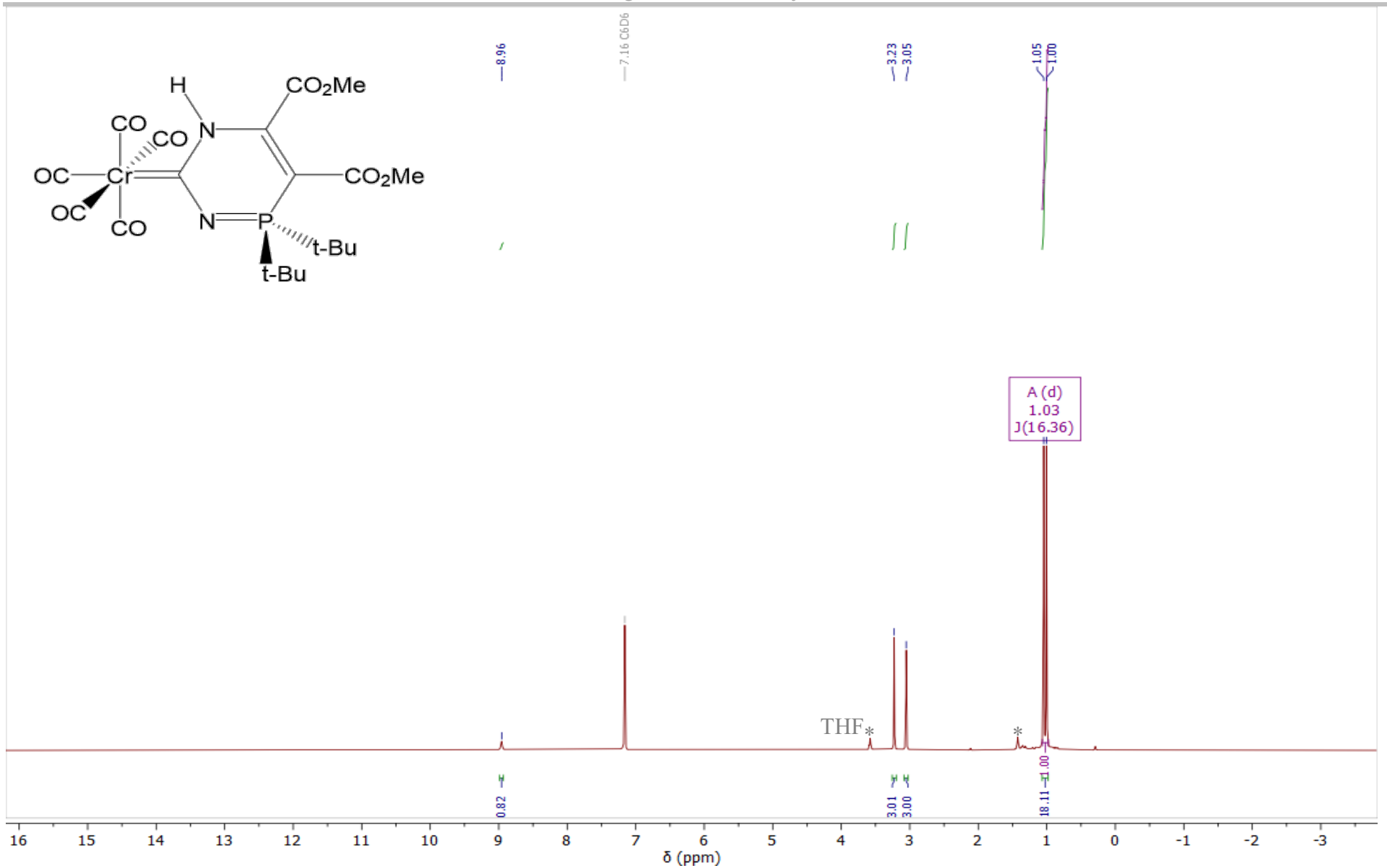

Figure S84: The ^{1}H NMR spectrum of [Cr{CNP^{t}Bu$_2$C(CO$_2$Me)C(CO$_2$Me)NH}(CO)$_5$] (C_6D_6, 400 MHz, 25 °C).

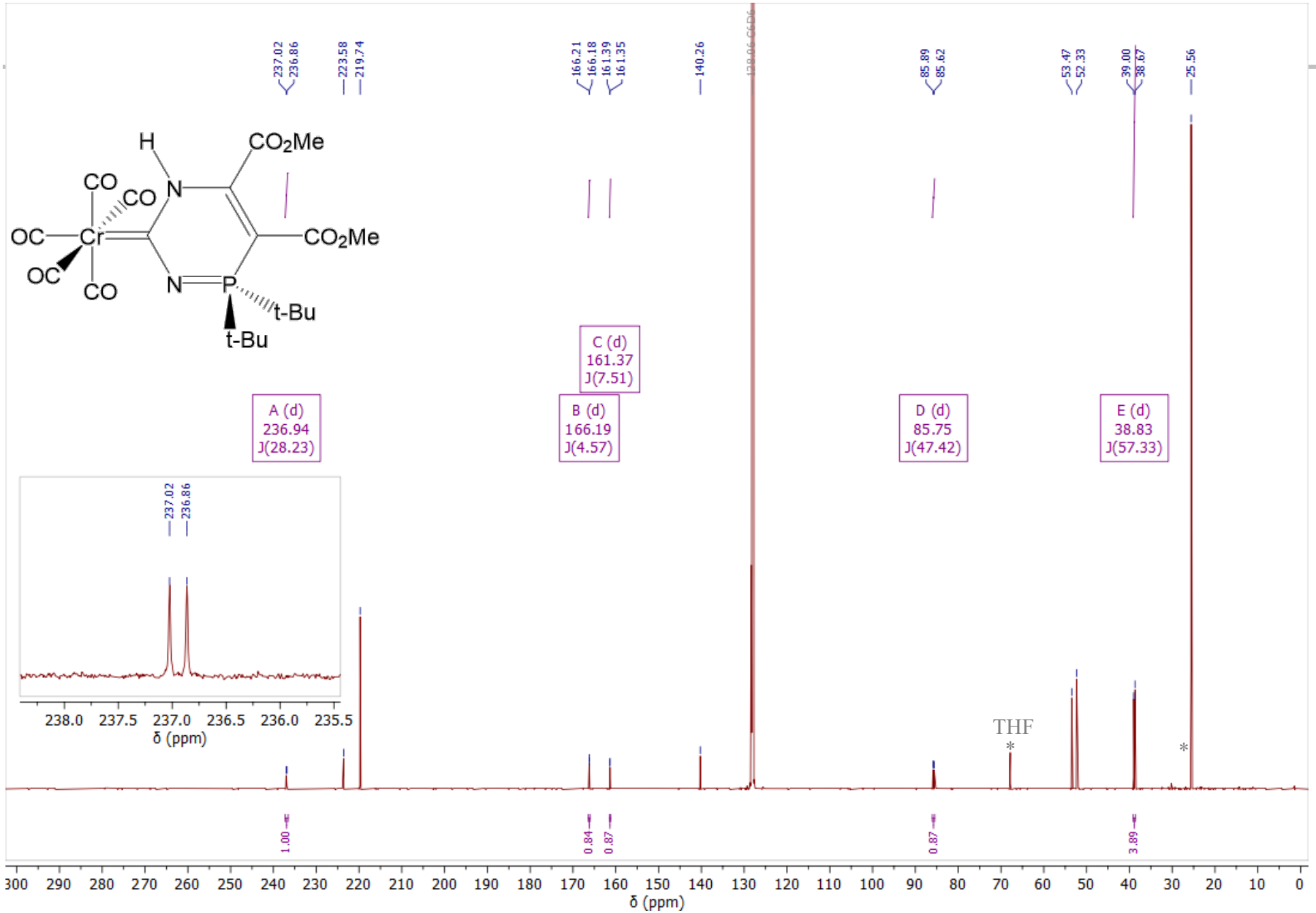

Figure S85: The $^{13}C\{^{1}H\}$ NMR spectrum of [Cr{CNP^{t}Bu$_2$C(CO$_2$Me)C(CO$_2$Me)NH}(CO)$_5$] (C_6D_6, 201 MHz, 25 °C).

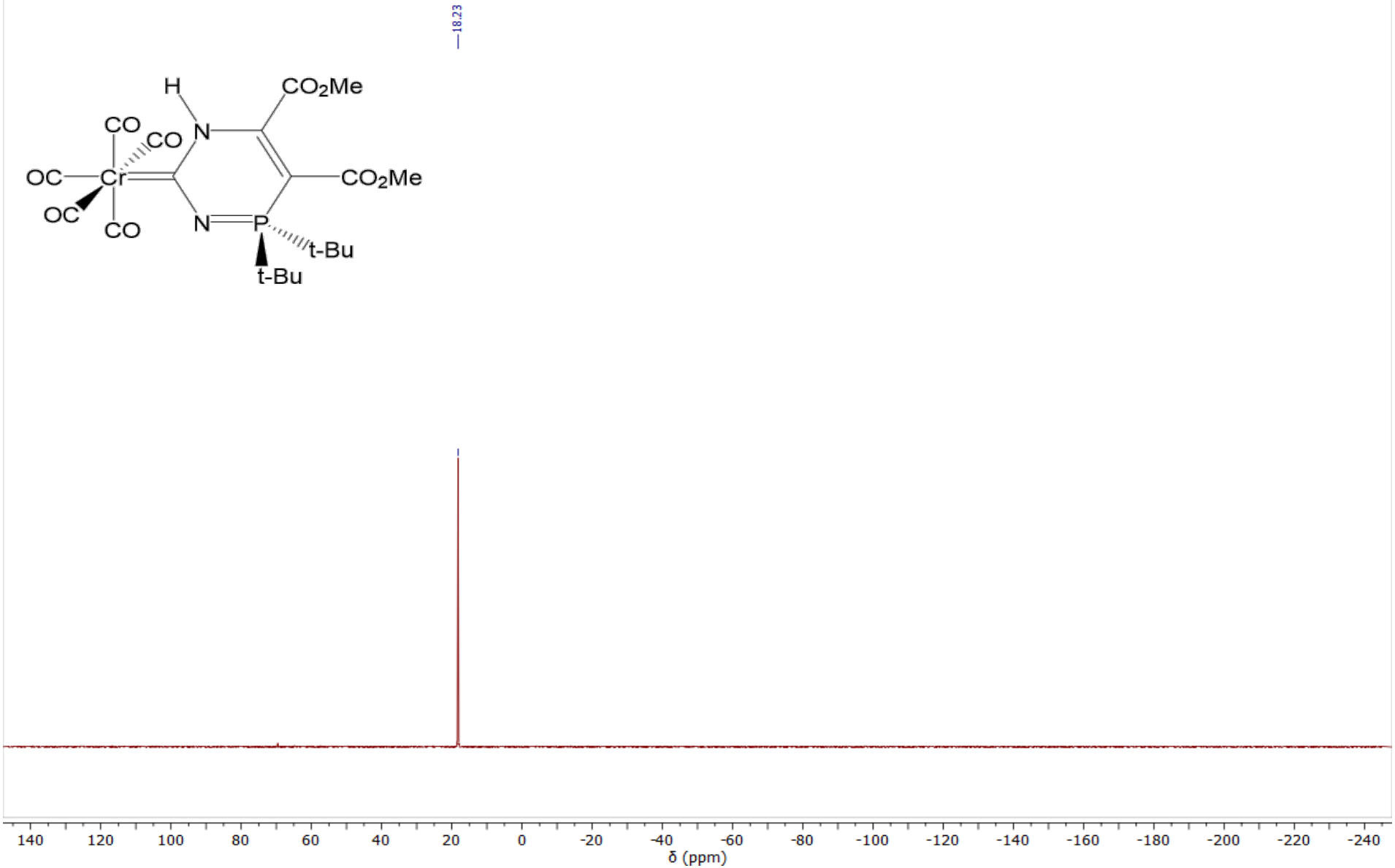

Figure S86: The $^{31}P\{^{1}H\}$ NMR spectrum of [Cr{CNP^{t}Bu$_2$C(CO$_2$Me)C(CO$_2$Me)NH}(CO)$_5$] (C_6D_6, 162 MHz, 25 °C).

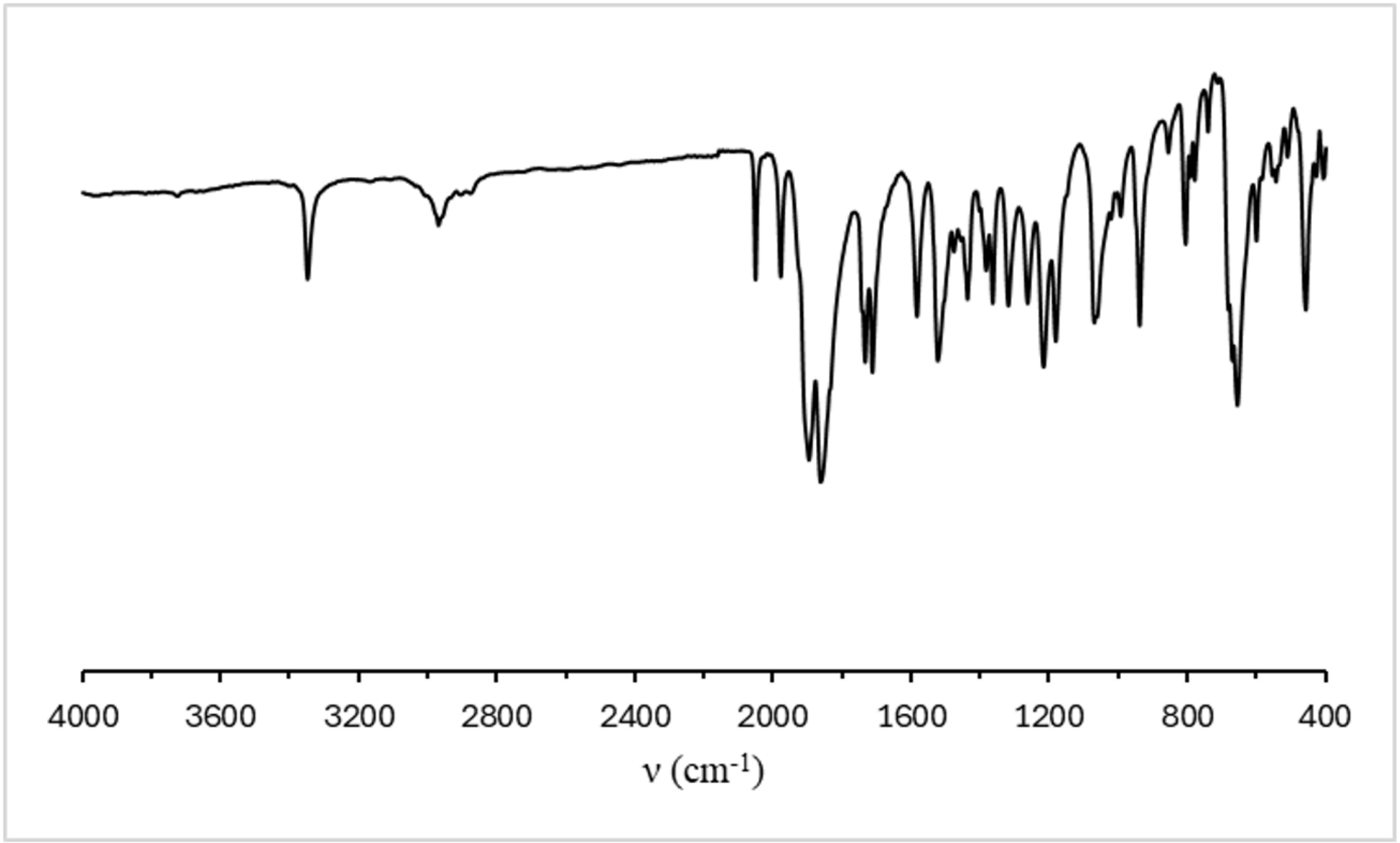

Figure S87: IR spectrum (ATR) of [Cr{CNP^{t}Bu$_2$C(CO$_2$Me)C(CO$_2$Me)NH}(CO)$_5$].

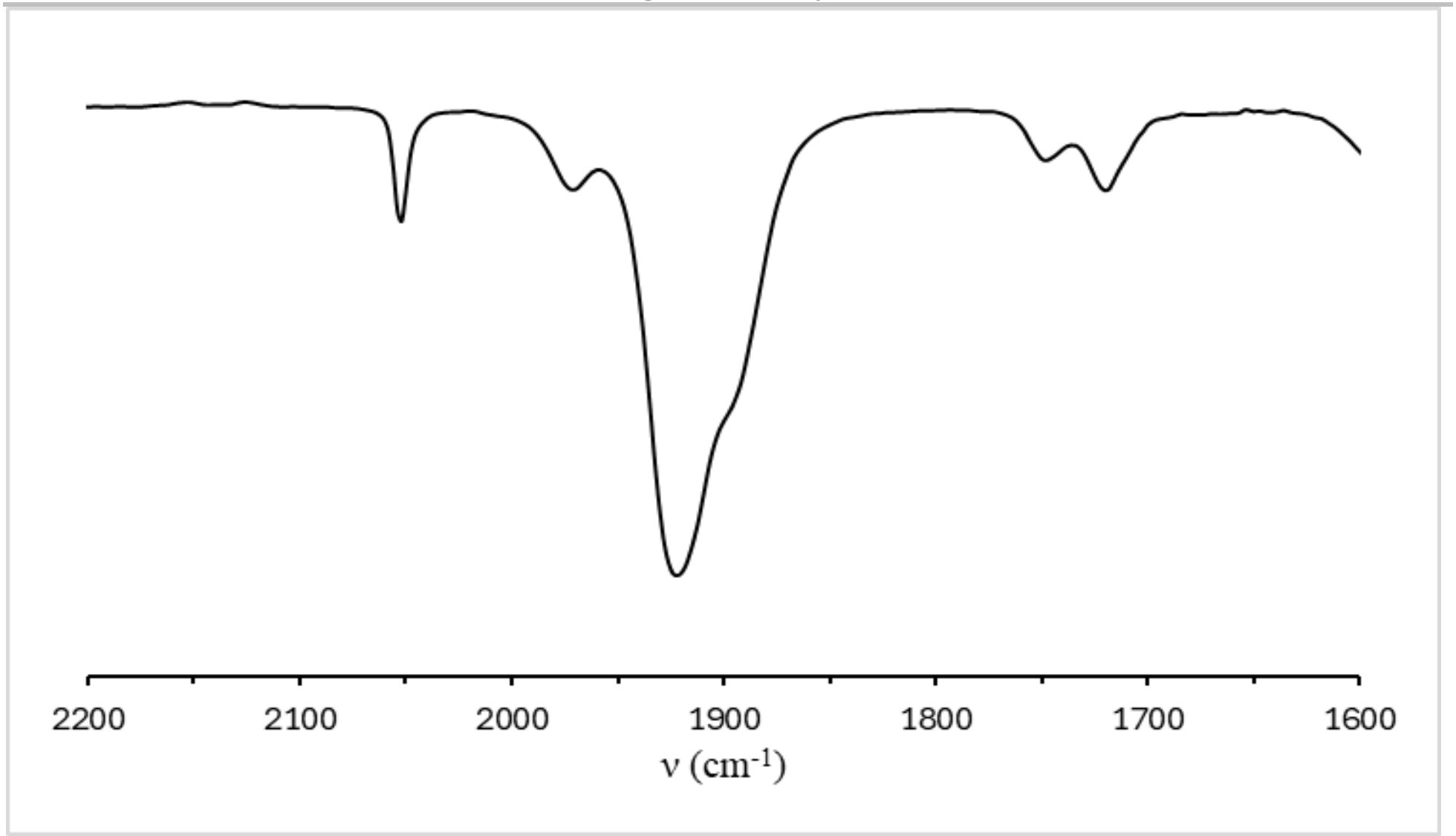

Figure S88: IR spectrum (CH_2Cl_2) of [Cr{CNP^{t}Bu$_2$C(CO_2Me)C(CO_2Me)NH}$(CO)_5$].

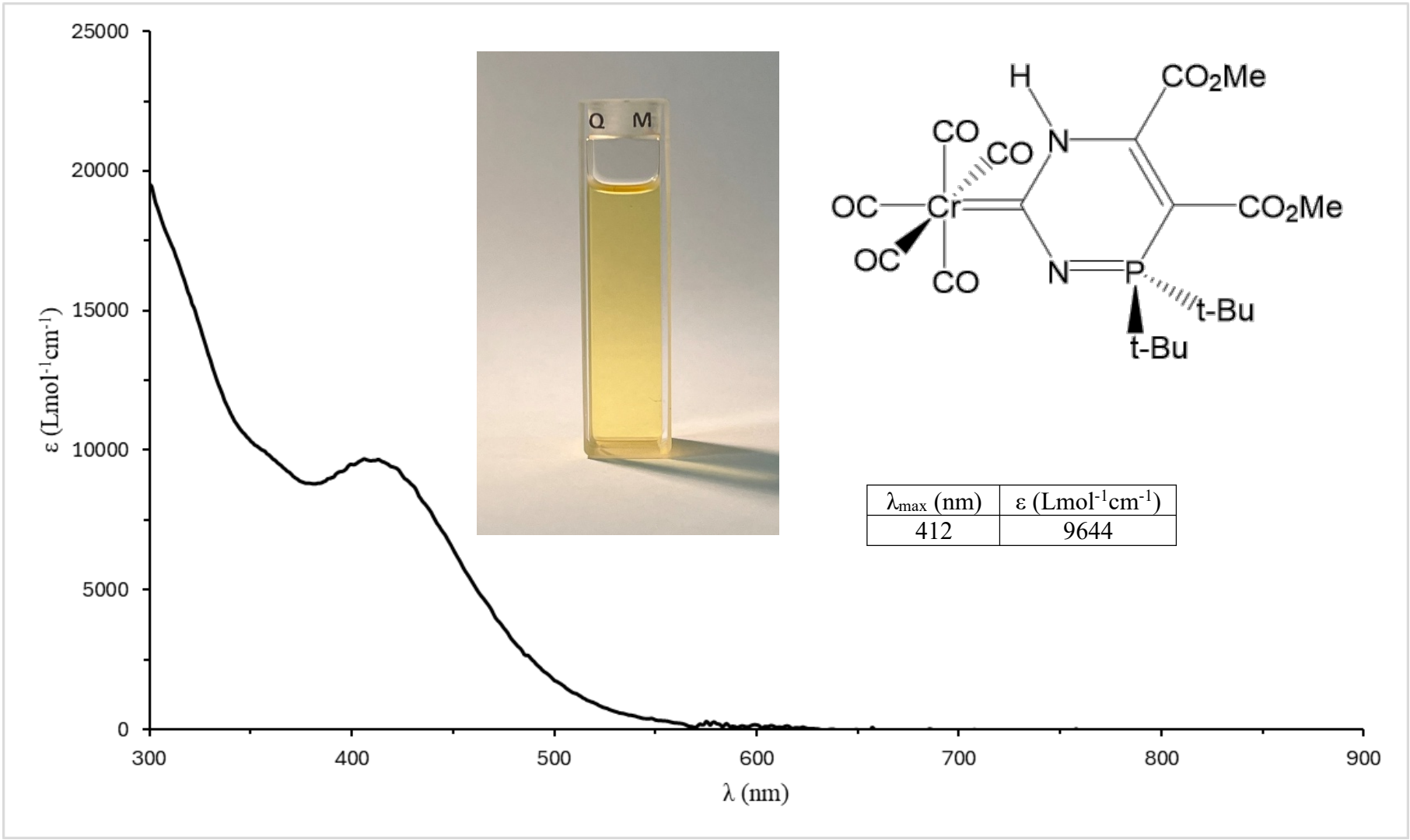

λ_{max} (nm)	ε ($Lmol^{-1}cm^{-1}$)
412	9644

Figure S89: The solution UV-Vis spectrum of [Cr{CNP^{t}Bu$_2$C(CO$_2$Me)C(CO$_2$Me)NH}(CO)$_5$] (*conc.* = 7.7 x 10^{-5} molL^{-1}, CH_2Cl_2, 25 °C). Inset: photograph of [Cr{CNP^{t}Bu$_2$C(CO$_2$Me)C(CO$_2$Me)NH}(CO)$_5$] in CH_2Cl_2 solution.

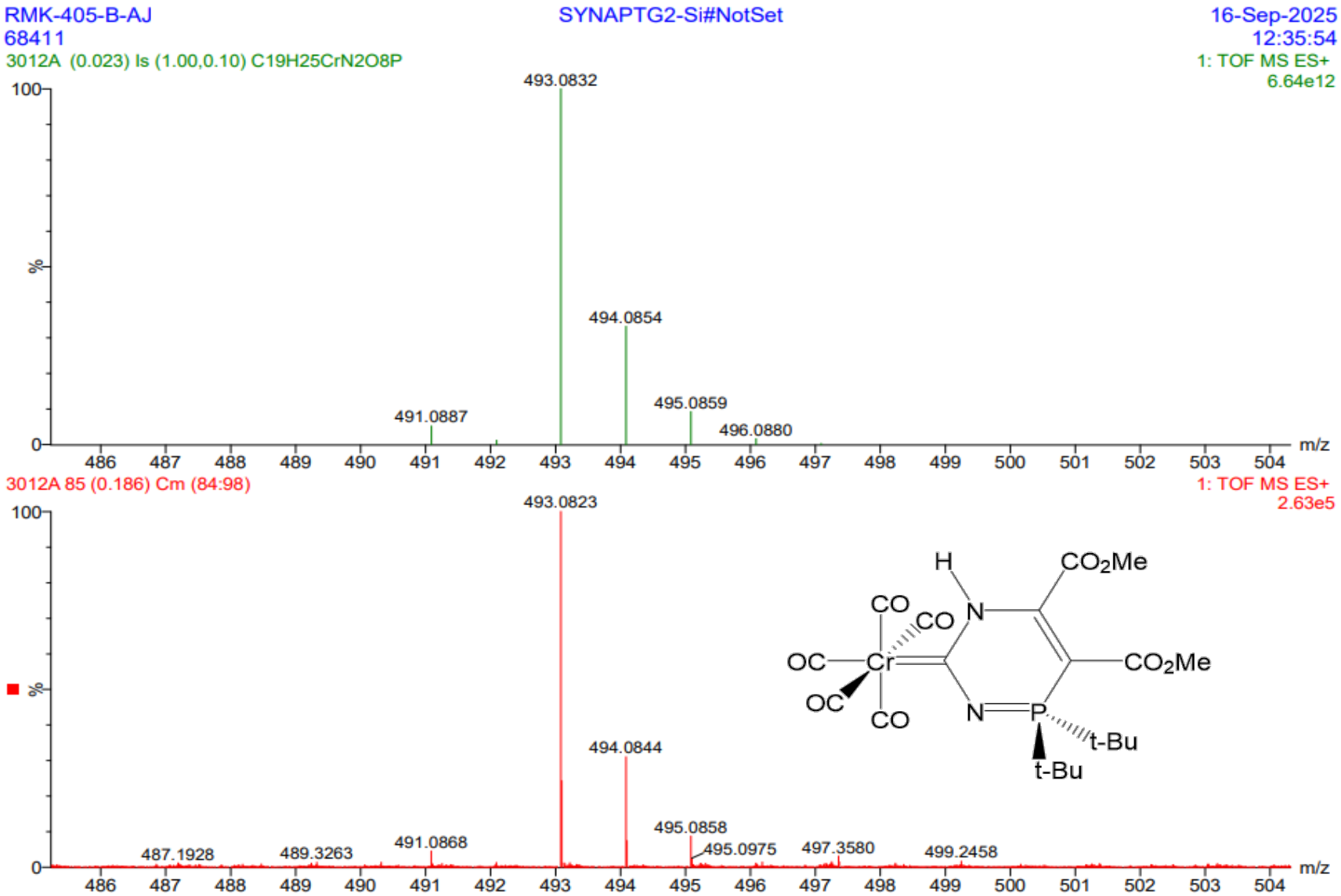

Figure S90: The HR-MS of [Cr{CNP^{t}Bu$_2$C(CO$_2$Me)C(CO$_2$Me)NH}(CO)$_5$] (ESI, MeCN, [*M* – CO]$^+$ ion).

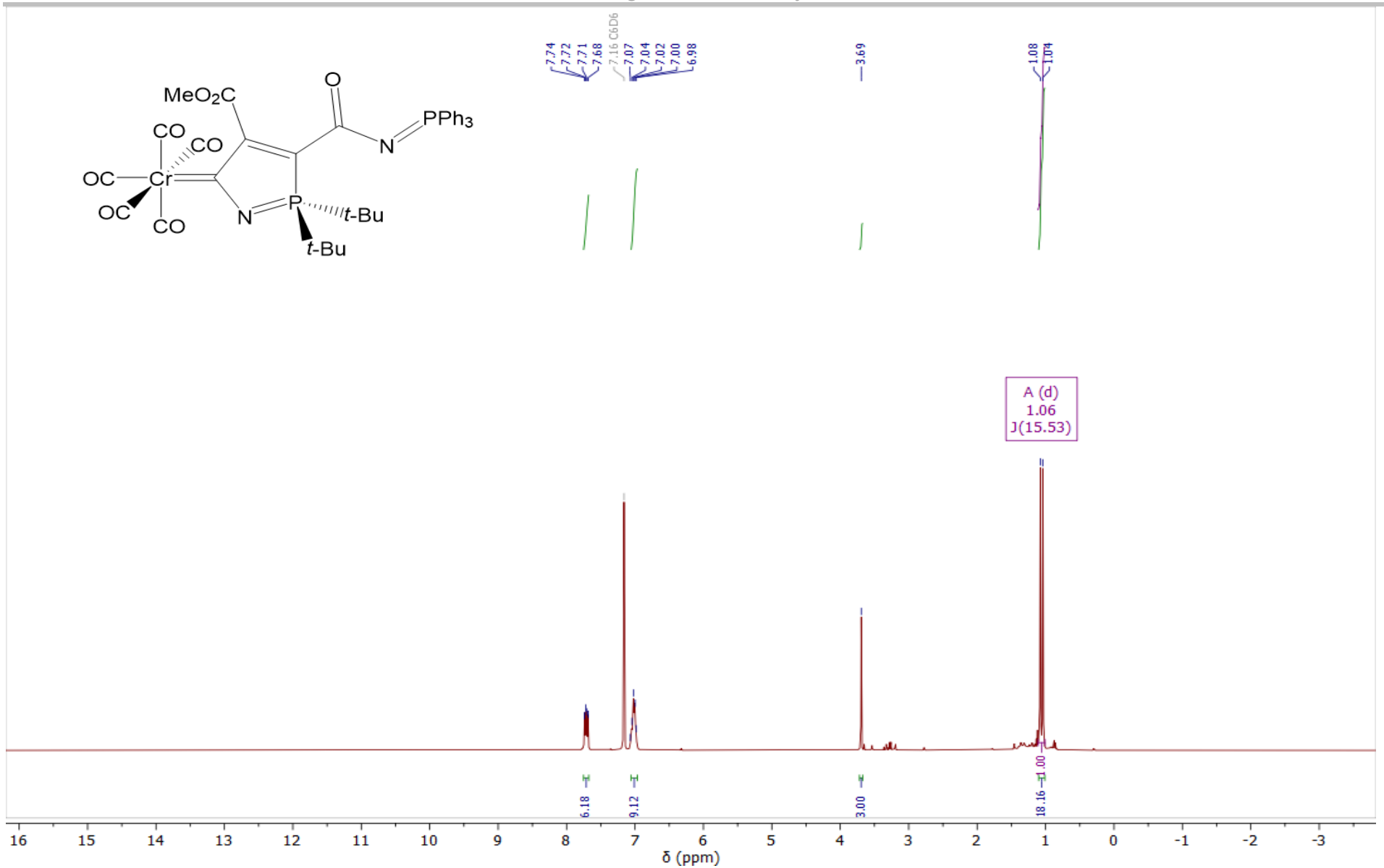

Figure S91: The ^{1}H NMR spectrum of [Cr{CNP^{t}Bu$_2$C(CO2Me)C(C(O)NPPh$_3$)}(CO)$_5$] (C_6D_6, 400 MHz, 25 °C).

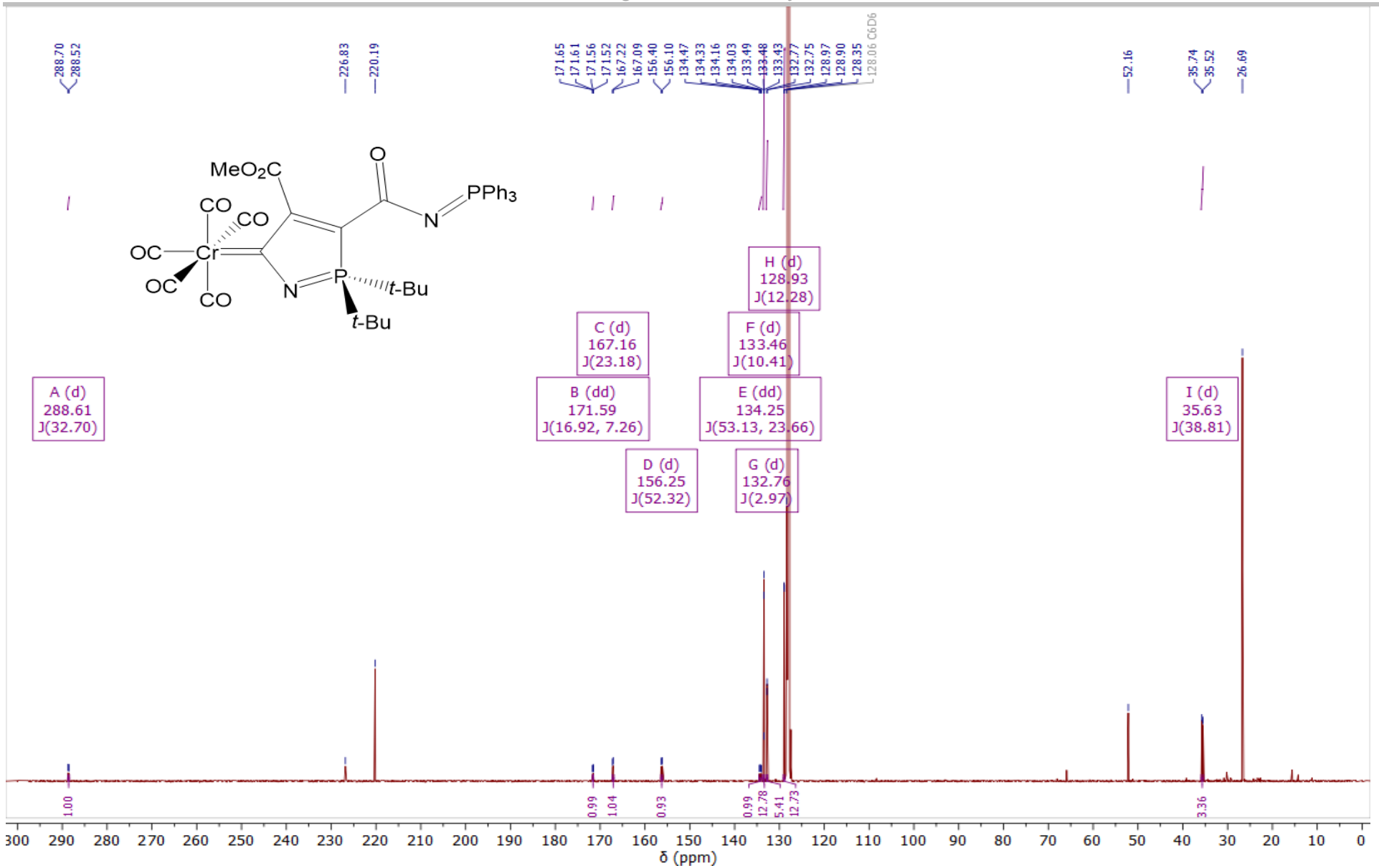

Figure S92: The $^{13}C\{^{1}H\}$ NMR spectrum of [Cr{CNP^{t}Bu$_2$C(CO$_2$Me)C(C(O)NPPh$_3$)}(CO)$_5$] (C_6D_6, 201 MHz, 25 °C).

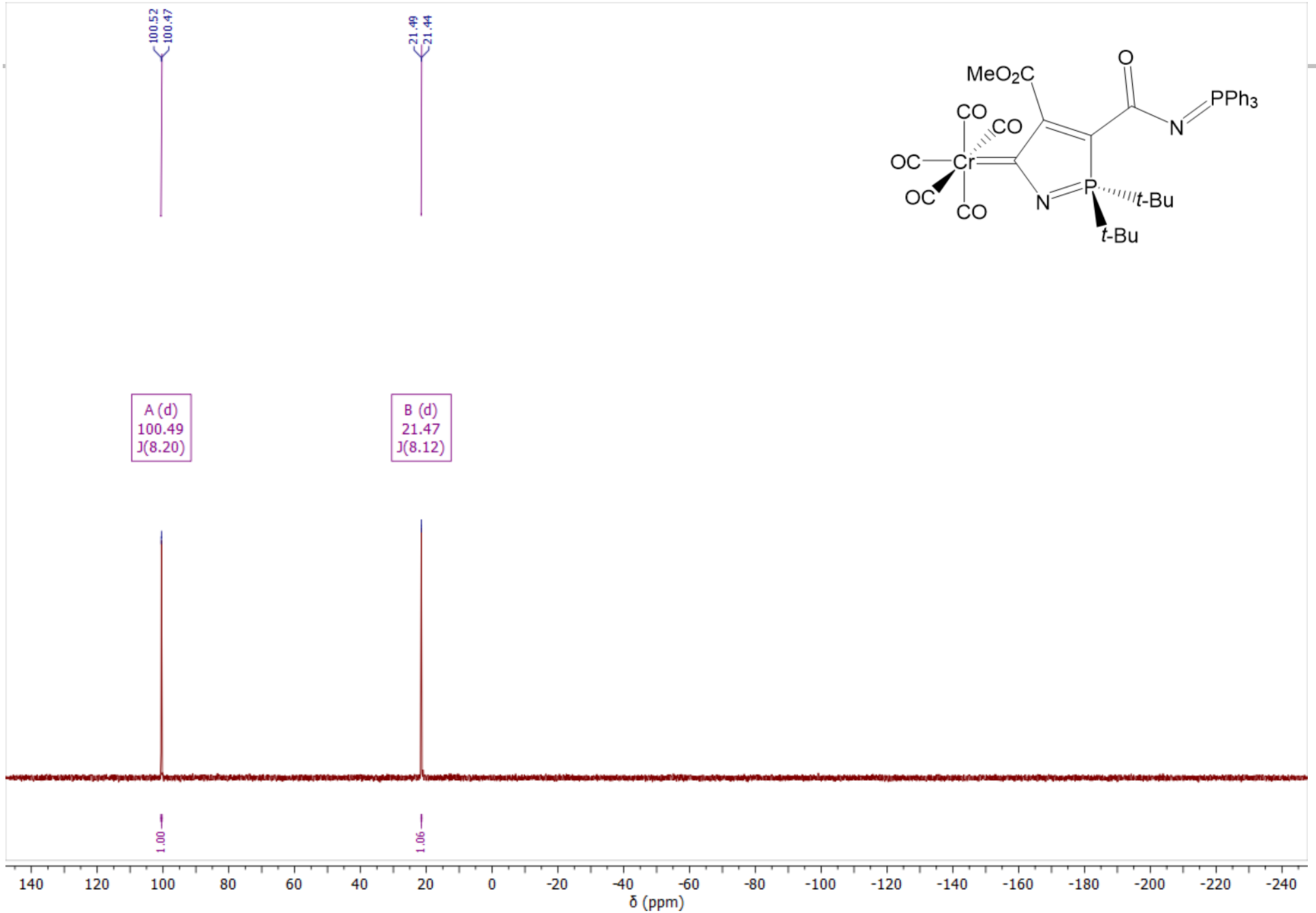

Figure S93: The $^{31}P\{^{1}H\}$ NMR spectrum of [Cr{CNP^{i}Bu$_2$C(CO$_2$Me)C(C(O)NPPh$_3$)}(CO)$_5$] (C_6D_6, 162 MHz, 25 °C).

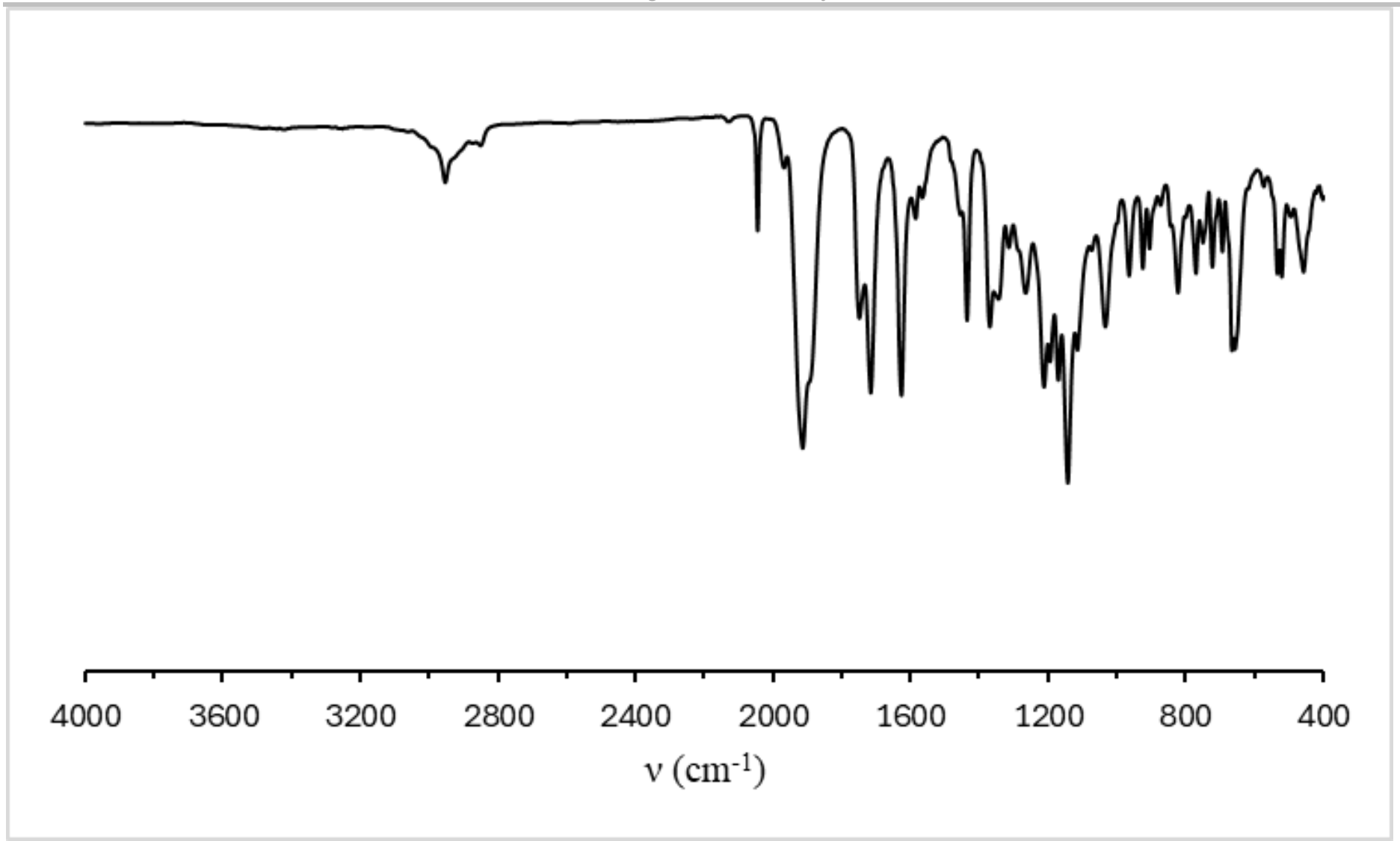

Figure S94: IR spectrum (ATR) of [Cr{CNP^{t}Bu$_2$C(CO$_2$Me)C(C(O)NPPh$_3$)}(CO)$_5$].

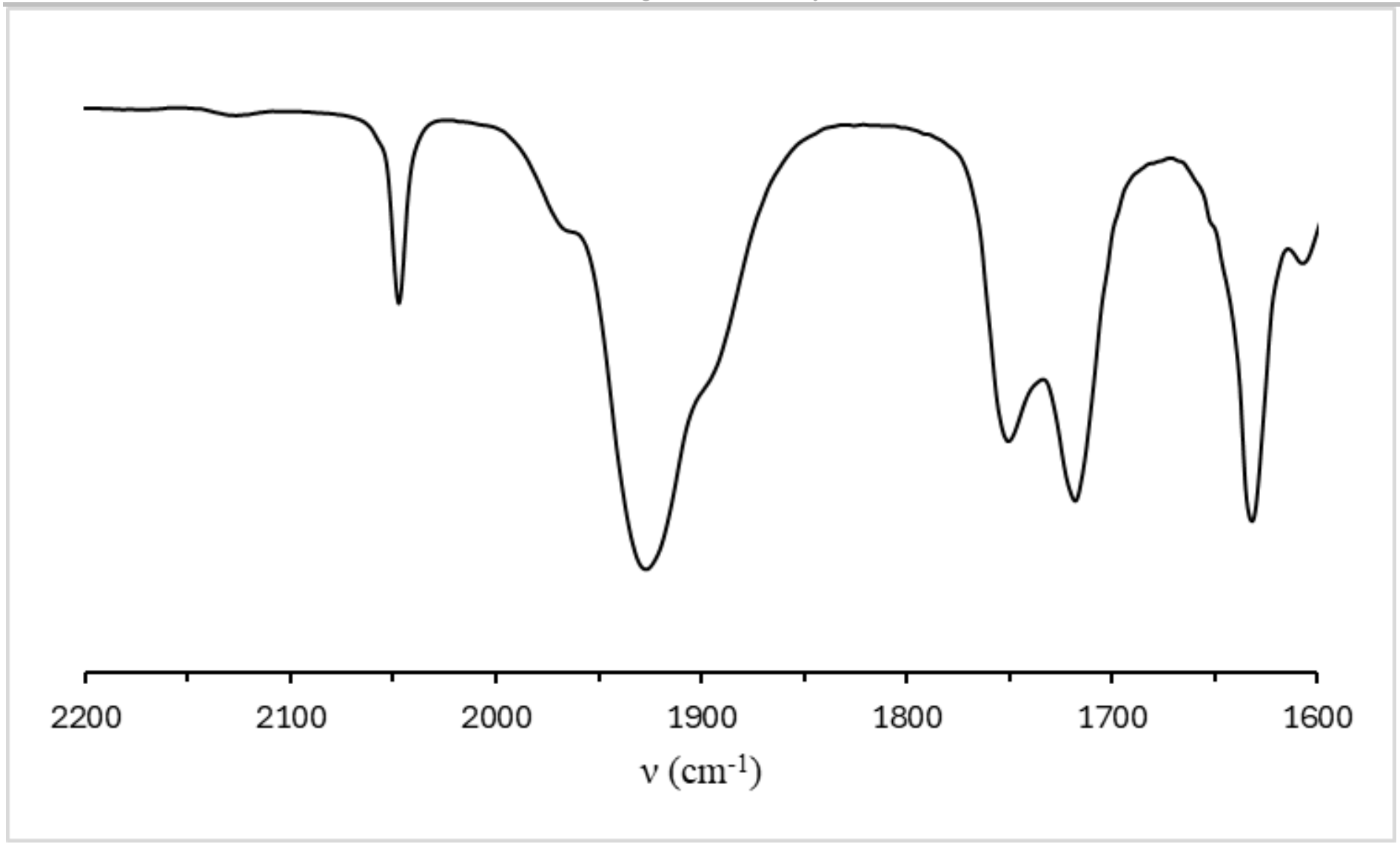

Figure S95: IR spectrum (CH_2Cl_2) of [Cr{CNP^{t}Bu$_2$C(CO_2Me)C(C(O)NPPh$_3$)}$(CO)_5$].

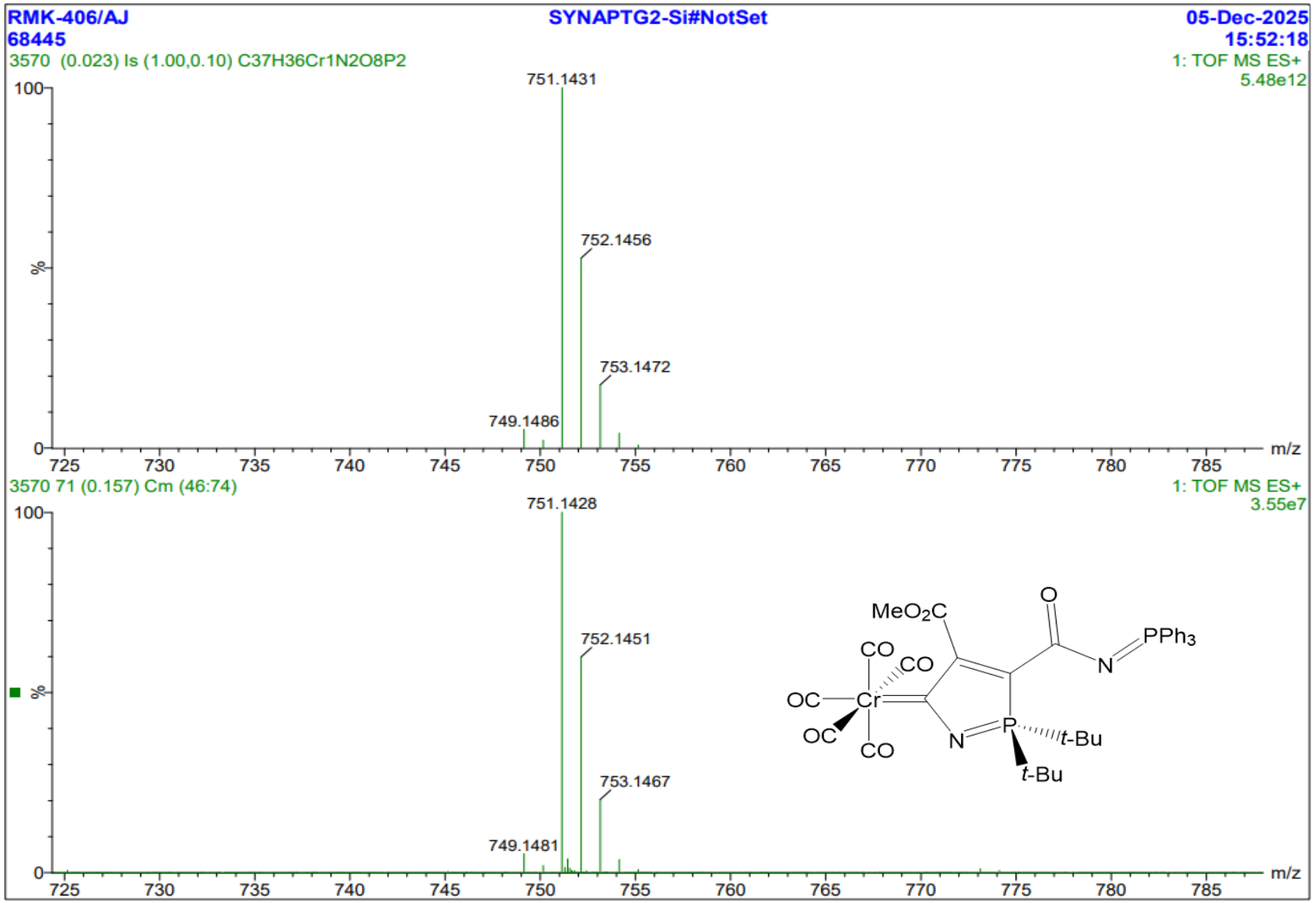

Figure S96: The HR-MS of [Cr{CNP^{t}Bu$_2$C(CO$_2$Me)C(C(O)NPPh$_3$)}(CO)$_5$] (ESI, MeCN, [*M* + H]$^+$ ion).

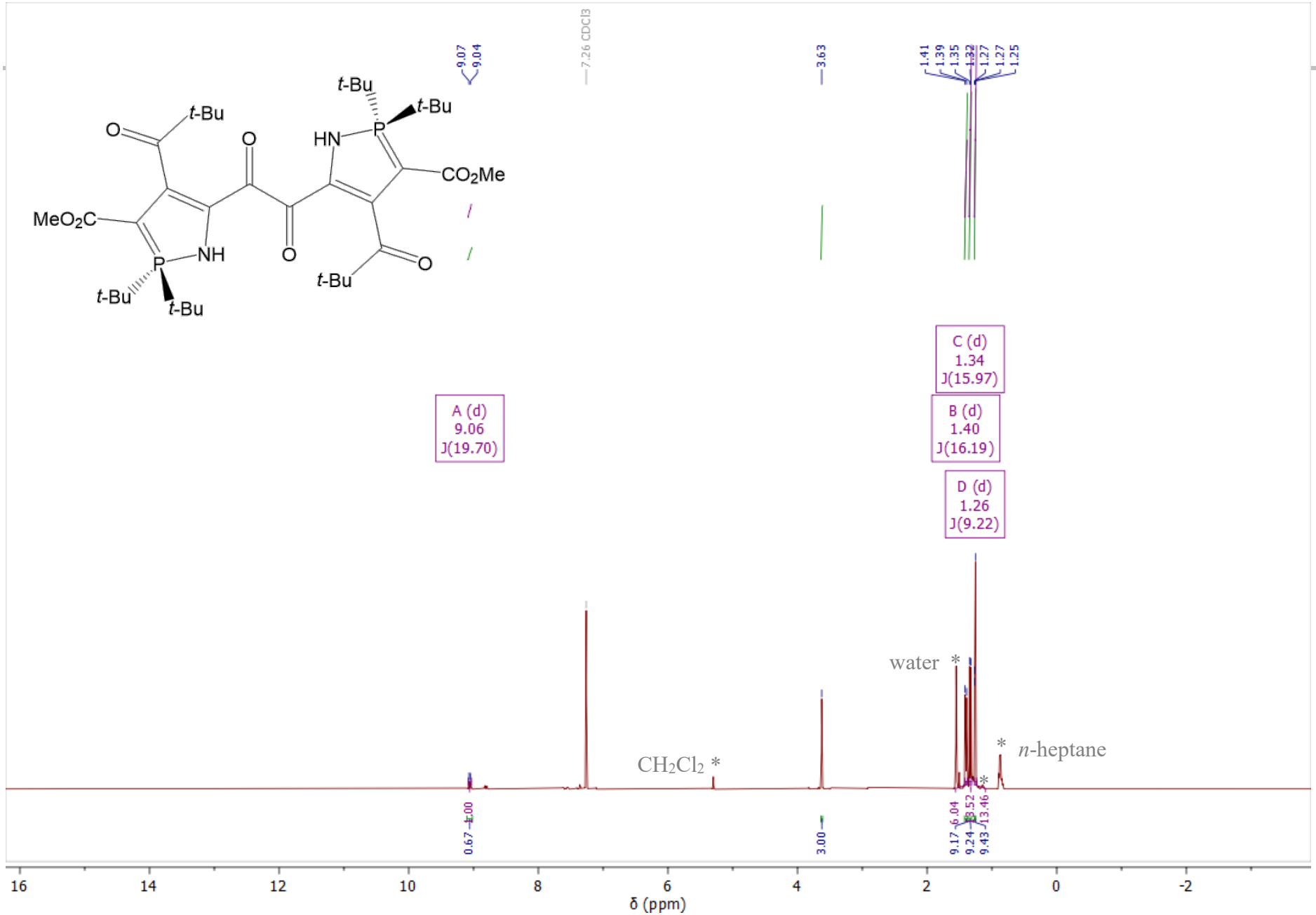

Figure S97: The ^{1}H NMR spectrum of $\{CN(H)P^{t}Bu_2C(CO_2Me)C(C(O)^{t}Bu)C(O)\}_2$ ($CDCl_3$, 400 MHz, 25 °C).

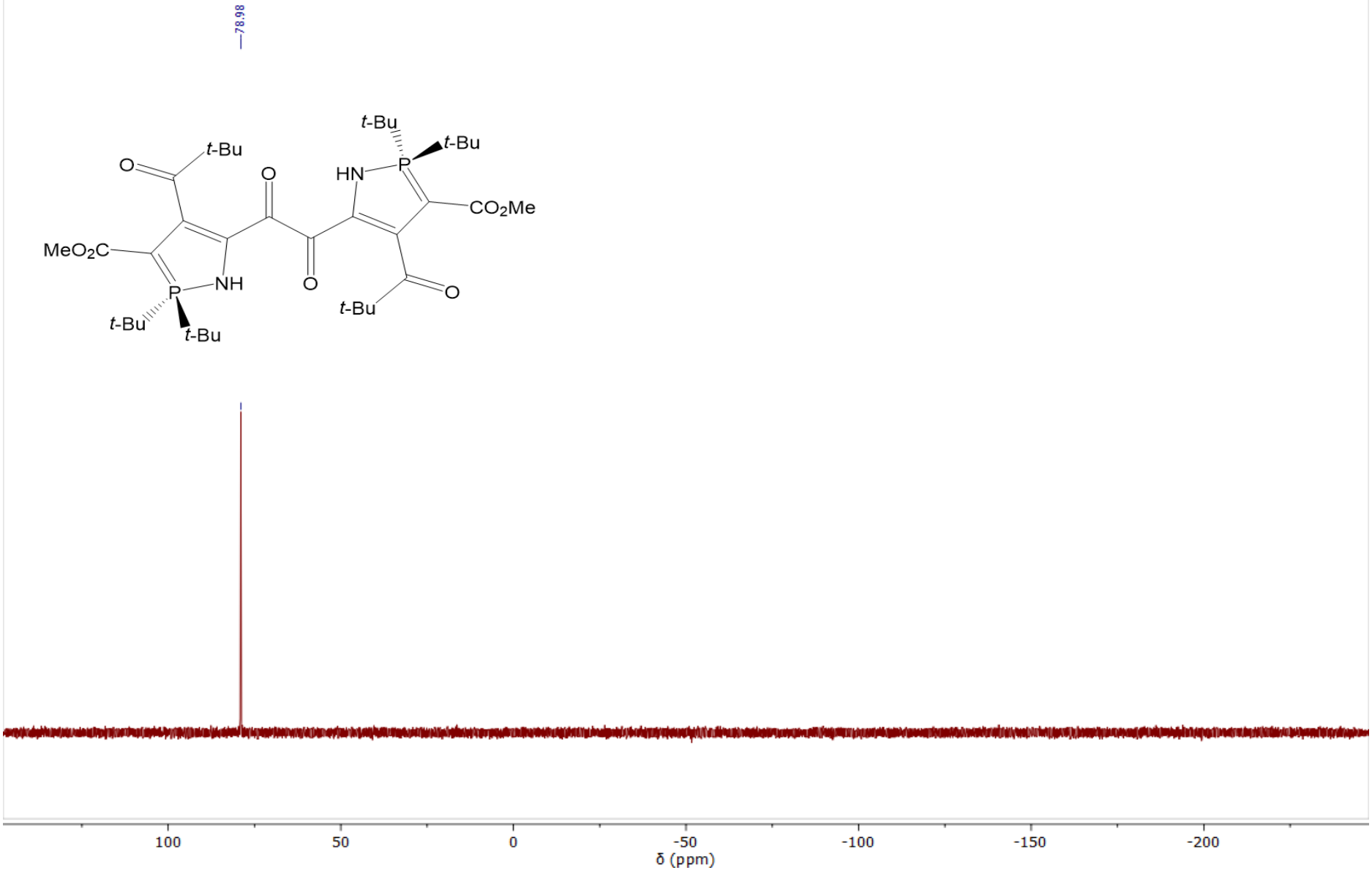

Figure S98: The $^{31}P\{^{1}H\}$ NMR spectrum of $\{CN(H)P^{t}Bu_2C(CO_2Me)C(C(O)^{t}Bu)C(O)\}_2$ ($CDCl_3$, 162 MHz, 25 °C).

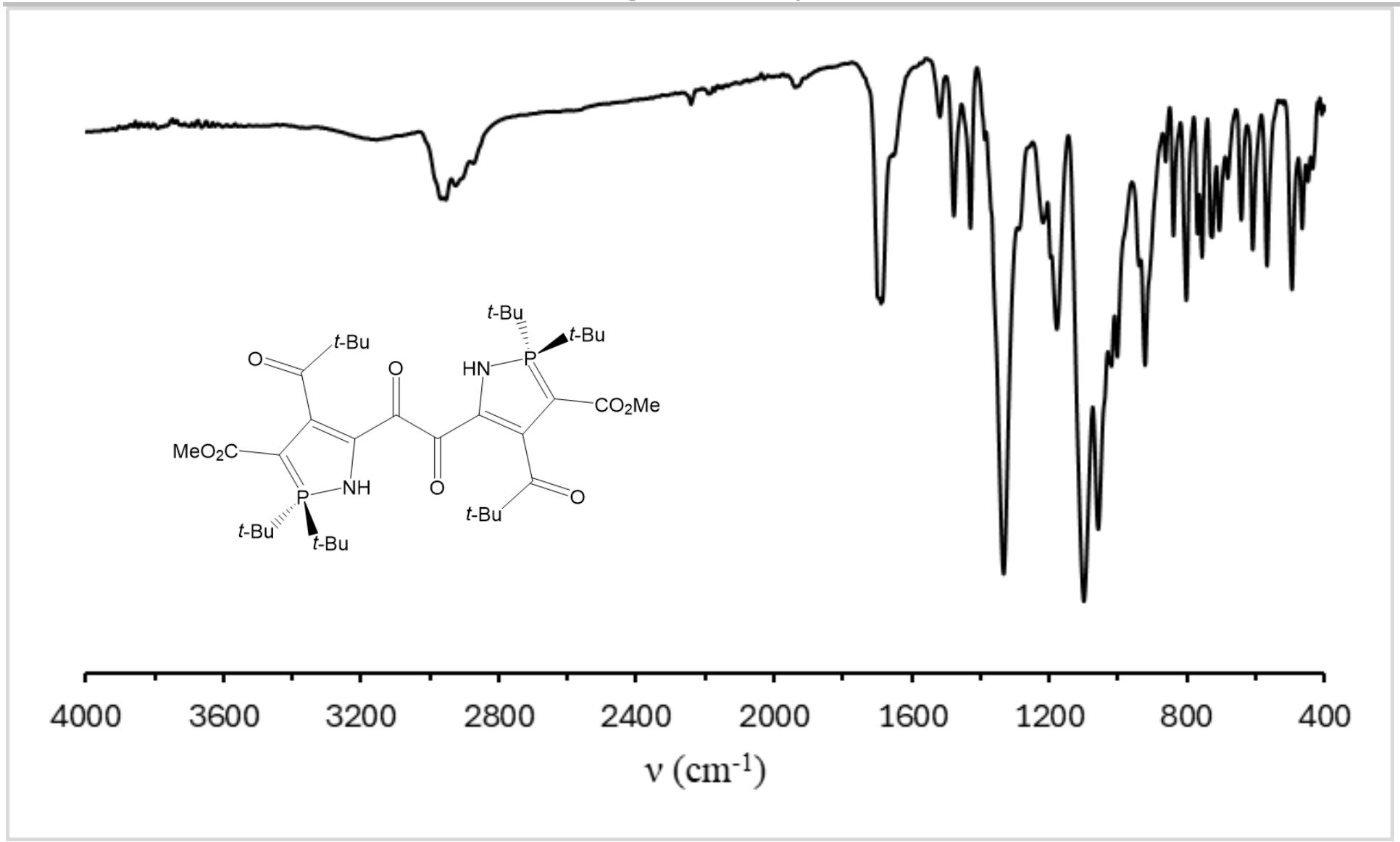

Figure S99: The ATR IR spectrum of {CN(H)P^{t}Bu$_2$C(CO$_2$Me)C(C(O)^{t}Bu)C(O)}$_2$.

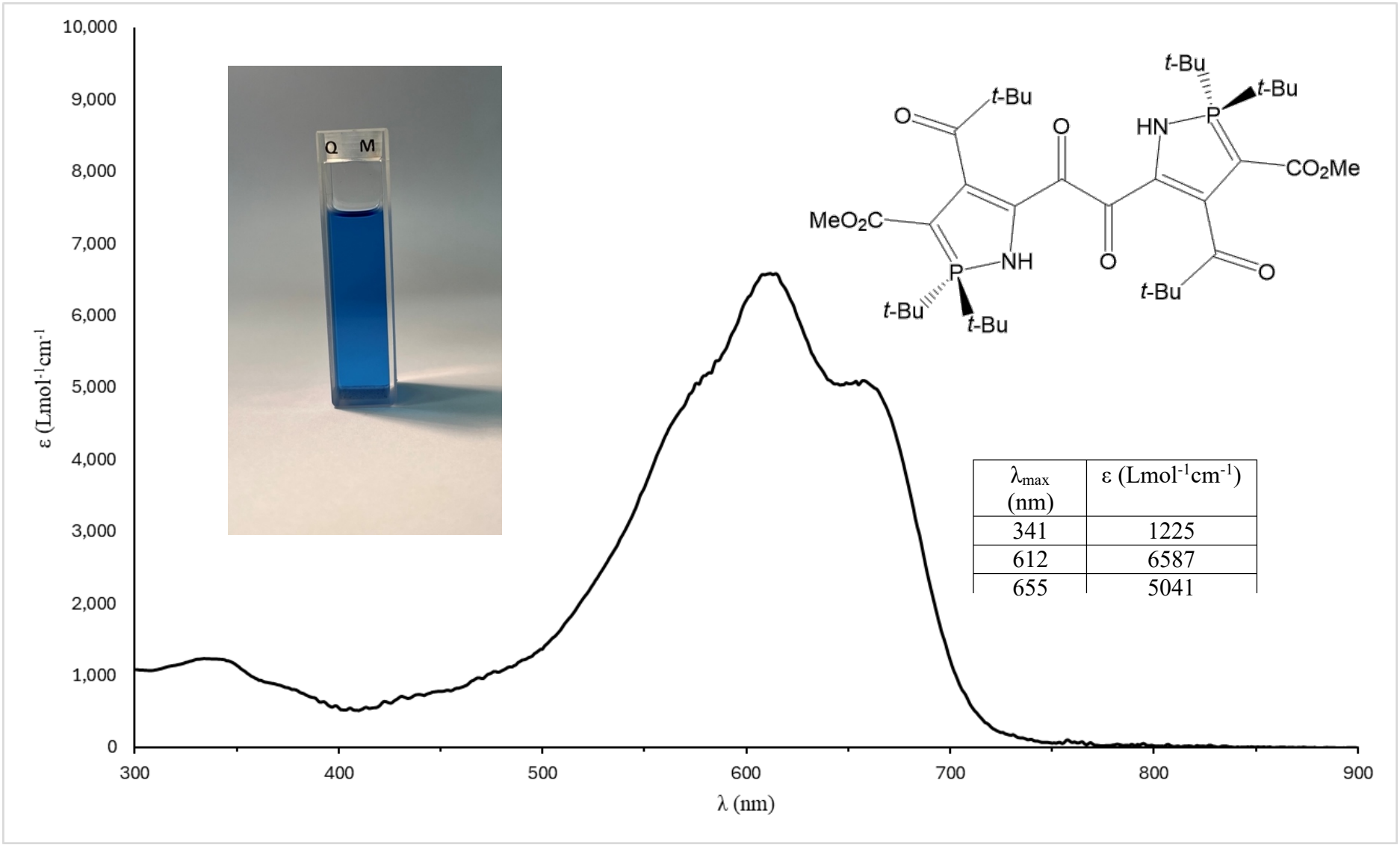

λ_{max} (nm)	ε ($Lmol^{-1}cm^{-1}$)
341	1225
612	6587
655	5041

Figure S100: The solution UV Vis spectrum of {CN(H)P^{t}Bu$_2$C(CO$_2$Me)C(C(O)^{t}Bu)C(O)}$_2$ (*conc.* = 1.3 x 10^{-4} molL^{-1}, CH_2Cl_2, 25 °C). Inset: photograph of {CN(H)P^{t}Bu$_2$C(CO$_2$Me)C(C(O)^{t}Bu)C(O)}$_2$ in CH_2Cl_2 solution.

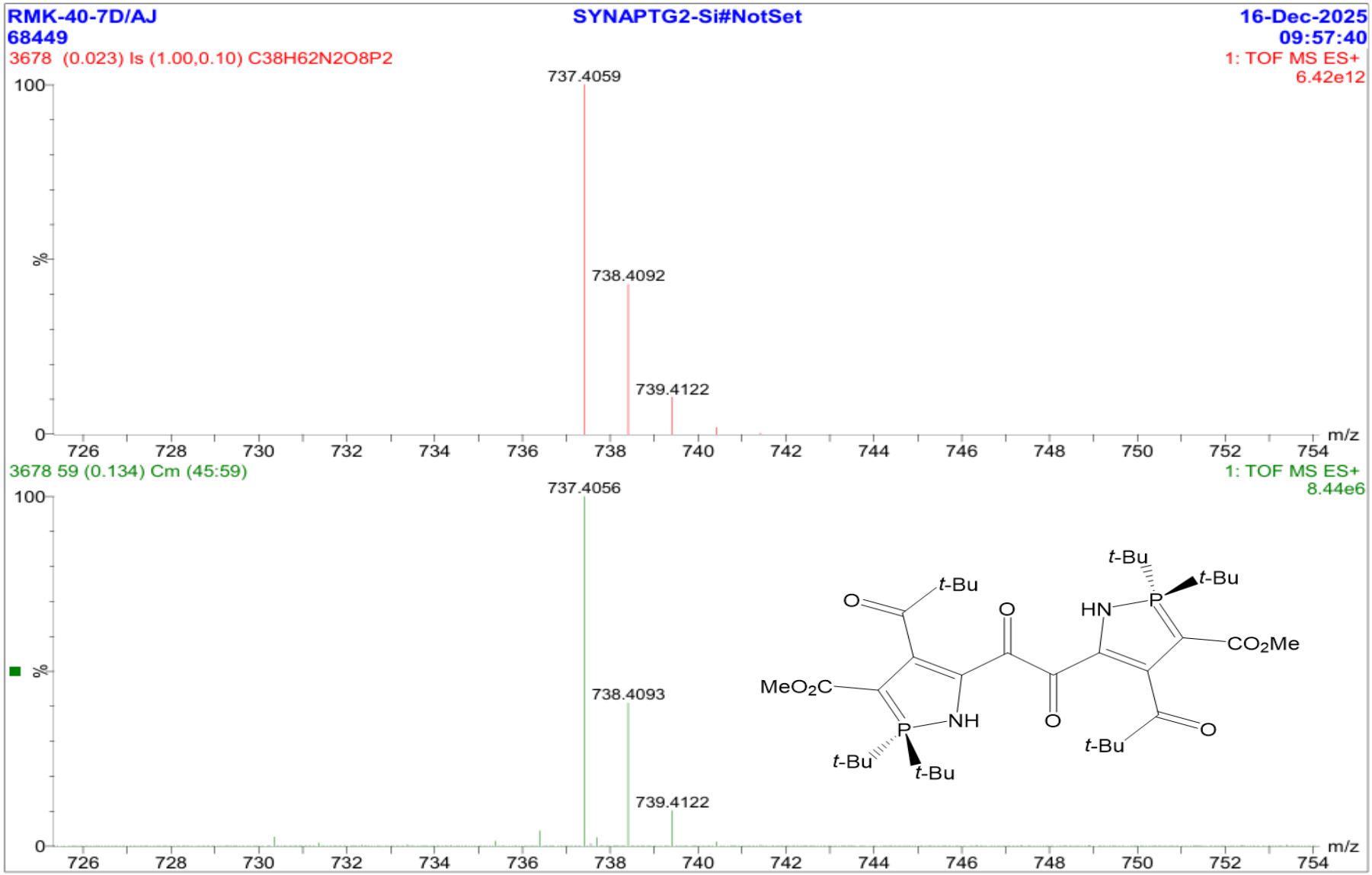

Figure S101: The HR-MS of {CN(H)P^{t}Bu$_2$C(CO$_2$Me)C(C(O)^{t}Bu)C(O)}$_2$ (ESI, MeCN, [*M* + H]$^+$ ion).